

**DESIGN AND CHARACTERIZATION OF METAMATERIAL ANTENNA
FOR MOBILE HANDSET APPLICATIONS**

By

N. PRASANTHI KUMARI

(SAP ID: 500010377)

COLLEGE OF ENGINEERING

Under the Guidance of

Dr. Piyush Kuchhal

(Associate Dean, Applied Sciences, UPES, India)

Dr. Prashant S Rawat

(HOD, Nuclear Science, UPES, India)

Dr. R. Gowri

(Director, Graphic Era Hill University, Dehradun, India)

Submitted



**TOWARDS PARTIAL FULFILLMENT OF THE REQUIREMENTS FOR
THE DEGREE OF DOCTOR OF PHILOSOPHY**

TO

UNIVERSITY OF PETROLEUM AND ENERGY STUDIES

DEHRADUN, INDIA

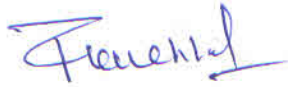
March, 2015

THESIS COMPLETION CERTIFICATE


This is to certify that the thesis on “**Design and Characterization of Metamaterial Antenna for Mobile Handset Applications**” by **N. Prasanthi Kumari**, towards partial completion of the requirements for the award of the Degree of Doctor of Philosophy (Engineering), is an original work carried out by her under our joint supervision and guidance. It is certified that the work has not been submitted anywhere else for the award of any other diploma or degree of this or any other University.



Internal Guide
Dr. R. Gowri



Internal Guide
Dr. Piyush Kuchhal



Internal Co-Guide
Dr. Prashant S Rawat

Dedicated to

My Parents and Lord, my creator, who has given me eternal life.

ACKNOWLEDGMENTS

Working on the Ph.D. has been a wonderful and awesome experience. It is good to say that right from the selection of the problem, to the design and wrestling to write the papers has been the real learning experience. I am grateful to many people for making this period an unforgettable experience.

I am deeply thankful to the honorable Chancellor Dr. S.J Chopra, the Vice chancellor, Dr. Parag Diwan, the Pro Vice Chancellor, Prof Utpal Ghosh, Dr. Shri Hari, the Campus Director, and Dr. Kamal Bansal, the Dean, College of Engineering, for their continuous moral support during this endeavour.

To work with my guides Dr. Ravi Gowri, Director, GEHU, Dr. Piyush Kuchhal, Associate Professor, and Dr. Prashant Rawat, Associate Professor, CoES, UPES, has been a real pleasure to me, with lot of enthusiasm and eagerness to know new things shared. They have been a constant influence throughout my Ph.D. career which has supported me with promptness and devotion, and have always been enduring and encouraging for both, new ideas and in times of difficulties. I met my external guide Dr. Ravi Gowri mostly at the closing hours of the day, yet she used to fill me with new ideas.

In addition, I have been very privileged to get to know and to collaborate with many other great people over the last several years. I learned a lot from them about life and research, and about how to tackle new

problems and to develop techniques to solve them. Thank you all for all the inspiring discussions I had every time I met you at the University of Petroleum & Energy Studies, Dehradun India.


N PRASANTHI KUMARI

EXECUTIVE SUMMARY

A metamaterial antenna with slots is investigated in this doctoral work for a new type of antenna for mobile application, which provides wide bandwidth, miniature size and high gain. This antenna exhibits handedness, left-handedness and right-handedness in the resonant frequency with good radiation characteristics with Composite Right/Left Handed Transmission line (CRLH TL) Split Ring Resonator (SRR) and PATCH as its central elements. The conventional microstrip antennas have a conducting patch printed on a grounded dielectric substrate and operate as resonant cavity elements. This operation, however, leads inherently to narrow impedance bandwidth, which is a barrier for microstrip antennas to be used for wireless communications. Hence, they are generally used for multi-standard wireless communication systems as they do not offer multi-band performance. Antennas for next generation wireless communication systems are required to exhibit resonance in multiple bands that are not harmonically related in order to accommodate multiple wireless standards within the same device. Additionally, they are required to have a compact form-factor and relatively high radiation efficiency.

Literature related to the compact antennas intended for use in handsets and other small wireless devices were studied in detail in the chapter -2. The nutshells proposed within the antenna, CRLH TL, SRR and Patch metamaterial concept were also surveyed in some of the relevant recent studies. Advantages of presence

of slot and feeding techniques employed for the metamaterial antenna for mobile applications are also investigated. On the basis of literature survey, an novel prototype antenna, which provides wider bandwidth, miniaturized size and high gain along with the above cited concepts is proposed in this work as the final design. The research described in this thesis is concerned with the analysis and design of mobile handset antenna types, based on the left-handed transmission line, S-SRR and patch with slot approach. The left handed transmission line concept can be extended to construct reduced-size planar antenna in the commercial frequency band which is thought to be a feature unique to these antennas. Efficiency is a key parameter of left handed antennas when split ring resonators are considered. A study of the efficiency of miniaturized mobile antennas loaded with a left-handed transmission line is described specially, and is compared with those of the conventional PCB antennas. Available literature shows the slot in the antenna helps in bandwidth enhancement. The bandwidth enhancement of the proposed antenna is achieved by unequal sizes of slots created on the radiating patch of various sizes.

The major aim of the third chapter of this thesis is to demonstrate the scheme of design development of a wideband handset antenna, for mobile range covering GSM, PCS, DCS and WIBRO bands. The design development is presented in terms of a flow chart. The prototypes have PCB type structures printed on both sides, covering frequency of mobile applications with unsymmetrical cells presented. The first part of this chapter deals with the dimensions of three antenna structures, and their simulation to obtain best

optimized results. Of the three antennas, while the first antenna has substrate of FR4, the second and the third have substrate of RT Duroid. The three antennas differ in structure and dimensions. The first of the prototypes has probe feed printed on both sides. The geometry of this two sided printed circuit CRLH -TL metamaterial antenna is discussed in some detail, mentioning the dimensions and copper conducting plane and substrate. The first design sample with FR4 substrate and coaxial feed is presented with FR4 ($\epsilon_r=4.4$), with dimensions of $40 \times 80 \times 1 \text{ mm}^3$. Antenna of miniaturized size, with dimensions of $40 \times 60 \times 0.762 \text{ mm}^3$, with a printed type on a substrate of RT Duroid 5880LZ ($\epsilon_r=2.2$) and edge feeding is subsequently proposed. The subsequent prototype designed has the same dimensions, and differs by the presence of slots of different sizes in the unsymmetrical patches of front side.

The third chapter later discusses the fabrication of these three antennas; 1st through chemical etching of the antenna which has FR4 substrate, 2nd through chemical etching of the antenna which has RT Duroid substrate and without slot, and the 3rd through mechanical etching, which has RT Duroid and slot in the patches. Of the two etching methods used, the mechanical one is found to be better and adapted, with reasons discussed. Simulations for the mentioned three prototypes are studied and compared by the output parameters, listed by, Return loss, Radiation Pattern, Gain, VSWR and axial ratio. Optimized simulation results are determined followed by characterization, for measurement of return loss through vector network analyzer, radiation pattern through anechoic chamber to measure HPBW hence gain and directivity. Design consists of unsymmetrical

cells with combination of different sized patches to resonate in the frequency range mobile applications. This dimensional variation in turn makes antennas to resonate with different central frequencies. The improvement in characteristics is observed right from the first prototype, progressing to the third antenna, along with increased number of center frequencies.

Analytically 'equivalent' antenna is determined for all the prototypes. Considering with the 'equivalence' of individual elements, for all the main elements including CRLH, S-SRR, and PATCH with slot of the prototype having slots on one side, the equivalent circuit of an antenna is drawn. The input impedance for analysis is derived from the overall circuit according to current from feed point to ground. The reactance component of input impedance is then plotted to obtain the resonating frequency. This parameter is discussed in section 4.4.

An extensive list of output parameters is discussed in chapter 4 for the antennas, which were fabricated according to the relevant existing literature. Of them, parameters like Return loss, Radiation pattern, Gain measurement and Input impedance plot are discussed in detail in chapter 4. The resonant frequency of the antenna is inferred from the plot of return loss. The simulation results show that the antenna resonates from 1.58 GHz to 1.95 GHz. The measurement results of prototype were shifted towards right, with -10dB frequency values 1.65 GHz to 1.99 GHz. The shift of the two values is attributed to the fabrication inconsistencies, like discontinuities at the outer contours of the conducting patch lines on the substrate. This antenna covers PCS and DCS bands.

The resonant frequency of the 2nd antenna prototype antenna is obtained from return loss plot. The simulation results show that the antenna resonates from 1.95 GHz to 2.45 GHz. The tested result of prototype was shifted towards left with 1.9 GHz to 2.3 GHz. The shift of the two results can be observed by fabrication inconvenience faced in the discontinuities at the outer contours of the conducting patch on the substrate. The low-frequency resonance at 1.9 GHz, the current distribution is good enough to get wider bandwidth. This antenna is covering PCS and DCS and BLUETOOTH. Limitation of this antenna is its feeding increasing thickness of mobile or wireless sets.

The 3rd antenna prototype which is a slot loaded metamaterial antenna exhibits distinct resonances at 1.91 GHz, 2.4GHz 3.35GHz and 4.62 GHz respectively. Return loss responses explains the four resonances that lie within the S_{11} with value equal to -10 dB line can be clearly seen. It can be observed that in all three cases the antenna has a dipolar pattern, exhibiting a linear electric field polarization in the y-direction. The 10% shift towards right is observed due to the losses of connector and fabrication anomalies. The sizes and placement of the slots etched on patches are defined, such that a multi-band version of the antenna can be achieved with a large lower frequency bandwidth. The prototype with slots on the radiating patches is proved to be resonating more number of bands compared to the prototype which doesn't have slots on the front side.

The mechanical etching method employed for final antenna fabrication also proved to be better in terms of accuracy, with respect to chemical etching used for antenna without slots. The resonating bands of antenna are discussed considering

the -10dB power of Return loss response of individual antennas. Radiation patterns, Gain, Voltage Standing Wave Ratio(VSWR) and Axial ratio are also plotted for the all three designs.

Thus, a very good agreement between the design (simulation) and experimental results was obtained. Moreover, a comparison of the measured and predicted antenna output efficiencies, as functions of frequency at 0 dBm input power done for both the simulated and measured results. Some differences in the results for the simulation and measurements are observed.

Next section in chapter 4, deals with the rectangular radiation pattern which is measured through anechoic chamber, by obtaining half power beam widths (HPBW) for Electric and Magnetic fields. The gain and directivity are further measured from this. It is clear that amongst the gain obtained for the three antennas, prototype based on RT Duroid and with slot, has the highest gain at resonant frequency.

The last section chapter 4 deals with the response of reactance of input impedance. It also confirms the values of resonating frequencies as same as those obtained from the return loss response at 1.9GHz of the antenna with slots.

The complexity in the designing of transceivers, which are vital for communications, are drawn out clearly from the present work. With increased sophistication in personal locator boards, there is a growing need for flexible high-speed communication with the 'outside' devices. Today communication is done by wireless sets which are embedded into MICS, and are used in numerous applications. Also, the present work throws up the possibility of using the 2.45

GHz band for mobile communications. Although, this band has the drawback of being heavily used by other applications, such as wireless computer networks and in Bluetooth applications. Thus, both theoretical limits and practical designs of the relevant antennas are described and discussed in detail in this work.

CONTENTS

THESIS COMPLETION CERTIFICATE.....	i
ACKNOWLEDGMENTS	iii
EXECUTIVE SUMMARY	v
CONTENTS.....	xii
LIST OF FIGURES	xvi
LIST OF TABLES.....	xix
ACRONYMS	xx
LIST OF ABBREVIATIONS	xxii
LIST OF SYMBOLS	xxiii
CHAPTER 1	
INTRODUCTION	1
1.1 The Radio Frequency Spectrum of Mobile Antenna Applications	2
1.2 Printed Circuit Board Antennas	2
1.3 Antenna Parameters.....	5
1.4 Feeding techniques	13
1.5 Metamaterials	20

1.6 Comparison between Conventional and Metamaterial Antenna	27
1.7 Software Tool.....	28
1.8 Thesis organization	28
 CHAPTER 2	
LITERATURE REVIEW	32
2.1 The Split Ring Resonators.....	32
2.2 The Composite Right/Left-handed (CRLH) Transmission line (TL)	36
2.3 Patch in the Antenna	38
2.4 Slot Loaded Patch.....	41
2.5 Feeding the Prototype.....	41
2.6 Effect of substrate on resonant Frequency	42
2.7 Meandered Structure for Bandwidth Enhancement	45
2.8 Implementation for Mobile Handsets.....	47
2.9 Equivalence of the Circuit.....	48
2.10 Need for the Work.....	49
2.11 Objectives.....	50
2.12 Summary of the Chapter	50
 CHAPTER 3	
DESIGN and fabrication.....	52

3.1 Design Flow	52
3.2 Geometry of the Structure	54
3.3 Simulation of Design.....	59
3.4 Fabrication of designed antenna.....	63
3.5 Characterization of Prototypes.....	70
3.6 Analytical analysis of an Antenna on RT Duroid and with slot.....	72
3.7 Summary of the Chapter	77
 CHAPTER 4	
RESULTS AND DISCUSSIONS.....	80
4.1. Antenna on FR4 Substrate	81
4.2 Antenna on RT Duroid and without slot.....	85
4.3 Antenna on RT Duroid and with slot	89
4.4 Comparison of Tested Return loss of three Antennas.....	93
4.5 Gain measurement.....	95
4.6 Input Impedance of Antenna on RT Duroid and with slot.....	101
4.7 Summary of the Chapter	102
 CHAPTER 5	
CONCLUSIONS.....	104

CHAPTER 6

FUTURE SCOPE..... 106

REFERENCES 108

APPENDIX 1..... 123

APPENDIX 2..... 124

APPENDIX 3..... 125

FREQUENCY CALCULATIONS..... 125

LIST OF FIGURES

Fig 1.1 Radiated field from antenna	5
Fig 1. 2 Radiation Lobes representation	8
Fig 1. 3 Beam Angle Representation	10
Fig 1. 4 Coaxial feed.....	14
Fig 1. 5 Quarter wave length line TL feed.....	15
Fig 1. 6 Capacitive Feed	16
Fig 1. 7 Inset feed.....	17
Fig 1. 8 Feeding through slot	17
Fig 1. 9 Antennas fed by coupling	18
Fig 1. 10 Edge Feeding	19
Fig 1. 11 Classification of Metamaterials	21
Fig 1. 12 Split Ring Resonator with wire on back of substrate	24
Fig 1. 13 CRLH T/L with lumped elements	25
Fig 1. 14 CRLH Realization	26
Fig 3. 1 Flow chart of antenna design.....	53
Fig 3. 2 Front and Rear Views of Antenna on FR4	54
Fig 3. 3 Front and back views of Antenna on RT Duroid and without Slot	57
Fig 3. 4 Front and back views of Antenna on RT Duroid and with Slot	59
Fig 3. 5 Over all view of antenna.....	60
Fig 3. 6 Simulated Structure of Antenna on FR4 substrate	61
Fig 3. 7 Simulated Structure of Antenna without slots.....	62

Fig 3. 8 Simulated Structure of Antenna on RT Duroid and with Slot.....	62
Fig 3. 9 Art Work Film maker	64
Fig 3. 10 Developer.....	64
Fig 3. 11 UV Light Exposure	65
Fig 3. 12 PCB Etching	65
Fig 3. 13 Fabricated Antenna on FR4.....	67
Fig 3. 14Fabricated Antenna on RT Duroid and without slot.....	68
Fig 3. 15 Fabricated Antenna on RT Duroid and with slot.....	69
Fig 3. 16 Circuit equivalent of Antenna.....	72
Fig 3. 17 Over all Equivalent Circuit.....	73
Fig 4. 1 Return loss for Antenna on FR4	81
Fig 4. 2 Radiation Pattern for Antenna on FR4	82
Fig 4. 3 Gain for Antenna on FR4	83
Fig 4. 4 VSWR for Antenna on FR4.....	84
Fig 4. 5 Axial Ratio for Antenna on FR4.....	84
Fig 4. 6 Return loss of Antenna on RT Duroid and without slot	85
Fig 4. 7 Radiation Patterns of Antenna on RT Duroid and without slot.....	87
Fig 4. 8 Gain of Antenna on RT Duroid and without slot	87
Fig 4. 9 VSWR of Antenna on RT Duroid and without slot.....	88
Fig 4. 10 Axial Ratio of Antenna on RT Duroid and without slot.....	88
Fig 4. 11 Return loss of Antenna on RT Duroid and with slot	89
Fig 4. 12 Radiation Pattern of Antenna on RT Duroid and with slot	91
Fig 4. 13 Gain of Antenna on RT Duroid and with slot	92

Fig 4. 14 VSWR of Antenna on RT Duroid and with slot.....	92
Fig 4. 15 Axial Ratio of Antenna on RT Duroid and with slot.....	93
Fig 4. 16 Tested Return loss for three Prototypes.....	94
Fig 4. 17 E Plane of Antenna on FR4	96
Fig 4. 18 H Plane of Antenna on FR4.....	96
Fig 4. 19 E Plane of Antenna on RT Duroid and without slot.....	97
Fig 4. 20 H Plane of Antenna on RT Duroid and without slot	98
Fig 4. 21 E Plane of Antenna on RT Duroid and with slot.....	99
Fig 4. 22 H Plane of Antenna on RT Duroid and with slot	100
Fig 4. 23 Input Impedance of the Antenna on RT Duroid with slot	101

LIST OF TABLES

Table 1. 1 Feeding Techniques	20
Table 4. 1BW of Antenna based on FR4	81
Table 4. 2 BW of Antenna based on RT Duroid and without slot.....	86
Table 4. 3 BW of Antenna Antenna based on RT Duroid and with slot	90
Table 4. 4 Comparison of Return loss of Three Prototypes.....	94
Table 4. 5 Directivity	100

ACRONYMS

AR	Antenna Ranges
AUT	Antenna Under Test
CRLH	Composite Right/Left
ACMPA	Aperture-coupled microstrip patch antenna
DCS	Digital communication system
DCS1800	Digital communication system at 1800 MHz
EGSM	European Digital Extended Group Special Mobile
FBW	Fractional bandwidth
FICA	Folded Inverted Conformal Antenna (FICA)
FDTD	Finite difference time domain
FR4	Flame Redundant
FSS	Frequency-selective surface
GPS	Global Positioning System
GSM	Global System for Mobile Communication
GPS	Global Positioning System/Satellite
GSM-900	Group Speciale Mobile (European GSM)
HFSS	High frequency structure simulator
HGA	High gain antenna
HPBW	Half Power Beam Width
HIPERLAN	High performance local area network

IMDN	Intelligent Mobile Data Network
LAN	Local area network
IF	Intermediate frequency
ISM	Industrial, scientific and medical (frequency bands)
PCB	Printed Circuit Board
PCN	Personal communications network
PCS	Personal communication service
PIFA	Printed Inverted F Antenna
PMA	Proximity feed microstrip antenna
RF	Radio frequency
RFID	Radio frequency identification
RT DUROID	ROGERS Technology Duroid
SHF	Super high frequency
SNA	Scalar Network Analyzer
SRR	Split Ring Resonator
UWB	ultra-wideband
VANA	Vector automatic network analyzer
VNA	Vector network analyzer
WAN	Wide area network
WLAN	Wireless local area network
WIMAX	World Wide Interoperability for Microwave Access
WIBRO	Wireless Broadband
WI FI	Wireless Fidelity

LIST OF ABBREVIATIONS

cm	Centimeter
μm	Micrometer
dB	decibel
dbm	decibel milliwatt
dB _i	decibel isotropic
Hz	Hertz
Km	Kilometer
Fig	Figure
KHz	Kilo Hertz
MHz	Mega Hertz
nm	Nanometer
W	watts

LIST OF SYMBOLS

Ω	Resistance
β	Phase Constant
ε	Permittivity
μ	Permeability
Γ	Reflection Coefficient
γ	Propagation Constant
δ	Shift
λ	Wavelength
f_H	Upper Frequency of Band
f_L	Lower Frequency of Band
P_i	input power
P_r	radiated power
R_x	Receiver
T_x	Transmitter
D	Directivity

CHAPTER 1

INTRODUCTION

“Use a poor antenna and you're simply not going to get your call through.”

An antenna is a device for transmitting and/or receiving signals, like the eyes and ears of a communication system. It is an important part of any wireless communication system as it converts the electronic signals, propagating in the (RF) Trans-receiver, into Electromagnetic Waves, which propagate in free space, efficiently with minimum loss. Thus, Antennas replace expensive cables and are used for difficult and rugged terrains, e.g. mountainous regions and for communication with mobile objects like the airplanes and missiles etc. A good antenna is designed to be "in-tune" with the signal it is seeking for a phone or a radio, and a clear conversation is obtained when the antenna is properly matched. To understand better the concept of antenna it is required to understand the behavior of Electromagnetic waves in free space.

The current chapter of this work describes the parameters of an antenna, the role of ‘metamaterials’ in antennas, the different feeding techniques used in antennas, and discusses a printed planar antenna, along with the selection of substrate to work in mobile communications frequency range. This chapter also introduces the software tool used to design an antenna and the methods of determination of gain and directivity suitable for a prototype.

1.1 The Radio Frequency Spectrum of Mobile Antenna Applications

The mobile communications use a part of radio frequency band for their signal transmissions. The Ultra High Frequency band (UHF), ranging from 0.3–3GHz, is suitable for line-of-sight propagation (LOS) and efficient portable antennas for Television, Radar, Satellite communications, Global Positioning Satellite (GPS), Personal Communications (PCS), besides those for Wireless Local-Area networking (LAN), land-mobile and mobile phones, have been developed to work in this band. The relatively higher frequency band, Super High Frequency (SHF) band with frequencies ranging between 3–30 GHz, is also suitable for LOS propagation, Radar, microwave links, land-mobile communication, satellite communication, UWB, wireless LANs and Personal Area Networks, fixed broadband, 3G and PCS communications. All of these different communication systems use specific frequency ranges in these frequency bands, and the allocation of these ranges, also known as ‘spectrum allocation’, is done according to protocols set up by the concerned governing bodies of individual countries [1].

1.2 Printed Circuit Board Antennas

Patch Antennas (also known as a *rectangular microstrip antennas*), which consist of a flat rectangular sheet or "patch" of metal, mounted over a larger sheet of metal called a ground plane were evolved in 1970s [2]. In these antennas, the two metal sheets together form a resonant piece of microstrip transmission line,

with its length approximately one-half of wavelength of the radio waves. The radiation mechanism arises from discontinuities at each truncated edge of the microstrip transmission line. A patch antenna is usually constructed on a dielectric substrate, using the same materials and lithography processes that are used to make printed circuit boards (PCB). PCB antennas are thus microstrip radiators which are wavelength dependent, and hence, on the physical dimensions of antenna's circuit. These PCB antennas are used in a wide range of wireless communications devices.

A PCB substrate with a higher Dielectric Constant (ϵ) value enables smaller circuit features and allows for reduced antenna size for a given operational frequency. An antenna may be called upon to either transmit (radiate energy), or receive signals or both. Materials with higher ϵ values tend to radiate less than circuit materials with lower ϵ values. To maximize the amount of energy delivered to and from the antenna's resonant structure, the loss of the feed lines should be minimized, which usually suggests the use of a PCB material with low dissipation factor. Thus, while a PCB material with high ϵ can help reduce the dimensions of the antenna's resonant structure, it will also result in a reduction of the physical width of the transmission lines, and hence, to reduction in the power fed to and from the resonant structure.

The ground plane on a printed circuit board is, the large area or layer of copper foil connected to the circuit's ground point, serving the return path for current. In multilayer PCBs, ground is often a separate layer covering the entire board. In digital and RF PCBs, the major reason for using large ground planes is

to reduce noise and interference. The Planar Inverted-F antenna (PIFA), which is similar to a microstrip antenna, has its limitations; as board space becomes critical when tuning is done by varying the length of the tail. This is accomplished by slicing the antenna tail to various lengths. If the range is not an issue then, a tradeoff of board space for frequency range can be employed as in a meandering inverted-F antenna. The inverted-F and the meandering inverted-F antenna are directional antennas and orientation of the antenna on the board affects their range. They are usually employed at UHF and higher frequencies because the size of the antenna is directly tied to the wavelength at the resonant frequency. It may be noted that an advantage inherent to patch antennas is their ability to have diversity in polarization features and can be designed to have vertical, horizontal, right hand circular (RHCP) or left hand circular (LHCP) polarizations, using multiple feed points or a single feed point with asymmetric patch structures. This unique property allows patch antennas to be used in many types of communications links that may have varied requirements. Though, this is usually not a big concern for well-tuned radios that only need to operate within a relatively small space such as a living room where the radio is being employed as a remote control [3]. While the inverted-F and meandering inverted-F antennas represent the lowest cost options for antennas, they are not necessarily the best choice for time-to-market due to the need to tune them. Mobile antennas should, however, have both directional properties and miniature designs. And for this, meta-materials are important as they aid space reduction and improvement of performance like directive gain [4] [21].

1.3 Antenna Parameters

Antenna parameters are the measurable quantities which help to characterize an antenna. Out of a set of numerous such antenna parameters, Return Loss, Radiation Pattern, Input impedance and Gain have been determined for the prototype antenna discussed in the present work. These are discussed below.

1.3.1 Antenna Field Regions

The electromagnetic field of an antenna can be divided into three regions or types. These are Reactive field, Radiation near-field and Radiation far –field and are shown in Fig 1.1.

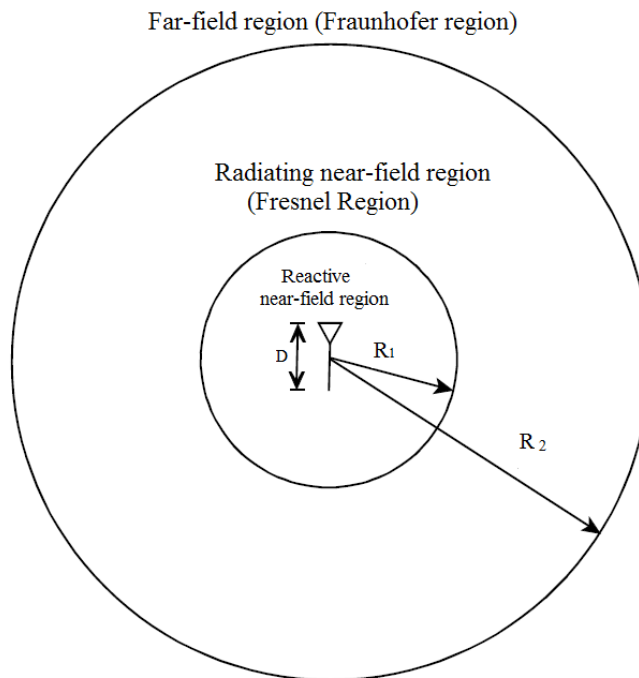


Fig 1.1 Radiated field from antenna

$$R_1 = 0.62 \frac{\sqrt{D^3}}{\sqrt{\lambda}} \dots\dots\dots 1.1$$

$$R_2 = \frac{2D^2}{\lambda} \dots\dots\dots 1.2$$

where D is maximum antenna dimension and λ is wavelength of input .

The Reactive field is the region just adjacent to the antenna and characterized by standing (stationary) waves which represent stored energy as mentioned in Eqn1.1. Radiation near field (Fresnel region) is just next to the reactive near field and bound between $R_1 \leq R \leq R_2$ as shown in Fig1.1. The far-field is region farthest away from the antenna. It is also called Fraunhofer region and is essentially independent of the distance from the antenna, referred in Eqn1.2. [5].

1.3.2 Reflection Coefficient and Return Loss

The voltage reflection coefficient is the ratio of the reflected voltage amplitude to that of the forward voltage amplitude, and is given as in Eqn 1.3 and is given by

$$\text{Voltage Reflection coefficient, } \Gamma = \frac{V^-}{V^+} = \frac{Z_L - Z_0}{Z_L + Z_0} \dots\dots\dots 1.3$$

The reflection coefficient is usually denoted by the symbol gamma [7]. The magnitude of the reflection coefficient does not depend on the length of the line, but only on the load impedance Z_L and the impedance of the transmission line, Z_0 . It is to be noted that if $Z_L=Z_0$, then the line is said to be "matched" where Z_L, Z_0 are load and characteristic impedances respectively. Mismatched impedances will lead to most of the power reflected away from the load. This can be measured

through a Vector Network Analyzer. This reflection loss is also measured in terms of return loss which is expressed in dB value of absolute reflection coefficient and given by the relation,

$$\text{Return Loss, } S_{11} = \frac{1}{1-\Gamma} \dots\dots\dots 1.4$$

1.3.2.1 Measurement through Vector Network Analyzer (VNA)

The most common equipment used in RF design laboratories is RF network analyzer. The RF network analyzer is used for characterizing or measuring the response of devices at RF or even at microwave and mm wave frequencies. By measuring the response of a device or network using an RF network analyzer, it is possible to characterize it and in this way understand how it works within the RF circuit for which it is intended. It is possible to use RF network analyzers for measuring a variety of components ranging from filters and frequency sensitive networks, to devices such as transistors, mixers and any RF orientated device. The vector network analyzer, VNA is a more useful form of RF network analyzer than the Scalar Network Analyzer (SNA) as it is able to measure more parameters about the device under test. Not only does it measure the amplitude response, but it also looks at the phase as well. As a result vector network analyzer, VNA may also be called a gain-phase meter or an Automatic Network Analyzer. The measurement of Return loss is discussed for the test antenna in the section 4.1.

1.3.3. Radiation patterns

Radiation Pattern of an antenna is a graphical representation of the antenna radiation properties as a function of position (spherical coordinates). Power/ Field Pattern is normalized power/ E or H Vs. spherical coordinate position. *Directional Pattern* is a pattern characterized by high intensity radiation in one direction than another. *Principal Plane Patterns* are the E-plane and H-plane patterns of a linearly polarized antenna. *E-plane* is the plane containing the electric field vector and the direction of maximum radiation. H-plane is the plane containing the magnetic field vector and the direction of maximum radiation. Main Lobe (major lobe, main beam) is the radiation lobe in the direction of maximum radiation. Side Lobe is a radiation lobe in any direction other than the direction(s) of intended radiation. Back Lobe is the radiation lobe opposite to the main lobe [6]. Radiation pattern of the test antenna is explained in Chapter 4.

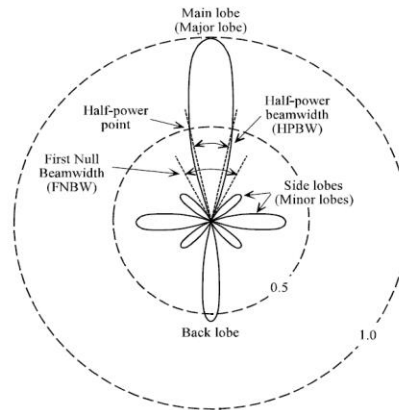


Fig 1. 2 Radiation Lobes representation

1.3.4 Voltage Standing Wave Ratio (VSWR)

To deliver maximum power to antenna, the impedance of the transmission line must be well matched to the antenna's impedance. VSWR is a measure of mismatch between transmission line and antenna reflected power. It is defined as a ratio of reflected power from antenna to incident power on it. When an antenna is not matched to the receiver, power is reflected (so that the reflection coefficient, Γ is not zero). This causes a "reflected voltage wave", which creates standing waves along the transmission line, if the reflection coefficient is given by Γ , then the VSWR is defined as

$$VSWR = \frac{1+\Gamma}{1-\Gamma} \dots\dots\dots 1.5$$

If the VSWR = 1.0, there would be no reflected power and the voltage would have a constant magnitude along the transmission line. VSWR can also be measured on the Smith Chart which is graphical representation of Γ . VSWR is only a scalar measurement, whereas the Smith Chart shows both magnitude and phase. As the VSWR increases, more power is reflected from the antenna and therefore not transmitted.

1.3.5 Axial ratio (AR)

Axial ratio by definition is the ratio of the two orthogonal components of E-field. For a circular polarized field it is one, because of two orthogonal E-field components of equal amplitude. It is interesting to look at the Axial Ratio beam width for Circularly Polarized antennas so as to understand the deviation from

circular polarization [6]. Axial ratio for an antenna under test is explained in Chapter 4.

1.3.6 Directivity and Gain

The directivity of an antenna is the ratio of the radiation intensity in a given direction to the radiation intensity averaged over all directions. Gain is defined as antenna directivity times a factor representing the radiation efficiency of an antenna, which is defined as the ratio of the radiated power (P_r) to the input power (P_i).

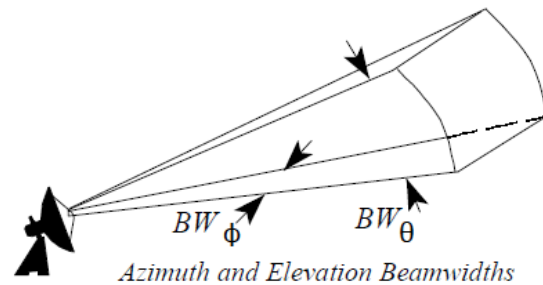


Fig 1. 3 Beam Angle Representation

The input power is transformed into radiated power and surface wave power while a small portion is dissipated due to conductor and dielectric losses of the materials used.

Half-Power Beamwidth (HPBW) is the angular width of the main beam at the half-power points. First Null Beamwidth (FNBW) is angular width between the first nulls on either side of the main beam [6]. The antenna equations mentioned in this section are related to Figure 1.3. In Figure 1.3, BW_ϕ is the

azimuthal beamwidth and BW_θ is the elevation beamwidth. Beamwidth is normally measured at the half-power or -3 dB point of the main lobe unless otherwise specified. Quite often directivity and gain are used interchangeably. The difference being that directivity neglects antenna losses such as dielectric, resistance, polarization, and reflection losses. Since these losses in most classes of antennas are usually quite small, the directivity and gain will be approximately equal. The directivity of an isotropic radiator is $D(\theta, \phi)$ is unity. The maximum directivity is defined as $[D(\theta, \phi)]_{\max}$ and denoted by D_o . The directivity range for any antenna is $0 \leq D(\theta, \phi) \leq D_o$. An antenna with one narrow major lobe and negligible radiation in its minor lobes, the maximum directivity can be approximated in terms of beam solid angle Ω_A by

$$D_o = 4\pi/\Omega_A \approx 4\pi/\theta_1\theta_2 \dots\dots\dots 1.6$$

where θ_1 and θ_2 are the half-power beam widths (in radians) which are perpendicular to each other in θ and ϕ planes. Simulated gain was presented for three antennas in this work. The gain measurement through anechoic chamber was given in detail for the prototype in the section 4.5, where beamwidths are measured in degrees and directivity is determined by Eqn 1.6. Gain can be determined by Eqn 1.7.

$$G = e_t D \dots\dots\dots 1.7$$

1.3.6.1 Gain Measurement through Anechoic Chamber

The antenna measurement sites are called antenna ranges (AR). They can be categorized as outdoor ranges and indoor ranges (anechoic chambers).

According to the principle of measurement, they can be also categorized as reflection ranges, free-space ranges, and compact ranges. Indoor ranges (anechoic chambers) suppress reflections (echoes) by lining the walls, the floor and the ceiling with special RF/Microwave absorbers. The source antenna has very low side lobes so that practically there is no energy directed toward the surface below (the ground) or the buildings behind. The line-of-sight is always clear. The slant ranges need less space than the elevated ranges. The test antenna is mounted at a fixed height on a non-conducting tower (e.g. made of fiber glass), while the source antenna is mounted near the ground. The source antenna must have its pattern null pointed toward ground. It is desirable that it has very low side lobes and narrow beamwidth. The anechoic chambers are the most popular antenna measurement sites especially in the microwave frequency range. They provide convenience and controlled EM environment. However, they are expensive to build and maintain. An anechoic chamber is typically a large room whose walls, floor and ceiling are first EM isolated by steel sheets. In effect, it is a huge Faraday cage, which provides ideal security against outer EM noise and interference. In addition, all inner surfaces of the chamber are lined with RF/microwave absorbers. A typical absorbing element has the form of a pyramid or a wedge. Pyramids are designed to absorb best the waves at normal incidence (nose-on). They do not perform well at large angles of incidence. They act, in effect, as a tapered impedance transition for normal incidence of the EM wave from the intrinsic impedance of 377Ω to the short of the chamber's wall. Their resistance gradually decreases as the pyramid's cross-section increases. The

tapered chamber has the advantage of tuning by moving the source antenna closer to (at higher frequencies) or farther from (at lower frequencies) the apex of the taper thus the reflected rays are adjusted at the test location. Measurement of far-field patterns in the compact chambers is through near-field/far-field (NF/FF) method in which field amplitude, phase and polarization are measured in the near field of the Antenna under Test (AUT), which is in radiating mode. The near-field data is transformed to far-field patterns via analytical techniques implemented in the sophisticated software run by an automated computer system, which controls the measurement procedure [8]. The magnitude and phase of the tangential electric field are measured at regular intervals over a well-defined surface: a plane or a cylinder (sphere is also a possibility) located close to the AUT. The presented prototype antenna was measured in tapered chamber and results are tabulated in chapter 4.

1.4 Feeding techniques

Microstrip patch antennas can be fed by a variety of methods. These methods can be classified into two categories as contacting and non-contacting. In the contacting method, the RF power is fed directly to the radiating patch using a connecting element such as a microstrip line. In the non-contacting scheme, electromagnetic field coupling is done to transfer power between the microstrip line and the radiating patch. The four most popular feed techniques used are the microstrip line, coaxial probe (both under contacting schemes), aperture coupling and proximity coupling (both under non-contacting schemes). Methods to feed

antenna are coaxial, microstrip feed, line feed, aperture coupling and by placing a probe-fed capacitor patch next to the patch of an antenna are studied according to the best impedance matching techniques[9]. Coplanar wave guide feeding is also extensively studied. CRLH transmission line feeding for the antenna in high frequency range applications are also studied along with conventional feeding techniques [10].

1.4.1 Coaxial Cable or Probe Feed

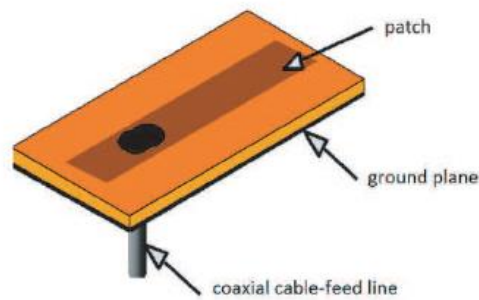


Fig 1. 4 Coaxial feed

Microstrip antennas can also be fed from underneath via a probe as shown in Figure 1.4. The outer conductor of the coaxial cable is connected to the ground plane, and the center conductor is extended up to the patch antenna. The position of the feed can be altered to control the input impedance. The coaxial feed introduces an inductance into the feed that may need to be taken into account if the height of the substrate gets large (an appreciable fraction of a wavelength). In addition, the probe will also radiate, which can lead to radiation in undesirable

directions. This increases the volume of the design ultimately causing the thickness of mobile handset and it is not implemented for the present design.

1.4.2 Fed with a Quarter-Wavelength Transmission Line

The microstrip antenna can also be matched to a transmission line of characteristic impedance Z_0 by using a quarter-wavelength transmission line of characteristic impedance Z_1 . If the impedance of the antenna is Z_A , then the input impedance viewed from the beginning of the quarter-wavelength line becomes (Z_{in}). This input impedance Z_{in} can be matched with Z_0 , by changing the width of the quarter-wavelength strip, as in Fig 1.5.

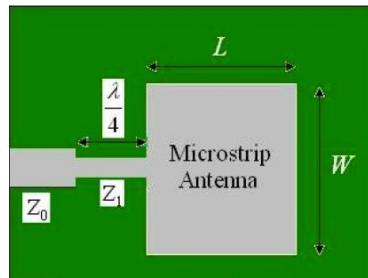


Fig 1. 5 Quarter wave length line TL feed

1.4.3 Proximity feeding

The proximity feed microstrip antenna (PMA) fed via a gap enables switching of the polarization with a simple operation of opening or shorting the end of the feed. However, since the PMA is coupled electromagnetically with the feed line printed on the same surface as the antenna, the effect of the feed line on the antenna characteristics is expected.

1.4.4 Capacitive feed

Patch antennas use feeding technique in which a capacitive patch next to patch antenna. The advantage of using this feeding technique is that the inductive impedance of the probe is effectively canceled by the capacitive patch. As a result a higher substrate (with longer probe) can be used to increase bandwidth. Figure 1.6 shows a section through the patch antenna with probe-fed capacitor patch in the $x-z$ -plane. Due to the placement of feed location point in the unsymmetrical structure is difficult.

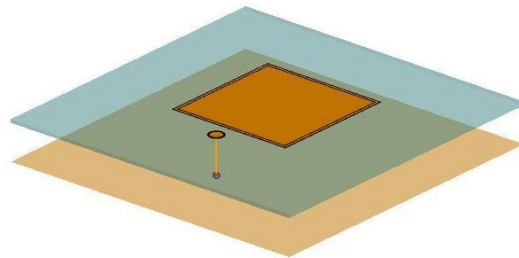


Fig 1. 6 Capacitive Feed

1.4.5 Inset Feed

Inset feed is type in which the patch antenna was fed at the end, as shown in Fig 1.7. Since this yields high input impedance and the current is low at the ends of a half-wave patch and increases in magnitude toward the center, the input impedance could be high and is not suitable for the design discussed in this work.

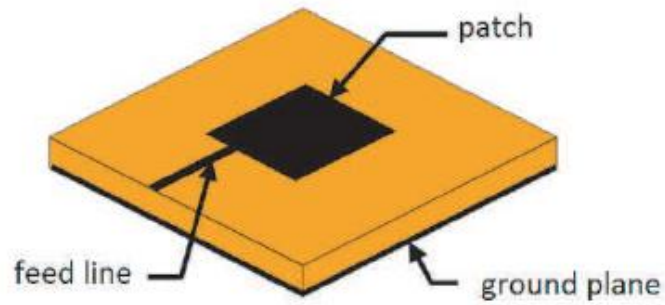


Fig 1. 7 Inset feed

1.4.6 Slot feed and feed by coupling

Antennas can also feed through the slot and by coupling [10]. These methods are suitable for double layer PCB antenna. This type of feed causes a capacitive coupling in the design.

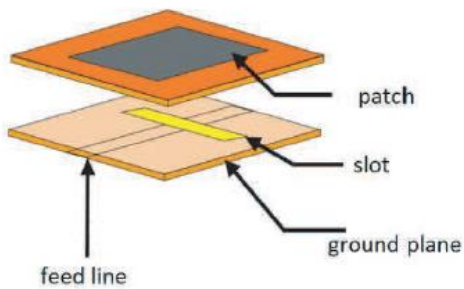


Fig 1. 8 Feeding through slot

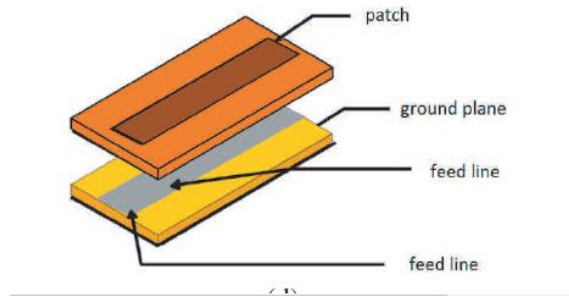


Fig 1. 9 Antennas fed by coupling

1.4.7 CPW feeding

A coplanar waveguide (CPW) is a one type of a planar transmission line structure for transmitting microwave signals. It comprises of at least one flat conductive strip of small thickness, and conductive ground plates. A CPW structure consists of a median metallic strip of deposited on the surface of a dielectric substrate slab with two narrow slits ground electrodes running adjacent and parallel to the strip on the same surface. Beside the microstrip line, the CPW is the most frequent use as planar transmission line in RF/microwave integrated circuits. It can be regarded as two coupled slot lines. Therefore, similar properties of a slot line may be expected. The CPW consists of three conductors with the exterior ones used as ground plates. These need not necessarily have same potential. When the substrate is metallized on its bottom side, an additional parasitic parallel plate is formed [11][12]. This method is not suitable for the antenna of size 40 mm x 1.4 mm.

1.4.8 Edge feeding

This scheme of edge feeding is shown in Fig 1.10. It is composed of a plurality of microstrip transmission line sections, periodically transposed at each junction with a period of d . The microstrip transmission line in this structure consists of two strip conductors of different widths, which are used to feed a patch printed on a dielectric material of permittivity ϵ_r and thickness h . These microstrip transmission line sections have the same characteristic impedance. Since the two microstrip transmission line sections are present, with the same dimensions, the small difference can be neglected in practice, so that the length of the structure can have equal width. A transposed microstrip line section can be considered as a junction between a microstrip line and a converted microstrip line. The discontinuity in dimensions, is usually much smaller than the wavelength in the microstrip and it can be modeled by lumped element T-equivalent. The equivalent circuit model is a periodically transposed microstrip lines [13]. For the presented second and third prototypes, edge feeding is selected due to the convenience to feed from one side of the antenna and to reduce volume.

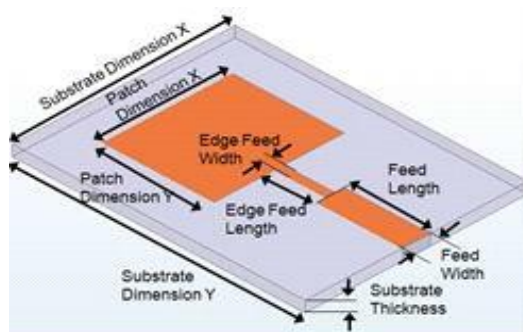


Fig 1. 10 Edge Feeding

Table 1.1 gives the summary of the different feeding techniques and the feed compatibility for the prototypes discussed in Chapter 3.

Table 1.1 Feeding Techniques

S. No	Technique	Compatibility
1	Coaxial feed	Used for one antenna with substrate FR4
2	Quarter wave TL	Not suitable
3	Proximity feed Yielded	poor Return loss
4	Capacitive	Not used
5	Inset feed	Not used
6	Slot feed	Structure is not double layer
7	CPW	Not suitable for geometry
8	Edge	Incorporated in the antenna with RT Duroid in this work, for volume reduction

1.5 Metamaterials

Metamaterials are artificial materials engineered to provide properties which “may not be readily available in nature”. These materials usually gain their properties from structure rather than composition, using the inclusion of small inhomogeneities to enact effective macroscopic behavior. The metamaterials have now entered into the main stream of electromagnetics [14][15]. The essential property in metamaterials is their unusual and desired qualities that appear due to

their particular design & structure. In particular composite media electromagnetic waves interact with the inclusions which produce electric & magnetic moments, which in turn affect the macroscopic effective permittivity & permeability of the bulk composite medium. Since metamaterials can be synthesized by embedding artificially fabricated inclusions in a specified host medium, they provide the designer with a large collection of independent parameters such as properties of

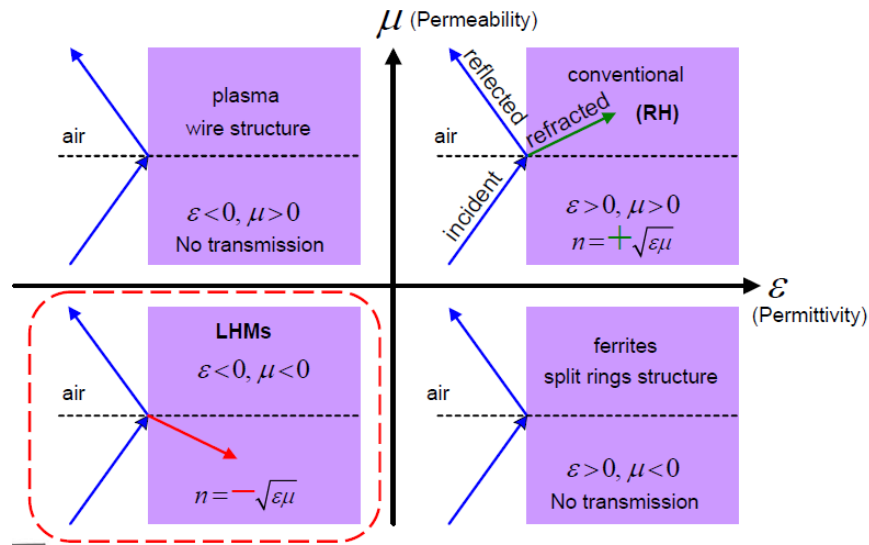


Fig 1. 11 Classification of Metamaterials

host materials, size, shape, and compositions of inclusions. All these design parameters can play a major role in getting the final result. In these the shape of the inclusions is one that provides a new possibility for metamaterial processing. The response of a system to the presence of Electromagnetic field is determined by the properties of the materials involved. These properties are described by defining the macroscopic parameters permittivity ϵ and permeability μ of these materials. By using permittivity ϵ and permeability μ the classification of metamaterials as follows, the medium classification can be graphically illustrated

as shown in Fig1.11. A medium with both permittivity & permeability greater than zero ($\epsilon > 0, \mu > 0$) are called as double positive (DPS) medium. Most occurring media (e.g. dielectrics) fall under this designation. A medium with permittivity less than zero & permeability greater than zero ($\epsilon < 0, \mu > 0$) are called as Epsilon negative (ENG) medium. In certain frequency regimes many plasmas exhibit this characteristics. A medium with both permittivity greater than zero & permeability less than zero ($\epsilon > 0, \mu < 0$) are called as Mu negative (MNG) medium. In certain frequency regimes some gyrotropic material exhibits this characteristic. A medium with both permittivity & permeability less than zero ($\epsilon < 0, \mu < 0$) are called as Double negative (DNG) medium[43] [59]. This class of materials has only been demonstrated with artificial constructs.

1.5.1 Metamaterials in Electromagnetism

In 1898, Jagadish Chandra Bose conducted the first microwave experiment on twisted structures, which are known as artificial chiral media[14]. Karl F. Lindman, studied artificial chiral media, a collection of randomly oriented spirals are called *metamaterials* [16]-[18]. In electromagnetic domain, a negative value for permittivity and permeability occurring simultaneously to produce the metamaterial [19]. These metamaterials have: (i) The index of refraction of a medium is negative. (ii)The field vectors E, H and the direction of phase propagation would form a left-handed triplet. (iii) Evanescent waves would increase as they propagate through a medium. (iv)The phase would advance lossless in a medium.

In 1967, Victor Veselago, presented a theoretical material that could produce extraordinary effects artificially by use of periodic structures with special elements that are difficult or impossible to produce in nature [19]- [21]. Hence, in electromagnetic domain, a negative value for permittivity and permeability occurring simultaneously was a requirement to produce the first metamaterials. Metamaterials are able to guide and control light on all scales, including the scale of nanometers, or billionths of a meter. Unlike natural materials, metamaterials are able to reduce the index of refraction less than one or less than zero. Natural materials typically have refractive indices greater than one. Metamaterials, however, can make the index of refraction vary from zero to one, which possibly will enable applications including the hyperlens [18]. The history of metamaterials is essentially a history of developing certain types of manufactured materials, which interact at radio frequency, microwave and optical frequencies. Andryieuski et al. explained that how the bulk metamaterials design, exhibiting a negative index in the near infrared region [30]. Negative index of refraction, is a principle for invisibility cloaking and metamaterial microwave lenses for miniature wireless system antennas. These antennas are more efficient than conventional and Sub wavelength focusing with the super lens.

1.5.2 Metamaterials in Antennas

Metamaterials are a basis for further miniaturization of microwave antennas, with efficient power and acceptable bandwidth. Novel antennas employing metamaterials offer the possibility of overcoming restrictive

efficiency-bandwidth limitations for conventionally constructed, miniature antennas [22][23]. Metamaterials permit smaller antenna elements that cover a wider frequency range, thus making better use of available space for small platforms or space [24]. Some applications for metamaterial antennas are wireless communication, space communications, GPS, satellites, space vehicle navigation, and airplanes [25]. In these instances, miniature antennas [26]-[28] with high gain are significantly relevant because the radiating elements are combined into large antenna arrays for these functions, and vehicles. Conventional microstrip antennas have a conducting patch printed on a grounded dielectric substrate and operate as resonant cavity elements. This operation leads inherently to narrow impedance bandwidth which is a barrier for microstrip antennas applications in wireless communications. There has been a growing interest for the design of one-, two-, and three-dimensional artificial structures (also called metamaterials). Among them, special attention has been devoted to double-negative media [59]. These are artificial periodic structures composed of sub-wavelength constituent elements

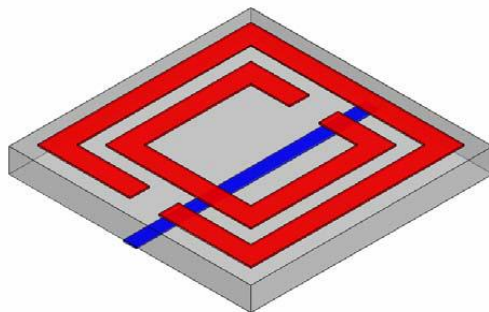


Fig 1. 12 Split Ring Resonator with wire on back of substrate

that make the structure behave as an effective medium with negative values of permittivity (ϵ) and permeability (μ) at the frequencies of interest. The properties of such media were already studied by Veselago[19]. A design of SRR for which a negative permittivity and a negative permeability do overlap in a wide frequency range. This is achieved by properly tuning the geometry of the rings into an S-type structure associated with an inverted image. The theoretical analysis, the numerical simulations and the experimental results confirm the left-handed property of the metamaterial. Negative values of ϵ and μ , along with the wave vector form a left-handed triplet, which results, antiparallel phase and group velocities, or backward-wave propagation. Due to left-handedness, exotic electromagnetic properties are expected for left-handed metamaterials (LHMs); namely, inversion of the Snell law, inversion of the Doppler effect and amplification of evanescent waves.

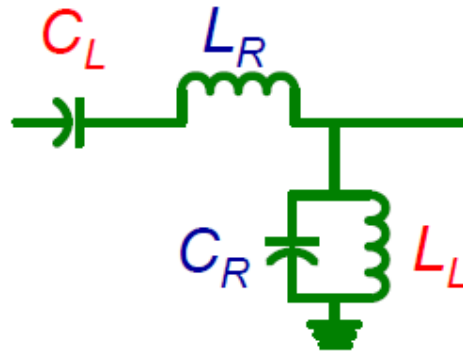


Fig 1. 13 CRLH T/L with lumped elements

This configuration is the dual circuit of the conventional transmission line, which contains cells constituted by a series right-handed (RH) inductance L_R and a shunt

RH capacitance C_R . The transmission-line (CRLH-TL) metamaterials is suitable for RF and microwave applications, exhibiting forward, backward possessing high radiation efficiencies, a compact size[25][27].

Several composite structures that emulate mediums with simultaneously negative permittivity and permeability (left-handed materials which are not readily available in nature) have been presented with high losses and narrow bandwidth. Left-handed (LH) artificial transmission lines partially overcome this problem because they are not of resonant type, so losses are smaller and hence the operating frequency band is wider. This type of artificial line is suitable for different microwave applications, such as couplers, delay lines, resonators, leaky-

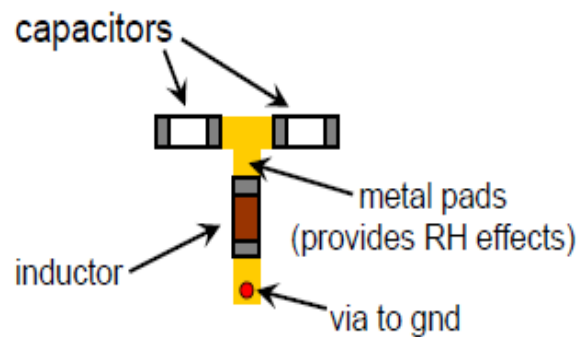


Fig 1. 14 CRLH Realization

wave antennas and dual-band components. A left-handed transmission line can be simulated by cascading cells constituted by two LH elements: a series capacitance C_L and a shunt inductance L_L . This configuration is the dual circuit of the conventional transmission line, which contains cells constituted by a series right-

handed (RH) inductance L_R and a shunt RH capacitance C_R . However, a pure LH line cannot exist due to the inherent right-handed effects of the physical LH elements which lead to a combined behaviour, the so-called composite right/left-handed transmission line (CRLH TL). The equivalent circuits of an asymmetric and a π -symmetric CRLH unit cell. For a balanced cell, the series ω_{se} and shunt ω_{sh} resonances are equal to the transition frequency ω_o .

1.6 Comparison between Conventional and Metamaterial Antenna

Metamaterial antennas are a class of antennas which use metamaterials to increase performance of miniaturized (electrically small) antenna systems. Their purpose, as with any electromagnetic antenna, is to launch energy into free space. However, these incorporate metamaterials, which are materials engineered with novel, often microscopic, structures to produce unusual physical properties. Antenna designs incorporating metamaterials can step-up the radiated power of an antenna. The newest metamaterial antennas radiate as much as 95 percent of an input radio signal. Standard antennas need to be at least half the size of the signal wavelength to operate efficiently [29]. At 300 MHz, for instance, an antenna would need to be half a meter long, in contrast, the experimental antennas are as small as one-fiftieth of a wavelength, and could have further decreases in size. With conventional antennas that are very small compared to the wavelength, most of the signal is reflected back to the source. The metamaterial, on the other hand, makes the antenna to behave as if it were much larger than it really is, because the novel antenna structure stores energy and re-radiates it. These novel antennas

appear to be useful for wireless systems that continue to decrease in size [31], such as emergency communications devices, micro-sensors and portable ground-penetrating radars to search for tunnels, caverns and other geophysical features.

1.7 Software Tool

Ansoft's Advanced HFSS Antenna Class is designed to build an understanding of HFSS's solution process and use this foundation to describe more advanced topics. Antenna design will be done on the advantage of various seeding operations and understand where they can be most effectively used. Various model creation rules of thumb are explored to highlight effective simulation setup techniques. HFSS's post-processing capabilities will be discussed as well, including use of the Field Calculator, displaying field results. The simulation software supports planar antennas like microstrip lines, with user specified dielectric, and conductive layers. Finally, more advanced simulation techniques are explored to improve simulation time and efficiency [32].

1.8 Thesis organization

In this dissertation, metamaterial structures are implemented with split ring resonators and CRLH transmission lines on PCB for wider frequency resonance. In which a representative of the general class of metamaterial antennas, are studied, and some of the unique phenomena observed with these structures are explored.

Chapter 1 provides a brief introduction of the Radio Frequency Spectrum of mobile Antennas, Planar Antennas and its importance. PCB Antennas, Parameters and main objective of feeding techniques to the planar antenna are explained. Lastly, Software Tool used and organization of the thesis.

Chapter 2, gives detailed road way for literature of SRRs CRLH and planar antennas which are used in wireless applications and mobile applications. Frequency bands of different mobile ranges were studied. Also, different approaches of fabricating the metamaterial implementation are described. The selection of substrate with low loss tangent for better performance, appropriate feeding technique according the mobile handset designs and various parameters of design behavior are explored, and the role of frequency resonance in the negative index of ϵ and μ are investigated. In the design process, a set of different substrates are simulated for prototype, and with help of the response, best selected substrate was substrate for wider bandwidth of the designed antenna. Additionally, new ways of improving the bandwidth of antenna by design parameters were also tried.

Chapter 3 describes simulation of prototype antenna using HFSS, to determine gain, axial ratio, polarization, directivity, radiation pattern, electric field distribution and current distribution. Characterization of metamaterial antenna is done using plane wave excitation. The first part involves investigations of various parameters related to the measurement. Since PCB antennas were studied, with nearby members resulted in near-field coupling effect of geometric arrangement on antenna response are described. All the planar PCB antennas characterization

involved in patterning using chemical etching of PCB antenna and details of the design, fabrication, and possible modifications are discussed, besides maintaining accuracy of chemical etching. In the later part, antenna design with feasible structure embedded in mobile handsets or smart transceiver systems WiFi systems and revolutionary aspects are studied and are implemented according to the need of the present design. Fabrication techniques of the antenna are studied and the feasible fabrication structure is implemented in the present design. The effects of gap size and antenna loading were also investigated. Connector of the 50 ohm resistance is used to excite the antenna and the connectors don't have other ohmic losses. This chapter also discusses equivalent circuit of CRLH, Split Ring Resonator and Patch and Slot. The Reactance of antenna circuit equivalent is derived and the response of the circuit is observed in frequency range and it was observed these are matching with simulation results of HFSS.

Chapter 4 discusses characterization an antenna measurement in terms of return loss/reflection coefficient through vector network analyzer, gain, VSWR axial ratio. Radiation plot is measured using anechoic chamber to derive half power beam widths. The standard horn antenna is used as reference antenna to measure the gain and directivity, antenna can excite completely different modes depending on its position, is identified for gain measurement through anechoic chamber.

Finally, Chapter 5 summarizes the findings and discusses the future outlook for metamaterial antennas. The bandwidth of various generations like 1G, 2G etc., of mobile network bands. Design and characterization of future antennas.

Field of Resonators has immense potential and several new products involving antennas are expected to evolve in the very near future. In light of this progress, possible directions and approaches for this ever growing field of antennas are highlighted.

CHAPTER 2

LITERATURE REVIEW

In this chapter, the literature for improving the bandwidth of antenna by design parameters like negative value of μ and ϵ of SRRs, CRLH and of planar antennas which are used in wireless applications and mobile applications is presented. The selection of substrate and feeding technique suiting the mobile handset designs are explored. Different approaches of fabricating the metamaterial implementations are described. PCB antennas details of the design, fabrication, and possible modifications are discussed

2.1 The Split Ring Resonators

Use of Electromagnetic metamaterials for antennas is one of the most important applications, Split-ring resonator (SRR), remains the popular choice since last decades. Chun Chun et al. reported that inclusion of SRR in PCB based low frequency antenna is able to miniaturize the antenna size. They have fabricated and characterized the low profile antenna with SRRs etched on the surface. [33].

Baena et al.[34] reported that the a new approach for the development of planar metamaterial structures with split-ring resonators(SRRs) and complementary split-ring resonators(CSRRs) coupled to planar transmission lines. Analytical equivalent-circuit models, stopband/passband characteristics of the

analyzed SRR/CSRR loaded transmission lines are derived which are suitable for the design of compact microwave devices.

Yuandan Dongh et al. [47] fabricated and presented the miniaturized patch antennas loaded with complementary split-ring resonators (CSRRs) and reactive impedance surface (RIS). The CSRR is incorporated on the patch to excite the antenna and the RIS is inserted below the patch to miniaturize the antenna size $0.099 \lambda_0 \times 0.153 \lambda_0 \times 0.024 \lambda_0$ and to improve the antenna radiation at 2.4 GHz. Then, a dual-band antenna with orthogonal polarization is developed by simply adjusting the feeding position in order to excite the initial patch resonance.

S. S. Karthikey et al. [48] presented a compact, wide fractional bandwidth band pass filter using a defected ground structure with compact microstrip resonating cell (CMRC). The band pass filter (BPF) is constructed by cascading low pass and high pass sections designed using CMRCs and OSSRR respectively.

Montero et al. [50] designed an novel square microstrip patch antenna loaded with split ring resonators (SRRs) for multi-frequency wireless communications systems like mobile communications (GSM, UMTS), wireless sensor (Zig Bee), personal area (Bluetooth) or wireless (WiFi) networks and radio navigation systems (GPS, Galileo).

Han et al. [52] fabricated the microstrip antenna with the combination of the Square Rectangular Split Ring and the Thin Wire Structure on an FR-4 by wet etching technique. The antenna is based on the focusing effect of the Left Handed metamaterials, which enhanced the gain and contributed to the betterment of the matching.

Wenquan Cao et al. [58] proved bowtie dipole elements loaded by split-ring resonator (SRR) has high gain compared to antenna using a parallel strip line (PSL) feed. These antennas radiate in the end-fire direction. The SRR-loaded antenna presents gain of about 6.2~9.9 dB in wireless communication frequency range.

Wook et al. [61] proposed a frequency-tunable waveguide antenna with a size-reduced aperture which they have achieved by adjusting the capacitance of the gap of a split-ring resonator. Comparison between measuring parameters of a capacitor-loaded split-ring resonator and a varactor-loaded split-ring resonator shows widening of bandwidth and 70% aperture reduction.

Alici et al. [62] demonstrated experimentally, an electrically small resonant antenna composed of split ring resonators (SRR) and monopoles. They have shown that resonance frequency depends on the geometry of the SRRs. They observed that an antenna with size $0.095\lambda_0 \times 0.100\lambda_0$ operates at 3.62 GHz and if the size is reduced to $0.074\lambda_0 \times 0.079\lambda_0$ frequency shift has occurred.

Sidana et al. [63] proposed a novel dual-band hexagonal patch antenna coupled with complementary split ring resonator (CSRR) etched at ground plane (underneath the hexagonal patch). It exhibits -10 dB bandwidth of 154 MHz from 3.203 GHz-3.357 GHz and bandwidth of 180 MHz from 5.140 GHz-5.320 GHz for first and second band respectively. The average gain at the two bands is 6.70 dB and 5.42 dB.

Kim et al. [64] presented a miniaturized planar antenna based on a broadside-coupled split ring resonator excited by an arc-shaped dipole. The

excitation dipole in their design, acts as a small tuning capacitor in series with a parallel RLC circuit represented by the SRR. The antenna resonance frequency and dimensions are essentially determined by the SRR, while by varying the dipole arm length the input resistance is changed in a wide range, thus matching the antenna to a feed line. This tuning technique is especially useful in practical applications wireless communications.

Gupta et al. [65] demonstrated a method to reduce the size of patch antennas by loading them with complementary split ring resonators (CSRRs) for linearly polarized radiators. This paper also demonstrates that the design can be extended for circularly polarized radiation by employing multiple CSRRs under the patch to generate a 900 rotationally symmetric antenna structure. It is also shown that, in this antenna configuration, the radiation efficiency becomes strongly dependent on the size of the ground plane that carries the CSRR metallization. To further miniaturize the antenna size without affecting its radiation efficiency, a new antenna structure was developed in which the CSRRs are formed within a truncated ground plane loaded with vertical inductive pins. The antenna operates at 2.24GHz with peak broadside realized RHCP gain of 3dB, corresponding to 75% radiation efficiency.

Mirza et al.[66] demonstrated that the miniaturization of a loop antenna through simulation and experiment using synthetic reactive elements, namely split ring resonators (SRRs), embedded in and out of the plane of the substrate of the antenna. Results show that antenna size can be reduced up to thirty eight percent for both designs.

2.2 The Composite Right/Left-handed (CRLH) Transmission line (TL)

Left-handed (LH) artificial transmission lines offer the wide operating frequency band, but a pure LH line [44] cannot exist due to the inherent right-handed effects of the physical LH elements which lead to a combined behaviour, so-called composite right/left-handed transmission line (CRLH TL). For a balanced cell, the series and parallel resonances are equal and resonates at single frequency. A left-handed transmission line can be simulated by cascading cells constituted by two LH elements: a series capacitance C_L and a shunt inductance L_L . This configuration is the dual circuit of the conventional transmission line, which contains cells constituted by a series right-handed (RH) inductance L_R and a shunt RH capacitance C_R . The transmission-line (CRLH-TL) approach of metamaterials is useful for microwave applications, such as couplers, delay lines, resonators, leaky-wave antennas and dual-band components. Furthermore, CRLH-TL maintains high radiation efficiencies, a compact size and a low profile, offering multi-band antenna which makes it amenable for integration onto small handheld devices. The resonant behaviour of the antenna can be adjusted by appropriately designing transmission line cells. Furthermore, the transmission-line and loading parameters of a unit cell can be used to independently tune the bands of the antenna.

Sanada et al. [40] presented composite right/left-handed (CRLH) transmission line (TL) as a general TL possessing both left-handed(LH) and right-handed(RH) natures. It is shown analytically that when the CRLH TL is

“balanced” two eigen frequencies at the Γ point ($\beta = 0$) of the Brillouin zone (BZ) degenerate at β_{Γ} and a seamless transition from the LH to the RH modes without a bandgap can be achieved. These phenomena are demonstrated experimentally in the case of CRLH microstripline for zeroth-order resonators, backward/forward leaky-wave antennas.

Yang et al. [41] presented that the composite right/left-handed (CRLH) transmission line (TL) based leaky-wave antennas (LWAs) with a substrate integrated waveguide (SIW) CRLH cell structure with dispersion sensitivity. This advantage makes the structure have a narrower fast wave region and thus have a potential application to the LWA with a large beam scanning range (BSR)/bandwidth ratio. The CRLH cell can be applied to the LWA for achieving large BSR/bandwidth ratio.

Sanchez Martinez et al. [42] presented a novel artificial transmission line with right/left-handed behavior in which the unit cell of the new artificial line consists of one series and one shunt wire bonded interdigital capacitors to achieve both capacitive and inductive behavior. It is a balanced structure, having a smooth, continuous transition from left-handed to right-handed propagation regions, wider frequency band of operation. It is important to mention that, when used in planar integrated circuits, to bias the circuits.

Yu et al. [67] have proposed a dual band antenna, based on the concept of composite right and lefthanded (CRLH) metamaterials. The same phase constants and current distributions on the ring antenna were achieved at two frequency bands having similar radiation patterns at both bands. The circular polarisation is

implemented by feeding two vertical ports from power dividers that provide equal magnitudes and quadrature phase excitations.

Chen et al. [70] proposed a homogeneous composite right/left-handed transmission lines (CRLH-TL) equivalent circuit model, an symmetric unit cell model for CRLH-TL metamaterials having left-handedness (LH), right-handedness (RH) at different frequencies. The CRLH TL unit model is a meta-structured TL composed of a series capacitance and a shunt inductance as well as a series inductance and a shunt capacitance. The series capacitance and the shunt inductance provide the LH nature at lower frequencies, whereas the series inductance and the shunt capacitance provide the RH nature at higher frequencies, unique characteristic of CRLH-TL. They have calculated the S-parameter analyzed for a unit cell at a desired center frequency.

2.3 Patch in the Antenna

A patch antenna is usually fabricated by etching the antenna element pattern in metal trace bonded to an insulating dielectric substrate. It is a printed circuit board antenna, with a continuous metal layer bonded to the opposite side of the substrate which forms a ground plane. Common microstrip antenna shapes are square, rectangular, circular and elliptical, but any continuous shape is possible. It offers a wide-beam but narrow band.

MUTIARA et al. [49] presented a fabricated planar, small and low cost broadband microstrip rectangular patch antenna for wireless communication. This rectangular microstrip patch antenna is designed as client antenna in computer for

wireless communication application that works at 2.4 GHz for outdoor place. It also has a wide angle of beam in its radiation pattern.

Some patch antennas do not use a dielectric substrate and instead made of a metal patch mounted above a ground plane using dielectric spacers; the resulting structure is less rugged but has a wider bandwidth. Because such antennas have a very low profile, and mechanically rugged, they can be shaped to conform to the curving skin of a vehicle. They are often mounted on the exterior of aircraft and spacecraft, or are incorporated into mobile radio communications devices. The most commonly employed patch antenna is a rectangular patch which is approximately a one-half wavelength long section of rectangular microstrip transmission line. When air is the antenna substrate, the length of the rectangular microstrip antenna is approximately one-half of a free-space wavelength. As the antenna is loaded with a dielectric as its substrate, the length of the antenna decreases as the relative dielectric constant of the substrate increases. The resonant length of the antenna is slightly shorter because of the "fringing fields" which increase the electrical length of the antenna slightly. An early model of the microstrip antenna uses a section of microstrip transmission line with equivalent loads on either end to represent the radiation loss. The dielectric loading of a microstrip antenna affects both its radiation pattern and impedance bandwidth. As the dielectric constant of the substrate increases, the antenna bandwidth decreases which increases the Q factor of the antenna and therefore decreases the impedance bandwidth. This relationship did not immediately follow when using the transmission line model of the antenna, but is apparent when using the cavity

model. Planar Inverted-F Antenna (PIFA) is common in cellular phones with built-in antennas and is increasingly used in the mobile phone market. The antenna is resonant at a quarter-wavelength (thus reducing the required space needed on the phone), and also have good SAR properties. This antenna resembles an inverted F, which explains the PIFA name. It is popular because it has a low profile and an omnidirectional pattern. These antennas are derived from a quarter-wave half-patch antenna. The shorting plane of the half-patch is reduced in length which decreases the resonance frequency. Often PIFA antennas have multiple branches to resonate at the various cellular bands. Sometimes, grounded parasitic elements are used to enhance the radiation bandwidth characteristics. The Folded Inverted Conformal Antenna (FICA) has some advantages with respect to the PIFA, because it allows a better volume reuse. This is an example of the meandered structure which helps to resonate for wider frequency range. This is the idea of mobile handset antennas which usually designed by random structure of the patch on the dielectric.

Sipal. V et al. [71] proposed relation between substrate dimensions and the antenna properties of an electrically small transmission line ZORA (zeroth-order resonator antennas). A small antenna that with large ground plane loses its competitive advantage and antenna radiation properties deteriorate as the substrate is reduced.

Zelenchuk D.E. et al.[36] did the numerical study for a low-profile and high-gain planar antenna. The antenna was realized with gain values between 9

and 11 dBi and the return loss better than 10 dB over the 5.6-6.3-GHz frequency band occupying area 20% smaller than a conventional microstrip patch antenna.

2.4 Slot Loaded Patch

The slot loading is made by two ways; one is on the conducting patch and the other on Ground plane. The dimensions and positions of slot can be properly selected in order to the first two broadside-radiation modes of the patch be perturbed such that their resonance frequencies get close to each other to form a wide impedance bandwidth. The slots of various shapes are particularly investigated for wide band antenna, suitable for handset devices.

Mazzinghi, A et al. [37] studied the effects of finite conductivity on the radial line slot array (RLSA) at high frequencies through simulation. The low cost metallization techniques were adopted with an arbitrary impedance surface.

Chen et al. [45] proposed a novel design of open slot antenna for bandwidth enhancement. The bandwidth enhancement of the proposed antenna was achieved by slot to the circular radiating patch. Experimental results indicate that an operating bandwidth over a wideband frequency range was from 2.57 to 14.23GHz obtained for small size of dimensions $20 \times 35 \text{mm}^2$ and found suitable for wideband applications in various wireless communication systems.

2.5 Feeding the Prototype

X. Sun et al [54], proposed a novel compact quad-band microstrip antenna using edge-feeding to support the four wireless communication bands of GPS,

WIMAX, WLAN and WLAN. To expand the bandwidth of the GPS and to further reduce the size of the antenna, an edge-fed technology was used.

Si, L. et al. [56] designed a compact planar microstrip antenna, composed of composite closed-ring resonator and split-ring resonator (SRR) fed by 50Ω coplanar waveguide (CPW) on FR4_epoxy substrate for wireless communications. The antenna has good impedance bandwidth and radiation characteristics in the (WLAN) and (WiMax) applications.

Deng et al. [69] designed and simulated an ultra wideband (UWB) rectangular monopole antenna through ANSOFT HFSS. They have observed a notched characteristic for (WLAN), (WiMAX) and the C-band satellite communications. In order to obtain the desired dual band rejections, a piece of pentagonal slot line and a pair of inverted L-shaped stubs were used. The antenna was CPW fed and printed on the FR4 substrate of 40 mm x 41 mm x 0.5 mm .

2.6 Effect of substrate on resonant Frequency

Substrate in the Printed Circuit Board antennas enable a wide range of RF/microwave antenna applications, in which dielectric constant (ϵ_r) is key characteristic. The dielectric constant and its thickness of a PCB affects antenna frequency response. PCB substrate with a high dielectric constant will enable us to fabricate smaller circuit features and hence reduced antenna size for a particular frequency. But on the other hand, high dielectric constant substrates are more lossy. To improve the radiation characteristics, the feed lines for the antenna can be significantly reduced.

Dielectric loading of a microstrip antenna affects both its radiation pattern and impedance bandwidth. As the dielectric constant of the substrate increases, the antenna bandwidth decreases which increases the Q factor of the antenna and therefore decreases the impedance bandwidth. This relationship did not immediately follow when using the transmission line model of the antenna.

2.6.1 Ceramic Substrate

The ceramic substrate is mainly used in small size applications with frequencies below 1 GHz. It has low loss tangent and has good chemical resistance, but is also very expensive. Besides that, ceramic is very hard to produce and handle. For instance it is very hard to drill holes in the substrate without breaking it. Some ceramic material has a high dielectric constant which is used where size reduction is needed [55].

2.6.2 Synthetic Substrate

Synthetic substrate is commonly made out of organic material like PTFE (also known as Teflon). These materials possess low loss tangent and low ϵ_r . The only problem is that this material is very soft and can therefore easily change the characteristics of a microstrip antenna if it is not handled properly.

Liu Y et al. [72] designed and tested a low cost and simple structure dielectric rod antenna array. It was composed of cylindrical dielectric rods acting as the radiation elements, which were made of low cost Teflon with relative permittivity of 2.08 rather than high permittivity dielectric that are commonly

used in dielectric resonator antennas. To achieve high gain, dielectric rods form an array and are connected with a microstrip corporate feeding network.

2.6.3 Composite Material Substrate

Composite material is made out of mixed chemicals between fibre glass, ceramic or quartz and synthetic material. There is a wide variety of composite material on the market which has been modified so they fit both to antenna fabrication and standard PCB design [55].

2.6.4 Low-Cost Low-Loss Substrate

Ceramic, Synthetic and Composite material substrate is usually used where other applications are needed or a microstrip antenna needs perfection and also it is too expensive to use in consumer electronics such as TV's, mobile phones, etc. Works mentioned above, focuses on the miniaturization of the antenna structure only. The study of the effects of the substrate size reveals that the Antenna radiation parameters deteriorate significantly as a result of the reduction of the substrate's lateral dimensions.

Kai et al. [51] proposed new approach for antenna miniaturization of antennas in ever increasing wireless systems. Substrates with high dielectric constants can be used for miniaturization. Another approach for reducing the antenna size is to change the boundary condition of the antenna, either using a shorting pin on a patch or replacing the two short circuits at the end of the resonant slot by inductive or capacitive loadings.

Dau chyrh chang et al. [73] presented a fabricated results of a high-gain multilayer four square patch antenna array for the application of WLAN (wireless local area network) AP (access point) which fabricated on FR4 substrate. The FR4 substrate is with air gap to the ground plane. Adjusting the thickness of FR4 substrate and geometry of antenna array the maximum gain of 13dBi can be achieved. The radiation efficiency for 2.4, 2.5 and 2.6 GHz are all larger than 65%.

D. Laila et al. [53] showed that a printed antenna with reduced radiation hazard from a mobile handset with RT Duroid. The printed metal stripes in the back side of the monopole modify the far field pattern ideal for mobile handset caused reduction of radiated power in one quadrant of the radiation pattern offers a reduction of radiation towards the users head. RT/Duroid 5880LZ laminates can be easily cut, sheared and machined to shape. They are resistant to all solvents and reagents, normally used in etching printed circuits, holes and suitable for smart wireless sets mobile handsets [5],[68].

2.7 Meandered Structure for Bandwidth Enhancement

Meander line antenna is one type of the micro strip antennas. The meander line antenna was proposed by Rashed and Tai to reduce the resonant length [60]. Meandering the patch increases the path over which the surface current flows and that eventually results in lowering of the resonant frequency. The structure of the antenna though it is considered out the combination effect of different implementation, but the structure is said to be meandered because it is flowing

from one side of antenna to the other. Bandwidth of an antenna is the difference between the upper and lower frequencies of operation(f_H and f_L respectively)

$$BW = f_H - f_L.$$

Y. Wang et al. [38] presented an effective modeling methodology for Ultra-wideband (UWB) antennas. The methodology is based on augmenting an existing narrow-band model with a macro-model while simultaneously perturbing component values of the narrow-band model. The narrow-band model is an empirical-based circuit and the macro-model described by rational functions is determined using data fitting approaches. The perturbation of component values of the narrow-band model is achieved by adjustments in SPICE for a 2.5 cm dipole antenna and a circular disc monopole antenna for UWB systems.

H. Mirzaei et al. [57] proposed and used miniaturization of electronics down to the nanoscale, to design Multiband/Broadband/ mutli- functional Smartphone/Tablet/Laptop Antennas. The combined effect with several additional strategies such as tuning with embedded varactors to extend the usable bandwidth, antenna design which fit in confined spaces (e.g. smartphones, tablets etc.), are suggested. The unique properties offered by metamaterials are used for the design of multiple antennas have to be integrated in the handheld devices.

The impedance frequency bandwidth of a microstrip antenna depends primarily on both the thickness and the dielectric permittivity of the substrate. Thus, a reasonable thickness should be considered in the selection of substrate and the bandwidth would be enhanced using additional techniques. The most common and effective of them, are: (a) the loading of the surface of the printed

element with slots of appropriate shape (b) the texturing of narrow or wide slits at the boundary of the microstrip patch. Other effective techniques used for the enhancement of the bandwidth is the utilization of a) stacked, shorted or not patches, and b) extra microstrip resonators. The utilization of additional parasitic patches of different size directly- or gap-coupled to the main patch is an effective method but results to an increased antenna size which would also be undesired. Superior to these methods is the techniques of slot loading or texturing the patches by slits because they ensure the small size and the low profile of the antennas.

Hyung Kuk Yoon et al. [74] proposed a research on the miniaturization of UWB antenna over wide bandwidth using tapering, modified sleeve and truncated ground plane. It was of compact size, $10 \times 8 \times 0.652 \text{ mm}^3$ and the ground size of $30 \times 30 \text{ mm}^3$, to support UWB services and can be easily integrated with the other RF circuit.

2.8 Implementation for Mobile Handsets

Now a day's due to rapid changes in wireless communication technologies, there is tremendous increase in data rate and at same time reduction in antenna size and weight is demanded. There are varieties of techniques to reduce the size of microstrip antennas: use of high permittivity substrates, shorting pins [51], and meander line. Inserting suitable slots in radiating patch is also a common technique in reducing the dimensions of patch antenna. The slots introduce parasitic capacitances which tend to reduce the resonant frequency of

the antenna. For wireless communications applications such as USB Dongle, radio frequency identification tags, Bluetooth headset, Mobile phone Meander line antenna is convincing solution.

2.9 Equivalence of the Circuit

Hamid et al. [34] derived an equivalent circuit for a dipole of any length and compared the input impedance versus frequency response of the resulting equivalent circuit with published analytical and experimental data.

Tang et al. [35] proposed a four-element lumped-parameter equivalent circuit, consisting of a resistance, an inductance, and two capacitances, to represent the feed-point impedance of a dipole antenna. The values of these elements were related only to the physical dimensions of the antenna, for which empirical formulas were given through SPICE, PSPICE, and MICROCAP.

Ansarizadeh et al.[39] proposed a method for the computation of the broadband matching potential of a microstrip antenna that requires the wideband lumped equivalent circuit of the antenna. The general topology of the equivalent circuit of rectangular microstrip patch antennas has been used to model the feed point impedance of microstrip antennas over a wide frequency band and equivalent circuit parameters are determined using optimization techniques, working frequency from 0.1 to 6 GHz.

Rogla et al.[75] studied an equivalent circuits for the open-ring resonators and split-ring resonators. The resonators were intrinsically described by simple LC circuits. They have proved that their resonant behaviour is caused by

conceptually different phenomena, either distributed or quasi-static resonances can be attributed for designs with similar geometrical dimensions. When inserted on the back-plane of a coplanar waveguide, and combined with short-circuiting wires on the top-plane, the periodic structures designed so far exhibit a certain pass-band where backward waves were generated. They have proved the left-handed behaviour of the different length transmission lines through the analysis and can be observed for both types of resonators. They have validated the prototypes with equivalent circuits through full-wave simulations and experiment. Detailed models for the different the unit-cells were provided on the basis of analytical approach.

Ansarizadeh et al. [76] proposed lumped equivalent circuit of the broadband microstrip antenna with matching potential. They have modeled the equivalent circuit and its parameters of rectangular microstrip patch antennas and the feed point impedance through optimization techniques. Applying this technique, wideband lumped equivalent circuits of a rectangular and E-shaped microstrip antenna have been computed which are in good agreement with measurement data from 0.1 to 6 GHz.

2.10 Need for the Work

As conventional antennas have a conducting patch printed on a grounded dielectric substrate and operates as resonant cavity elements, this operation leads inherently to narrow impedance bandwidth in wireless communications. So, the enhancement of the bandwidth and the achievement of multifrequency operation

is still a challenge for the antenna designer. To meet this challenge, an unsymmetrical design is chosen with combination of different structures including CRLH, SRR and PATCH in the present study.

Antenna sizing possibilities can be done by including split ring resonators with possible shapes, while the multifrequency response may be obtained by considering the slots in the patches. Antenna is to be designed for the mobile applications such that it will meet the following requirements: (i) cost effective when compared with earlier designs (ii) low weight (iii) miniature in size and competent reliable entity. The objectives are framed by considering all the above.

2.11 Objectives

- (i) To design a multiband antenna resonating at various mobile frequency applications.
- (ii) To design a miniaturized handset antenna with competent reliable entity for mobile application.
- (iii) Fabrication and measurement of designed antenna.
- (iv) To realize the equivalent circuit of the multi-band antenna.

2.12 Summary of the Chapter

Antennas for next generation wireless systems are required to exhibit multiple bands accommodate multiple wireless standards within the same device. In this chapter literature related to compact antenna, intended for the use in a handsets is investigated with a metamaterial concept. The aspects of the

metamaterials for the antenna applications are derived out of the literature survey and finally objectives are framed for the process of design of antenna. The analysis of metal metallic strips wires and split-ring resonators (SRRs), which are planar structures, is reviewed. In microstrip technology, SRRs etched in the upper substrate side, in proximity to the conductor strip, have been found to provide metamaterial effects in planar configurations for the design of compact antennas. An S-shaped SRR structure (S-SRR) which, produces an electric and magnetic response within the same frequency range, thus realizing simultaneously a negative permittivity and a negative permeability, i.e., a left-handed metamaterial. The CRLH transmission-line (TL) approach to synthesizing metamaterials, that exhibit forward, backward with many of applications, multi-frequency operation. Enhancement of the bandwidth and the achievement of multifrequency operation are major challenges, the combined effect of CRLH and SRR metamaterial is studied for the design of a prototype. Different substrates have been studied suitable for printed antenna fabrication. The impedance frequency bandwidth of a microstrip antenna depends primarily on both the thickness and the dielectric permittivity of the substrate. The frequency controlling methods are: a) the loading of the surface of the printed element with slots of appropriate shape b) the texturing of narrow or wide slits at the boundary of the microstrip patch. c) utilization of additional parasitic patches of different size directly- or gap-coupled to the main patch. Superior of techniques is slot loading or texturing the patches by slits. Need for the present research and objectives are also presented.

CHAPTER 3

DESIGN AND FABRICATION

This chapter expounds the design aspects involved in the development of the prototype antenna e.g., the design of wideband handset antenna for mobile frequency ranges covering the GSM, PCS, DCS and WIBRO bands. More specifically, it deals with the dimensions, simulation and fabrication of three antenna structures considered preliminarily in the present work, along with the circuit equivalence of the final prototype.

3.1 Design Flow

The methodology adopted to develop the prototype antenna is shown in Fig 3.1. In principle, the design of the prototype consists of asymmetrical cells, with combination of different structures including CRLH, S-SRR and PATCH, with a slot to resonate in the frequency range of the anticipated mobile applications [76]. Design samples with FR4 and RT Duroid 5880 LZ substrates and edge feeding are considered, and the antenna designed using the antenna design kit in HFSS.

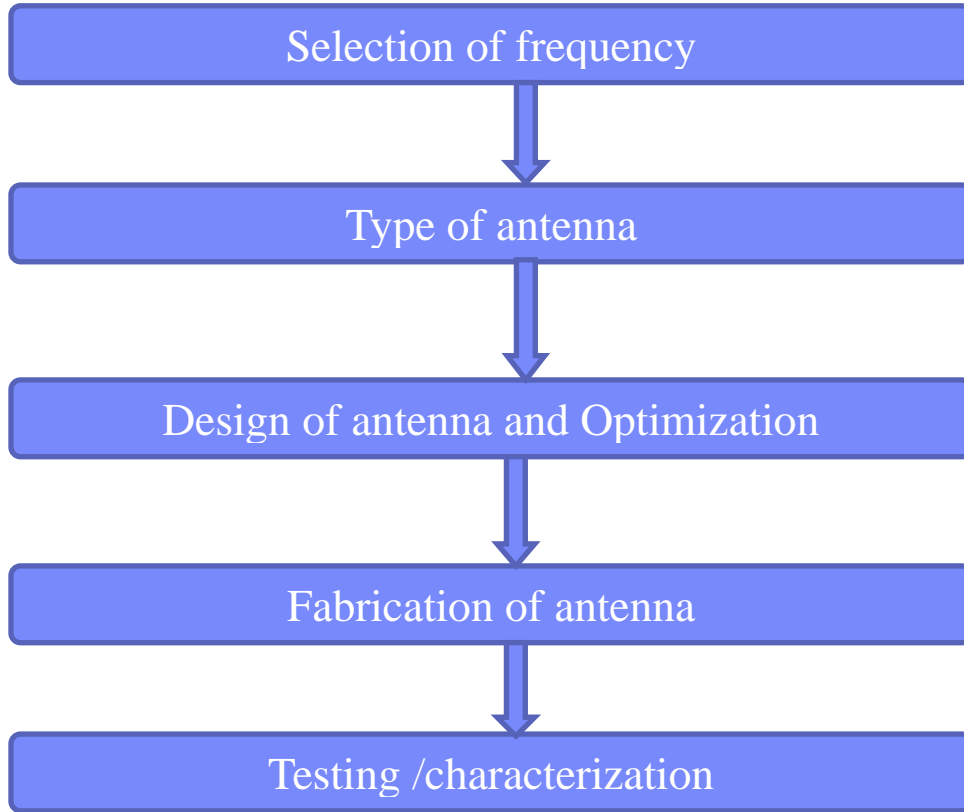


Fig 3. 1 Flow chart of antenna design

Initially, the antenna was proposed with coaxial probe feed and FR4 substrate with epsilon $\epsilon_r=4.4$. However, subsequent prototypes designed have edge feed and they differ from the earlier ones by the presence of slots of different sizes in the asymmetrical patches of front side. The section 3.2 provides the details of the dimensions involved. The ultimate dimensions are derived from optimization of the simulation results. Equivalent circuit of prototype with RT Duroid and slot is also derived in this chapter.

3.2 Geometry of the Structure

Among the three prototype antennas considered, the first antenna has FR4 substrate, while the second and the third had a substrate of RT Duroid. The three antennas differed in structure dimensions printed on their both sides. The first prototype had probe feed with metallic lines, while the second and the third antenna had edge feeds. The ‘sizing’ was done for latter two antennas which had same dimensions but differed by presence of slots in the patches on one side. The variation in their structural dimensions, make antennas to resonate at different center frequencies. Improvement of characteristics is observed beginning from the first prototype antenna to the third with respect to gain, radiation pattern and increased number of center frequencies.

3.2.1 Antenna on FR4

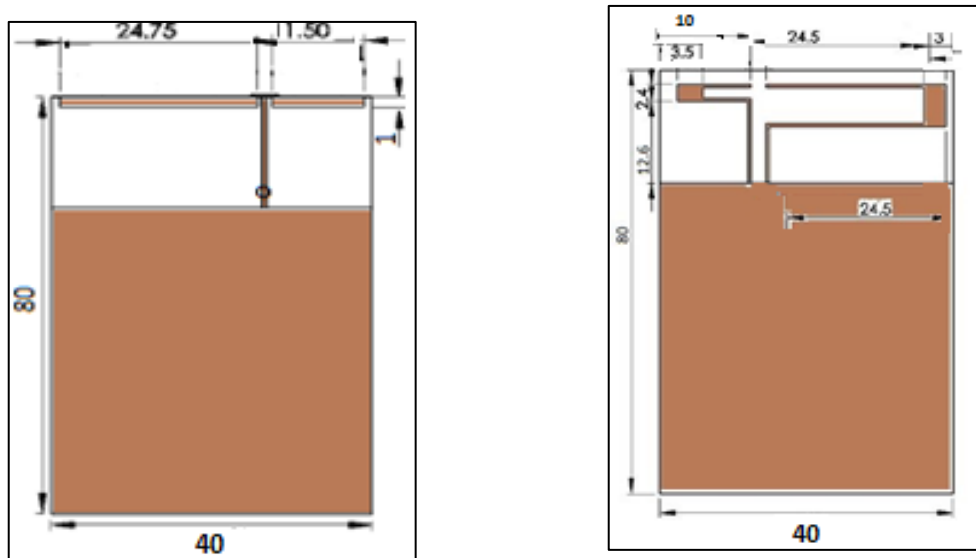


Fig 3. 2 Front and Rear Views of Antenna on FR4

The original antenna design which is the first antenna proposed in [17] consists of combination of metallic wires and split-ring resonators (SRRs) placed on a substrate in unsymmetrical dimensions. Since, SRRs are actually planar structures and wires can be easily substituted by metallic strips. Hence, the extension of these designs to planar configurations can be made easily and these can open the way to new planar microwave devices and also for coplanar waveguide technology for miniaturized stop band and band pass filters. Fig 3.2 shows the geometry of the proposed metamaterial antenna, without any slot in the patch on rear side. The dimensions are defined such that the antenna operates with controlled radiation in the resonating band at 1.8GHz. The dimensions of the structure of printed type on a substrate of FR4 ($\epsilon_r=4.4$) is $40 \times 80 \times 1 \text{ mm}^3$, which is small enough to be built in mobile or wireless devices. The space for PCB embedded type antenna is $40 \times 15 \text{ mm}^2$ and PCB ground of the front and rear sides are connected through vias. Radiating patch lines of width $24.75 \times 1 \text{ mm}^2$ and $11.5 \times 1 \text{ mm}^2$ are excited by a coaxial fed transmission line passing through a small gap in between and lines are finally connected with the rear side of ground. The proposed antenna has two different unit cells. The width of via lines and the width of feeding line is 0.5 mm and the feed point is indicated with circle symbol in the front side of antenna as shown in Fig 3.2. The gap between each unit cell and feeding line is 0.2 mm, which is the distance between radiating patches and feeding line. The major issue regarding the design is the arrangement of the feeding network, and the isolation between the cells while current passes from one side of the PCB to the other side till the ground. For further miniaturization of

the prototype antenna and to overcome the issue regarding the coaxial feeding, material of the substrate and the feed are altered, and discussed in the following section.

3.2.2 Antenna without slot

Designing a wide band high gain planar antenna with controlled radiation aperture is a difficult task. Antennas with conformal designs are usually based on the edge feeding of individual radiating elements that lie in a conducting plane. The advantage of this meander arrangement of different cells is that it results in better gain increment of resonant bands without any adverse impact of the feeding network. This Planar metamaterial antenna is based on reactively loaded transmission lines (TL), with an S-shaped SRR structure (S-SRR) [17]. They do not need additional rods to produce negative permittivity and negative permeability within the same frequency range as in original i.e., a left-handed metamaterial [22]. The SRRs have their advantages, such as miniature size and high quality factor, and therefore these types of resonators have been used to obtain miniature designs. Hence to realize meander structure, split ring resonators are coupled with patches on the other side of the antenna. Theoretical analysis of the radiation of an S-shaped split ring resonator (S-SRR) metamaterial, exhibiting left-handed property shows enhancement of radiation [33]. It is seen that the structure is resonant due to its internal capacitances and inductances, which can be adjusted by individual dimensions. Two S-SRRs and patches resonances fall within the same frequency band. Using this same idea, presently some extended

S-SRRs are used for mobile band with suitable physical dimensions [47]. The overall dimension of the intended structure was reduced to $40 \times 60 \times 0.762 \text{ mm}^3$, by using a printed type on a substrate of RT Duroid 5880LZ (with $\epsilon_r=2.2$), which is also small enough to be built in mobile or wireless devices. The space for antenna is $40 \times 14 \text{ mm}^2$ and can be PCB embedded type. PCB ground of front and rear side is connected through vias. Radiating patches of $24.75 \times 5.5 \text{ mm}^2$ and $11.5 \times 5.5 \text{ mm}^2$ are introduced, instead of lines in the previous prototype antenna. Radiating patches are excited by edge fed transmission line through a small gap in between, and lines are finally connected with rear side of ground. The proposed antenna has two different unit cells. The width of via lines is 0.5 mm . The width of feeding line is also 0.5 mm . The gap between each unit cell and feeding line is 0.2 mm which is the distance between radiating patches and feeding line. The diameter of vias is 0.5 mm , as shown in Fig. 3.3.

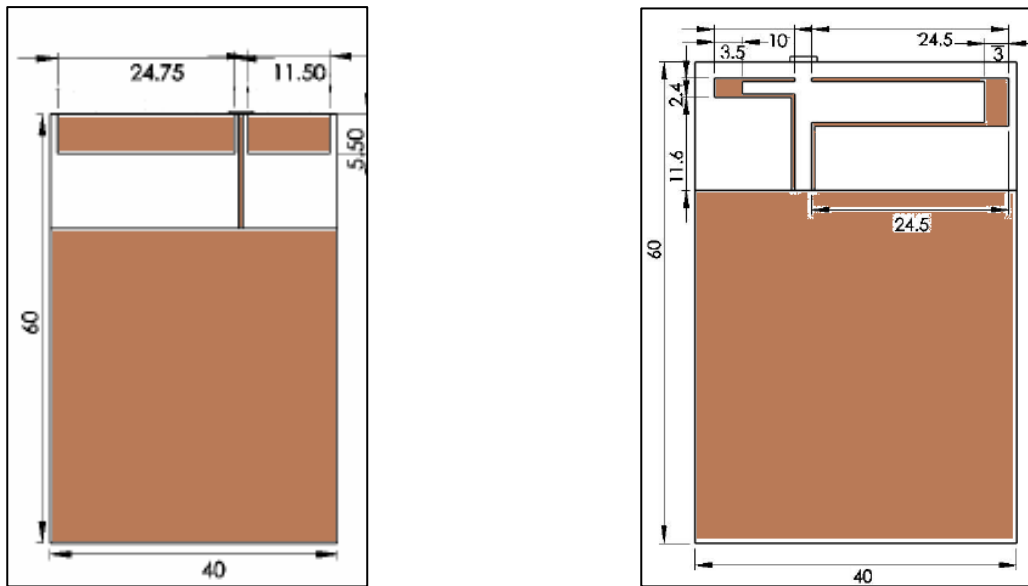


Fig 3. 3 Front and back views of Antenna on RT Duroid and without Slot

The prototype antenna size is reduced by 20mm of PCB with 1mm for antenna when compared to the antenna on FR4. This antenna exhibits shift in frequency bandwidth and better gain which is clearly dealt in Chapter 4. The dimensions of the structure are defined such that the antenna operates independently with controlled radiation in the resonating bands at 2.25 GHz and at 3.35 GHz. The SRRs are active to resonate at the 2.25 GHz frequency band, preventing in the second band with center frequency at 3.35 GHz. It is fabricated using the Wet Etching Technique/Chemical and discussed in section 3.4 in detail.

3.2.3 Antenna on RT Duroid with slots

In this prototype antenna, SRRs and the patches have the same dimensions as in the previous prototype. However, to achieve the multi-band response, slots with unequal dimensions are introduced. Slot with dimensions 14mm is introduced in 24.75mm patch and the other slot of 6mm is introduced on the 11.5mm patch as shown in Fig 3.4. These slots are so placed in the patches, so as to give good resonance characteristics [54]. The combination of patches with slots and SRRs achieve high magnetic coupling at resonance. The presence of the rings leads to an effective negative-valued permeability in a narrow band at resonance. By simply adding shunt metallic strips between the central strip and ground planes, the sample demonstrated wide resonating characteristics. This effect has been interpreted as due to the coexistence of effective negative permeability and permittivity (the latter introduced by the additional strips).

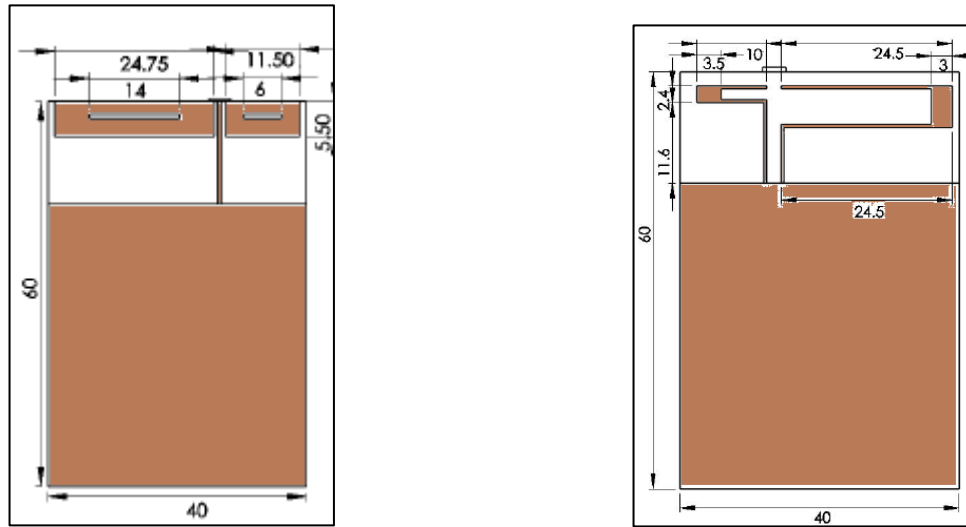


Fig 3. 4 Front and back views of Antenna on RT Duroid and with Slot

3.3 Simulation of Design

The proposed three antenna designs are simulated in HFSS (High Frequency Structure simulator) and the results obtained are presented and explained in Chapter 4. The overall view of the antenna on RT Duroid and with slot, is shown in Fig 3.5, and the slot is indicated there with violet coloured patch line. The final prototype in Fig. 3.5 has a feeding line (TL), and P1 and P2 are radiating patches which are connected to SRRs, R1 and R2 through vias (Via). Feeding line (TL) and radiating patches (P1 and P2) are located on front side of PCB. SRRs (part R1 and R2) are located at the rear side. FEED is the edge feeding incorporated in the antenna. These radiating patches are excited by line (TL) through a small gap in between. Finally, lines extending from SRRs are connected to ground, GND on the rear side. The overall view of rest two antennas is similar to the overview presented here for the third antenna.

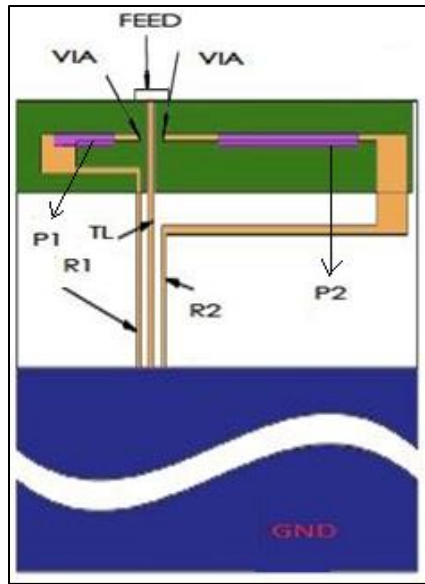


Fig 3. 5 Over all view of antenna

The dimensions of each part of the three prototypes are shown in Fig. 3.2, Fig3.3 and Fig 3.4 respectively. The third antenna is based on idea of metamaterials point and edge feeding. It has two different unit cells. One is composed of part P1 and R1 with via, and the other is composed of part P2 and R2 with via. Those two unit sections appear to have a similar kind of structure, but not symmetric. These cells share the feeding line (part TL). The width of via lines is 0.5 mm. The width of feeding line (TL) is also 0.5 mm. And the gap between each unit cell and feeding line is 0.2 mm, which is the distance between radiating patches (P1 and P2) and feeding line (TL). The diameter of vias is 0.5 mm. This CRLH structure may be modelled in terms of series inductance, series capacitance, shunt inductance, and shunt capacitance which are responsible for the resultant value of resonant frequency [78]. The three prototype antenna designs are simulated before fabrication, to achieve gain required for the mobile communications.

Optimization for the structure dimensions of an antenna is done in accordance with a view to counter-act the fabrication defects. The simulation is carried out to calculate the performance of designed antennas in terms of far field functionality of the antenna, return loss, radiation pattern, gain, VSWR and axial ratio values. Simulation also explained the improvement in resonance characteristics and the added gain achieved by inclusion of slots in the antenna. The resonating frequency bands could also be adjusted by changing the unit cell parameters.

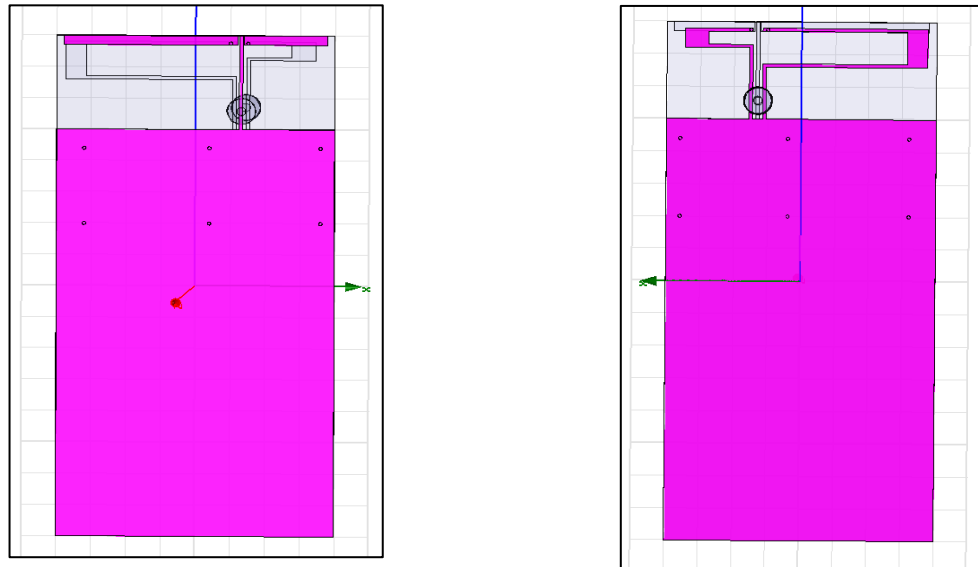


Fig 3. 6 Simulated Structure of Antenna on FR4 substrate

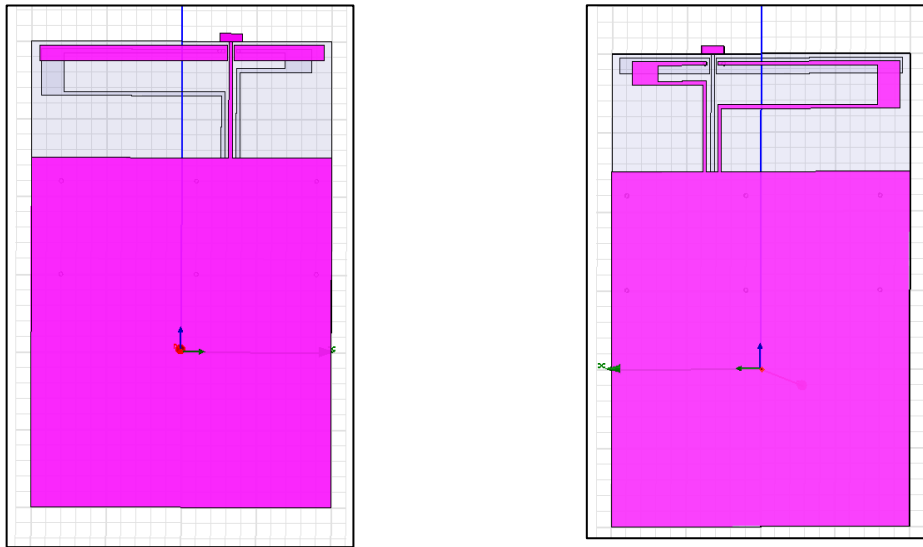


Fig 3. 7 Simulated Structure of Antenna without slots

Simulated view of antenna on FR4 and RT Duroid without slots in the patches are shown in Fig 3.6 and Fig 3.7 respectively.

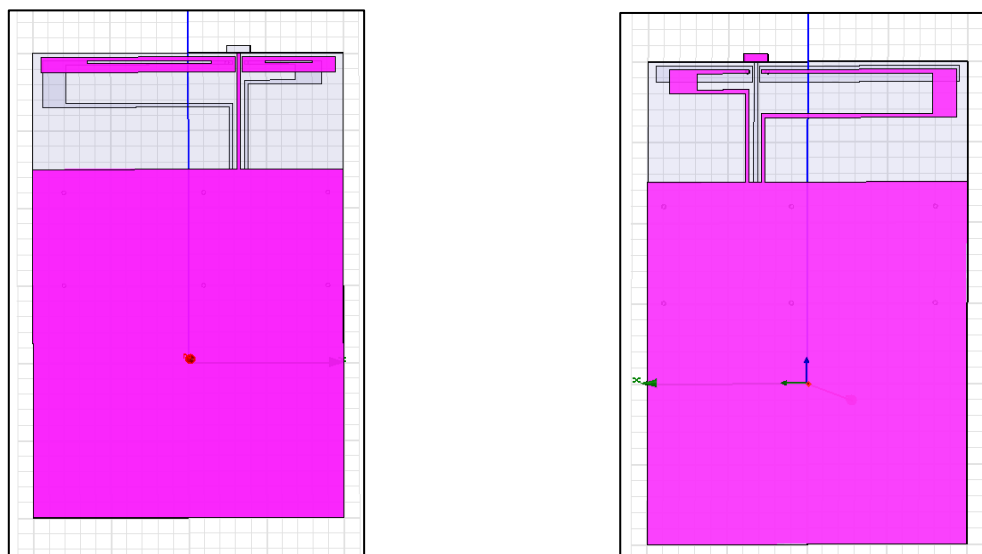


Fig 3. 8 Simulated Structure of Antenna on RT Duroid and with Slot

Simulated view of antenna on RT Duroid with slots in the patches is shown in Fig 3.8 respectively.

3.4 Fabrication of designed antenna

The three prototype antennas were fabricated as follows. The antenna 1, on FR4 substrate, and the antenna 2 on RT Duroid (without slot), used the chemical etching process, while mechanical etching was used for the antenna 3, on RT Duroid, with slot in the patches .

3.4.1 Wet Etching/Chemical Etching

Chemical Etching fabrication is implemented for the first and second antennas of this work. Transitioning from hypothetical metamaterial central elements to an antenna is quite challenging, since it requires the fabrication of different unsymmetrical unit cells. The SRRs are etched on the rear side of antenna while CRLH with metallic patches on the complementary side of the substrate. To fabricate two sided PCB antenna, .dxf file of antenna is taken from simulation file of HFSS. This file is then transformed to image file with the dimensions.

There are four main stages in the fabrication process of the antenna structures using two substrates FR4 and Roger's 5880 Duroid. These stages are:

- 1) Spinning and coating the board with photoresist;
- 2) Exposing the board to UV light;

3) Developing; and

4) Etching.



Fig 3. 9 Art Work Film maker



Fig 3. 10 Developer

Originally, an air-brush technique was developed to coat the boards. This approach was found to significantly save on the amounts of the photoresist that were being used in the processing. However, the air-brush approach was found to be unsatisfactory because it was difficult to achieve a thin, uniform coating. Because of the sizes involved, a standard spinner was used for the final fabrication process. It gave a coat with a thickness between 1.0 and 1.5 microns versus the 4 to 5 micron thickness that was achieved with the airbrush. A piece of 60 mm x 40mm x.762mm board size was selected, and it yielded two SRR-unit cell structures. After spinning, the boards were placed in a 100⁰ C furnace for one minute to dry them. The printed mask of the design was generated and placed



Fig 3. 11 UV Light Exposure



Fig 3. 12 PCB Etching

over the board. The boards were then exposed for 1.5 min with UV light. The boards were then placed in a developer. Developing time was under one minute. Once the photoresist was removed, the boards were rinsed with deionized water and dried with nitrogen. Finally, the boards were placed in a Ferric Chloride etching solution. This process took between 10 to 15 min to complete, while care was exercised to not over-etch the boards. The boards were rinsed with acetone to remove any remaining photoresist from the board. The boards were finally rinsed with deionized water and dried with nitrogen.

For Antenna Fabrication it is required to reduce or etch the copper clad on one side of the dielectric to form the desired mobile antenna, while leaving the back intact to function as a ground plane. The two general possibilities for material removal are machining by mill or chemical etch. Copper PCB etchant was selected over milling due to unavailability of a mill and the tediousness involved in milling by hand with a rotary tool. It is possible to mask off the un-

etched portion with marker or to selectively remove the protective plastic coating from the laminate. Both methods worked in tests, and the later method was selected for ease of measurement of dimensions and homogeneity of the resultant metal patch. The feed point was chosen to be in the middle of the short dimension, the length on the long dimension is due to impedance considerations. A hole was drilled at the desired location or vias and an SMA connector was soldered into place, taking care not to short the ground plane and antenna surface, allowing for more compact planar antennas for a given wavelength. Two techniques of fabrication were tested as suitable methods, a metal lift-off, and a metal etch. Negative masks of the antenna were made by laser printing on overhead transparency. The negative mask is needed for the lift-off. In a lift-off, photoresist is left under the unwanted metal so that a solvent may undercut and lift off the areas where metal is not desired, and after which it is cleaned and spin-dried in order to drive the solvent out of the polymer. The wafers were exposed to UV light through the negative mask for 15s at a dose of $14\text{mW}/\text{cm}^2$. This is a higher than typical dose adjusted for the facts that the plastic mask is expected to absorb a significant portion of the UV, and the negative mask is dark-field. After the metallization, the etched wafers proceeded to photolithography. This process was successful in creating the desired metallic pattern patch on substrate. The exposed copper metal layer was then wet etched in a ferric chloric acid and surfactant solution for 20mins at 40°C . The remaining photoresist was then stripped of with n-methyl pyrrolidone. However, a crippling setback to the investigation of the RT Duroid substrate was the difficulty involved in attaching a

feed point. Aluminum grows a native oxide, which makes soldering to the surface impossible. Plumber's soldering flux did not alleviate the problem. Possible solutions to this problem include the use of a proper wire bonder, probe station, or clamping devices. In this type of etching the resolution and precision of the dimensions are not reaching the mark and is not ecofriendly. So the prototype was attempted to fabricate through the mechanical etching.

Photograph of fabricated antenna with FR4 is shown in Fig 3.13.

3.4.1.1 Photograph of fabricated Antenna on FR4



Fig 3. 13 Fabricated Antenna on FR4

3.4.1.2 Photograph of fabricated Antenna on RT Duroid and without slot



Fig 3. 14Fabricated Antenna on RT Duroid and without slot

Photograph of fabricated antenna without slot is shown in Fig 3.14. Miniaturization was observed from earlier antenna to this antenna and is achieved by changing the feed and substrate.

3.4.2 Mechanical Etching

Mechanical etching is done by drilling bits with .dxf file is fed to the system where it automatically takes the path to etch the conducting layer on the antenna. Antenna print was crafted on the both sides of the antenna, and this has high precision. Vias which connect patches and SRRs are created through hole drilling. Later the feed point is connected / soldered with 50Ω SMA connector. This method is employed to fabricate the third prototype antenna on RT Duroid,

and also slots on the patches on front side. The very reason is to maintain accuracy of the dimensions of slots in the patches.

3.4.2.1 Photograph of fabricated Antenna with slot



Fig 3. 15 Fabricated Antenna on RT Duroid and with slot

Final prototype result is an antenna with slots on the radiating patches, as can be seen in the photograph of fabricated antenna in the Fig 3.15. In this photograph the refinement of fabrication detail is observed mainly with slot in the patch. The slot was also etched according to exact dimensions without any precision error. This antenna is not only compatible with handset, but also improvement of bandwidth, gain and radiation pattern was observed. This is discussed in chapter 4 in detail, with respect to the return loss of simulated as well as tested results. Structural variations from first prototype antenna to third prototype antenna was

clearly seen, as is also clear from the photographs shown in Fig3.13, Fig3.14, and Fig3.15.

3.5 Characterization of Prototypes.

After the designing and fabrication, the prototype antennas underwent characterization. This is done by the determination of output parameters listed by Return loss, Radiation Pattern and Gain.

(i) Return Loss S_{11} :

The return loss of prototype antenna is measured through Vector network analyzer, as described in section 1.4.3. For this the test antenna is fed for a 0.0 dBm (1.0 mW) input power level along the resonating frequency range. In the analysis, the fundamental definition of the bandwidth of an antenna is the difference between the upper and lower frequencies of operation (f_H and f_L respectively) $BW = f_H - f_L$. The center frequency is defined as the arithmetic average of the upper and lower frequencies. An arithmetic average yields the central frequency when frequency is considered on a linear scale. It is used for characterizing or measuring the response of desired antenna at resonant frequency through a -10dB Bandwidth (dealt in detail in Chapter 4).

(ii) Radiation Pattern:

Antenna Radiation Pattern is a plot between, normalized power versus angles of two perpendicular fields. The θ and ϕ components of Electric field and magnetic field, respectively are simulated and presented in Chapter 4. Major

Lobes of the radiation pattern for an antenna prototype are demonstrated at different frequencies.

(iii) Gain Measurement

The half power beam width (HPBW) is needed to measure the gain and directivity. The antenna prototype was rotated from -180° to $+180^{\circ}$ and the rectangular plot of received power Vs angle is plotted for all θ and ϕ orientations. From the plot, HPBW, angle which covers half of the maximum power in θ and ϕ , are obtained. The antenna gain measurement was done in anechoic chamber. With the relation of gain and directivity, gain is calculated and tabulated and presented in Chapter 4 [79],[80].

(iv) VSWR

VSWR is determined from the voltage measured along a transmission line leading to an antenna. When an antenna is not matched, power is reflected causing "reflected voltage wave", which creates standing waves along the transmission line. Low VSWR, which is equal to 1.0, in the plot of VSWR Vs frequency shows the resonant frequency range of the prototype antenna. VSWR of three prototypes are dealt in Chapter 4.

(v) Axial Ratio (AR)

Axial ratio (AR) is the ratio of the two orthogonal components of E-field. AR equal to one represents circular polarization (CP). AR beam width for CP based antennas is considered to explain the resonant frequency. AR for three prototypes are presented to observe deviation from circular polarization in the resonating band.

(iv) Input Impedance

The input impedance is obtained from the overall circuit according to the flow of current from feed point to ground for the final prototype. The graph of reactance component of input impedance is plotted along the resonating frequency range. This parameter will be discussed in section 4.6.

3.6 Analytical analysis of an Antenna on RT Duroid and with slot

Analytical analysis deals with the equivalent circuit of an antenna with slot described in section 3.2.3. The equivalent circuit of individual components, SRR, CRLH and patch with slot are shown in Fig 3.16. The input impedance, reflection coefficient and return loss have been computed and expressions are given below.

3.6.1 Equivalent circuit

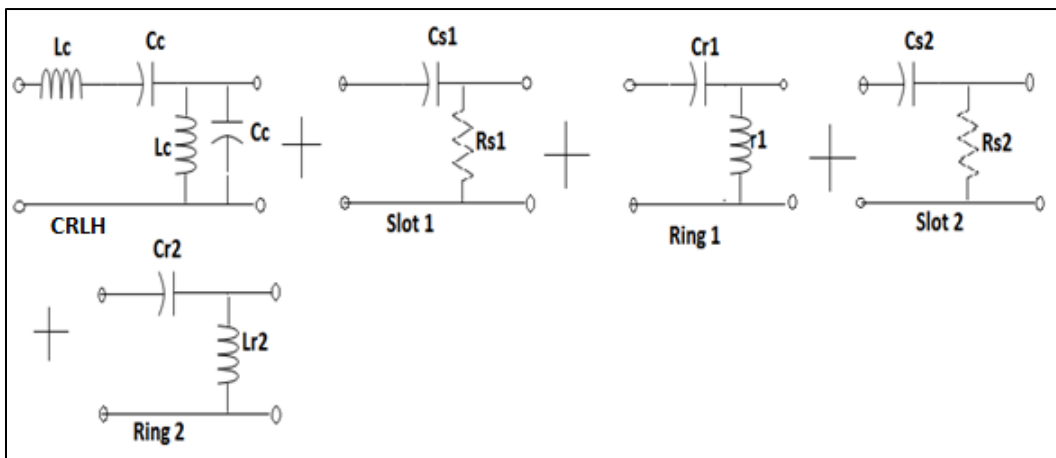


Fig 3. 16 Circuit equivalent of Antenna

The individual parts of antenna are considered and their circuit equivalent is presented to derive the overall impedance of the circuit, as shown in Fig 3.16. The CRLH TL, radiating patches and SRRs are the main elements to promote the radiation. The circuit is connected with the above mentioned elements according to Fig 3.17 to derive the impedance [82].

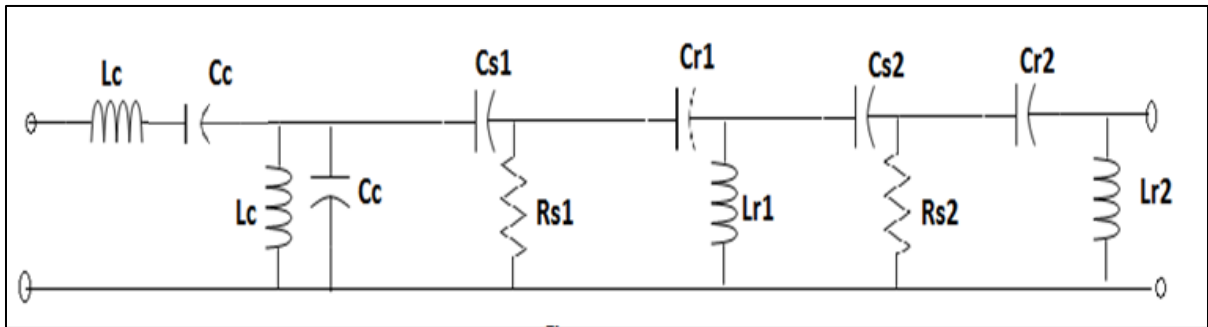


Fig 3. 17 Over all Equivalent Circuit

The CRLH-TL is basically the combination of conventional and dual of conventional transmission line. Examples are series inter-digital capacitors and shunt stub inductors, which are introduced in a microstrip transmission line, as given by a nonlinear equation.

$$\beta_1 = \omega \sqrt{L'_R C'_R} - \frac{1}{\omega \sqrt{C'_L L'_L}} \dots\dots\dots 3.1$$

where β is the propagation constant, ω is the angular frequency, and L_R, C_R, L_L, C_L are characteristic inductances and capacitances of the CRLH transmission line. The characteristic inductances and capacitances, L_R, C_R, L_L, C_L are equal to L_C, C_C, L_C, C_C respectively as shown in Fig 3.17. The resonant frequency is

given by the equations Eqn3.1 and Eqn3.3. The impedance can also be obtained by Equation 3.2.

The metamaterial transmission line allows the existence of backward waves, in other words, negative propagation constants. Thus, two different frequencies can have the same propagation constant (in the sense of absolute value) through this dispersion relation. As a consequence, the same mode and current distribution are achieved in the two different frequency bands. This property is utilized in this work to design a dual band antenna, where Z_c is the characteristic impedance of the feeding line. Thus, yet another freedom is left for the determination of the four design parameters. In order to have the ring resonate at another frequency f_2 , the fourth restriction can be written as following based on the negative propagation constant of the CRLH transmission line:

$$\sqrt{\frac{L'_R}{C'_R}} = Z_c$$

$$\sqrt{\frac{L'_L}{C'_L}} = Z_c \dots\dots\dots 3.2$$

$$\omega_{r1}, \omega_{r2} = \frac{1}{\sqrt{L_R C_L}}, \frac{1}{\sqrt{L_L C_R}} \dots\dots\dots 3.3$$

$$\beta_2 = -\frac{2\pi}{L} = \omega_2 \sqrt{C'_R L'_R} - \frac{1}{\omega_2 \sqrt{L'_L C'_L}} \dots\dots\dots 3.4$$

The minus sign indicates that the CRLH transmission line is supporting a backward wave at the second frequency f_2 . It's clear that the propagation constants at these two frequencies have the opposite signs but the same absolute values. Thus, the current distributions at these two frequencies are the same. It consists of the CRLH transmission line in which the series inductance and capacitance and shunt inductance and capacitance exist and resonate for two frequencies named f_L and f_H . The antenna, on the other hand, in fact, on its other side, has ring resonators, which also resonate at f_L . The patch on the side which has transmission line, resonates in both frequencies. The resonant frequency of the prototype antenna is calculated and observed as 1.9 GHz and 4 GHz. These two frequencies represent the low and high frequencies of CRLH which are the resonant frequencies of SRR and complement wires on the other side of PCB antenna [84]. The values of the inductance and capacitance of equivalent circuit are derived from the MURTA CHIPS DATABASE. The equivalence in terms of circuits gives the input impedance of the antenna, which is simulated in the MATLAB.

3.6.2 Input Impedance

The equivalent circuit of an antenna is drawn considering all the main elements of the prototype having slots on one side. The input impedance is derived from the overall circuit according to current from feed point to ground. The reactance component of input impedance is then plotted to observe the resonating frequency. This parameter is discussed in section 4.4. The input

impedance of equivalent circuit specified in Fig 3.16 is derived in terms of S, where is $S = j\omega$ and given by Eqn 3.5

$$Z_{11} = \frac{50 \times 10^{-94} s^9 + 12.5 \times 10^{-80} s^8 + 99.5 \times 10^{-75} s^7 + 5.23 \times 10^{-54} s^6 + 17.4 \times 10^{-54} s^5 + 2.4 \times 10^{-24} s^4 + 2.4 \times 10^{-33} s^3 + 2.16 \times 10^{-21} s^2 + 13.2 \times 10^{-12} s + 1}{49.8 \times 10^{-85} s^8 + 12.4 \times 10^{-73} s^7 + 17.4 \times 10^{-45} s^6 + 2.4 \times 10^{-45} s^5 + 17.4 \times 10^{-45} s^4 + 6.42 \times 10^{-30} s^3 + 14.3 \times 10^{-24} s^2 + 1.08 \times 10^{-12} s} \dots\dots\dots 3.5$$

$$\Gamma = \frac{Z_{in} - Z_o}{Z_{in} + Z_o} \dots\dots\dots 3.6$$

The impedance of the antenna equivalent is calculated from Eqn 3.5 and the reflection coefficient can be calculated by using Eqn 3.6.

3.6.3 Return loss

The return loss can also be calculated by the relation as

$$S_{11} = \frac{1}{1 - \Gamma} \dots\dots\dots 3.7$$

The response of the (i) input impedance (reactance) (ii) reflection coefficient and (iii) return loss is obtained for the frequency range from 1GHz to 5GHz.

It may be noted that metamaterial concepts like CRLH were proposed and applied for enhancement of antenna characteristics. They are basically the dual of traditional transmission lines and follow the same analysis as that for the

conventional transmission line. Substituting the equation Eqn 3.5 in the Eqn 3.6, the reflection coefficient is obtained.

$$\Gamma = \frac{50 \times 10^{-94} s^9 + 12.5 \times 10^{-80} s^8 + 99.5 \times 10^{-75} s^7 + 5.23 \times 10^{-54} s^6 + 17.4 \times 10^{-54} s^5 + 2.4 \times 10^{-24} s^4 + 2.4 \times 10^{-33} s^3 + 2.16 \times 10^{-21} s^2 + 13.2 \times 10^{-12} s + 1 - 50}{49.8 \times 10^{-85} s^8 + 12.4 \times 10^{-73} s^7 + 17.4 \times 10^{-45} s^6 + 2.4 \times 10^{-45} s^5 + 17.4 \times 10^{-45} s^4 + 6.42 \times 10^{-30} s^3 + 14.3 \times 10^{-24} s^2 + 1.08 \times 10^{-12} s + 50} \dots\dots\dots 3.8$$

Equation 3.8 gives the reflection Coefficient for the antenna. Return Loss can be determined by substituting Eqn 3.8 in the Eqn 3.7.

$$S_{11} = \frac{49.8 \times 10^{-85} s^8 + 12.4 \times 10^{-73} s^7 + 17.4 \times 10^{-45} s^6 + 2.4 \times 10^{-45} s^5 + 17.4 \times 10^{-45} s^4 + 6.42 \times 10^{-30} s^3 + 14.3 \times 10^{-24} s^2 + 1.08 \times 10^{-12} s + 50}{-50 \times 10^{-94} s^9 - 12.5 \times 10^{-80} s^8 + 12.4 \times 10^{-73} s^7 + 17.4 \times 10^{-45} s^6 + 2.4 \times 10^{-45} s^5 - 2.4 \times 10^{-24} s^4 + 6.42 \times 10^{-30} s^3 - 2.16 \times 10^{-21} s^2 + 11.2 \times 10^{-12} s + 99} \dots\dots\dots 3.9$$

The return loss of the antenna with slots is given by the Eqn 3.9

The response for the (i) input impedance (reactance) (ii) reflection coefficient and (iii) return loss S_{11} are obtained and analyzed. The standard set of equations for conversion between VSWR, return loss, and reflection coefficient (Γ) are also used for the purpose. [87].

3.7 Summary of the Chapter

This chapter presented the scheme of development of a wideband handset antenna for mobile range covering GSM, PCS, DCS and WIBRO. The schematic of this was presented in the form of a flow chart, and three prototypes were

considered. The working frequency of a planar antenna depends upon the substrate selected. Among the three antennas presented, the first antenna has substrate FR4 while second and third has substrate RT Duroid. The prototypes are having meander structure printed on both sides with CRLH-TL, S-SRRs. The first part of this chapter deals with the dimensions of the three antenna structures. First design sample with FR4 and coaxial feed with FR4 ($\epsilon_r=4.4$) is $40 \times 80 \times 1$ mm³ in its dimensions. The second is an antenna of miniaturized size, $40 \times 60 \times 0.762$ mm³, with a printed type on a substrate of RT Duroid 5880LZ ($\epsilon_r=2.2$) and edge feeding. Third antenna prototype has the same dimensions as those of second antenna and slots of different sizes are introduced in it to increase the number resonant frequencies. Latter part of this present chapter discusses the fabrication of three antennas. Chemical etching was implemented for (a) antenna which has FR4 substrate and also for (b) the antenna which has RT Duroid and without slot. Mechanical etching was used for the third antenna, which has RT Duroid and slot. Valid reason for adapting mechanical etching is mentioned. Simulation presents the optimized output parameters listed by return loss, radiation pattern, gain, VSWR and axial ratio. Return loss and radiation pattern are measured through vector network analyzer and anechoic chamber respectively. HPBW derived from radiation pattern is used to determine gain and directivity. For the improvement of antenna characteristics, right from the first prototype to the third prototype antenna, concept of patch and inclusion of slot is implemented sequentially. Betterment of results is observed clearly through the parameter of return loss response, which is being dealt in Chapter 4 in detail.

Analytical equivalent of the third antenna is determined by the equivalence of individual elements. The main elements include CRLH, S-SRR and PATCH with slot. The input impedance is derived from the overall circuit according to current flow from the feed point to ground. The reactance component of input impedance is then plotted to observe the resonating frequency. This last parameter will be discussed in Chapter 4.

CHAPTER 4

RESULTS AND DISCUSSIONS

A multi-frequency operation is essential for many mobile applications. Hence, enhancement of bandwidth for achieving multi-frequency operation is generally a major challenge for antenna designers. Many techniques have been proposed to achieve this purpose [77]. While the previous chapter gave the design and fabrication details, this chapter presents the characterization of the three prototypes through simulated and measured results, with a view to demonstrate amongst other properties, the frequency ranges in which these antennas resonate. The simulated and measured values for different parameters are then used for comparison. For example, the return loss response is used to compare the bandwidth of the different antenna prototypes. The simulation results include those for *radiation pattern*, *gain*, *VSWR* and *axial ratio*. The working band width of the antenna is determined from the return loss response measured through the vector network analyzer. The working bandwidth for is decided at the level where the return loss response crosses -10dB line. Likewise, the *Directivity* is determined through HPBW, from the rectangular radiation plot measured in anechoic chamber.

4.1. Antenna on FR4 Substrate

The prototype antenna on FR4 Substrate, discussed in Section 3.2.1 has yielded the following results.

4.1.1 Return loss

Return loss graph containing, both, the simulated and measured values, demonstrates the functioning range of the antenna.

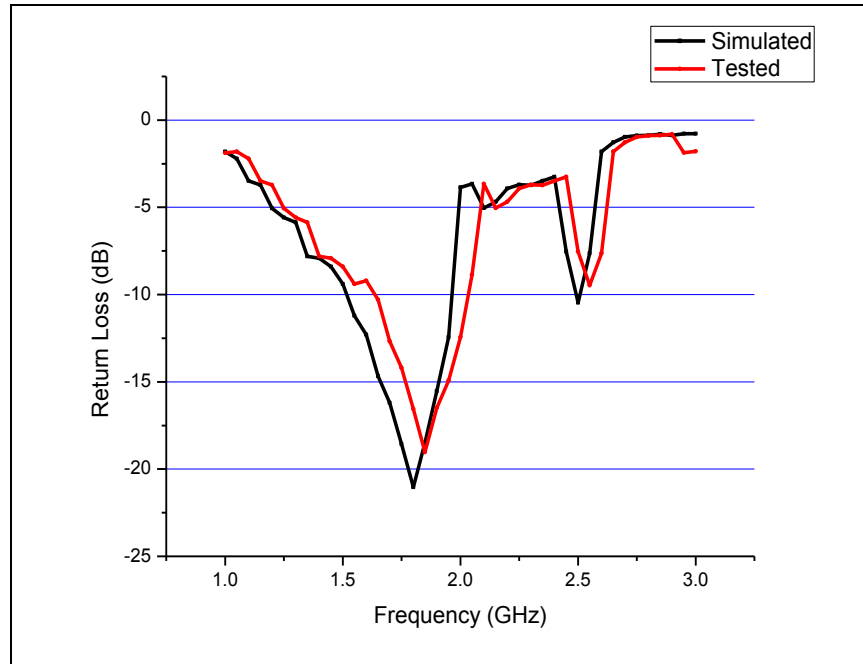


Fig 4. 1 Return loss for Antenna on FR4

Table 4. 1BW of Antenna based on FR4

-10 dB BW	f_1 GHz	f_2 GHz
Simulated S_{11}	1.58	1.95
Tested S_{11}	1.65	1.99

The resonant frequency of the antenna as inferred from Fig 4.1, is tabulated in Table 4.1. The simulation results show that the antenna resonates from 1.58 GHz to 1.95 GHz, while the tested result of the prototype is observed to be shifted towards right, with -10dB frequency values of 1.65 GHz to 1.99 GHz. The shift may be explained on the basis of the fabricational reasons, irregularities arising in the discontinuities at the outer contours of the conducting patch lines on the substrate. This antenna covers Personal Communications (PCS) and Digital Communications (DCS) bands.

4.1.2 Radiation Pattern

The simulated result of the radiation pattern of this antenna is shown in Fig4.2, which demonstrates the variation of E field and H field with ϕ is equal to 90^0 and 0^0 , respectively.

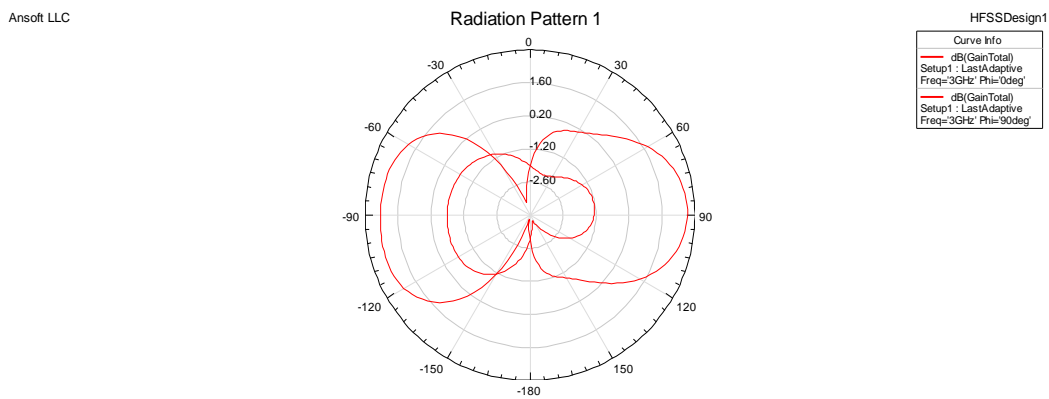


Fig 4. 2 Radiation Pattern for Antenna on FR4

From the pattern, it is observed that the Electric field component has a higher gain value of 1.6 dB.

4.1.3 Gain

The simulated gain for this antenna is plotted in between 1GHz and 3GHz, and shown in Fig 4.3.

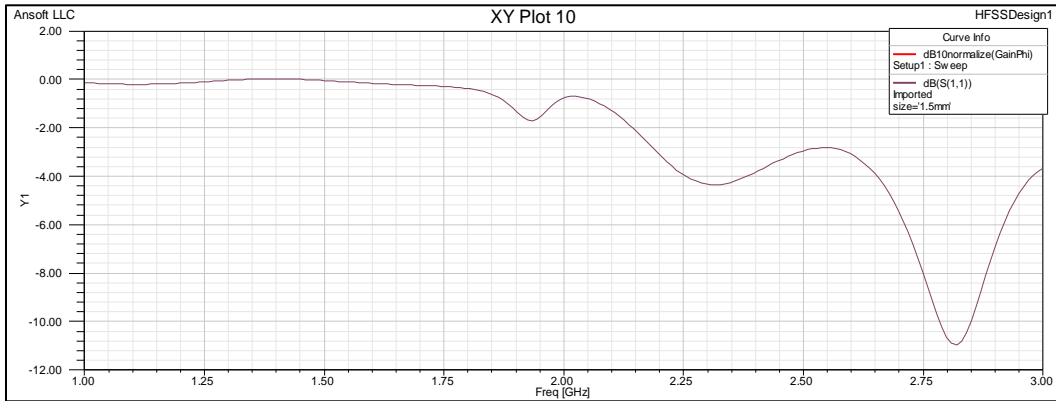


Fig 4. 3 Gain for Antenna on FR4

It is showing lower gain of value -0.1dB at 1.8 GHz in the resonating frequency range.

4.1.4 VSWR

The antenna prototype on FR4 has VSWR, represented in the frequency range of 1 to 3 GHz, as shown in the Fig 4.4, and it shows a lower value equal to 0.01 at 1.80 GHz. This is the center frequency of the antenna, as discussed in Section 3.2.1.

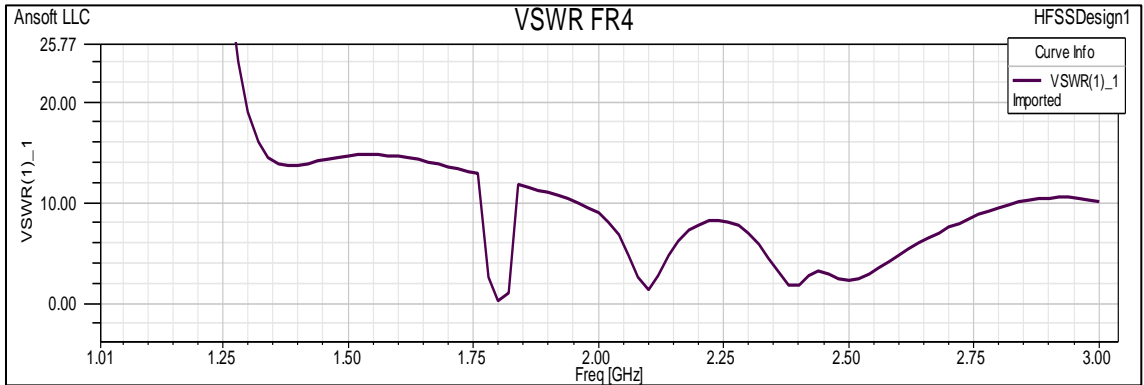


Fig 4. 4 VSWR for Antenna on FR4

4.1.5 Axial Ratio

The axial ratio of the antenna is shown in the Fig 4.5, and is used to identify the working range.

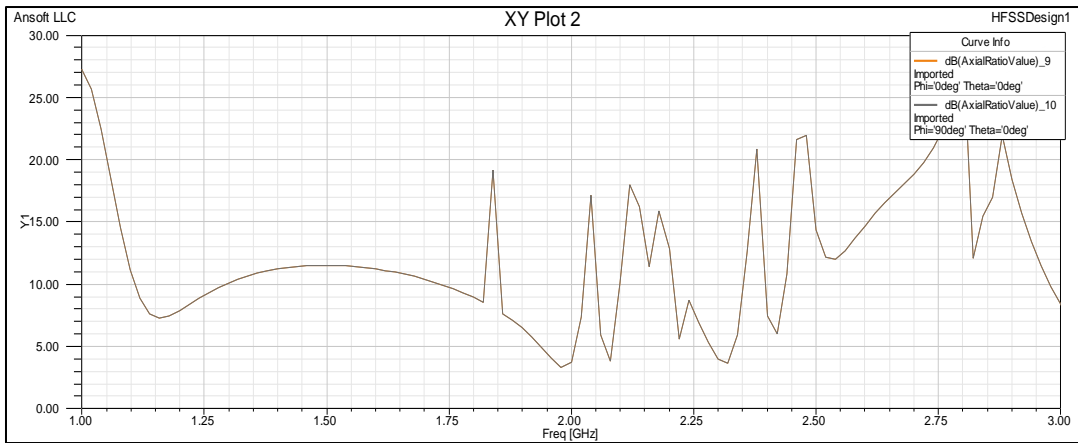


Fig 4. 5 Axial Ratio for Antenna on FR4

The plot of axial ratio derives a value 8dB at 1.8GHz, as shown in Fig 4.5, and evidently explains the resonating range.[88]

4.2 Antenna on RT Duroid and without slot

A miniature design is essential in mobile applications. One of the many techniques proposed, edge feeding along with RT Duroid, was incorporated here for the same purpose. As discussed in Chapter 3, adjusting the size of the patch on the front side of double sided prototype resulted in this wideband antenna.

4.2.1 Return loss

The prototype antenna on RT Duroid and without slot, discussed in Section 3.2.2, has produced the following results. The bandwidth and the center frequency of the antenna are obtained from the plot of return loss, Fig 4.6 and reported in Table 4.2. The main aim here was to increase the gain and the directivity of the planar antenna by metamaterial implementations.

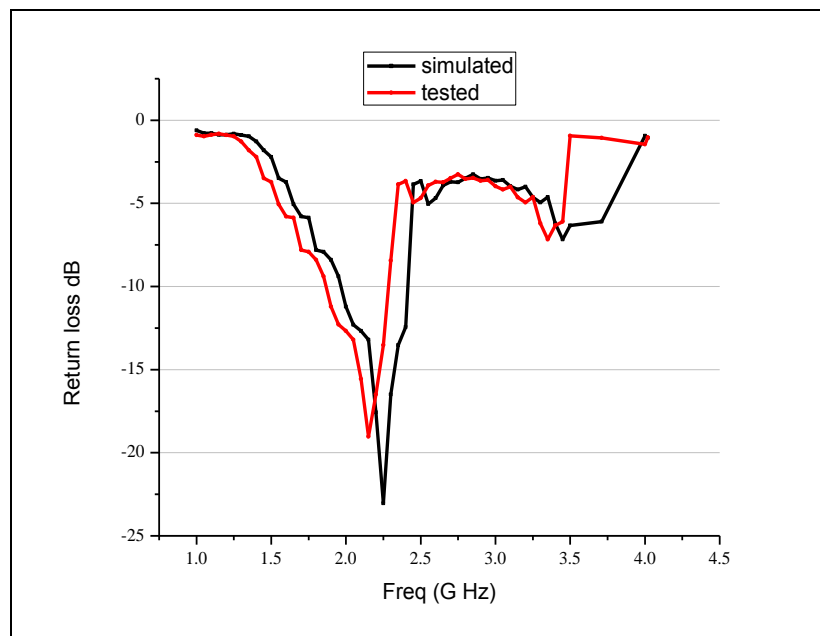


Fig 4. 6 Return loss of Antenna on RT Duroid and without slot

Table 4. 2 BW of Antenna on RT Duroid and without slot

-10 dB BW	f_1 GHz	f_2 GHz	Center frequency
Simulated S_{11}	1.95	2.45	2.15 GHz
Tested S_{11}	1.9	2.3	2.10 GHz

The simulation results show that the antenna resonates in the range of 1.95 GHz to 2.45 GHz. The ‘test’ results are observed to be shifted towards left with extreme values of 1.9 GHz and 2.3 GHz. The shift between the two results may be, again, due to fabrication reasons, i.e., due to irregularities arising in the discontinuities at the outer contours of the conducting patch on the substrate. At the low-frequency resonance at 1.9 GHz, the current distribution is good enough to get a wider bandwidth. This antenna is covers the PCS, DCS and partial BLUETOOTH bands [91].

4.2.2 Radiation Pattern

The simulated result for radiation patterns at 1.95 GHz, 2.15 GHz and 2.3 GHz frequencies are shown below in Fig 4.7. Radiation pattern presents both, the azimuth component (red) and the elevation component (black). The magnitude of the azimuth component is reduced, as the frequency increased. The shape of the vertical component is deteriorated at the right side with the increase of frequency.

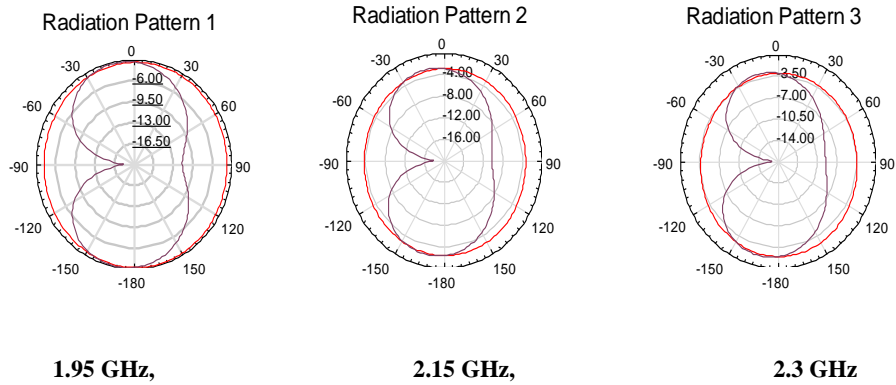


Fig 4. 7 Radiation Patterns of Antenna on RT Duroid and without slot

4.2.3 Gain

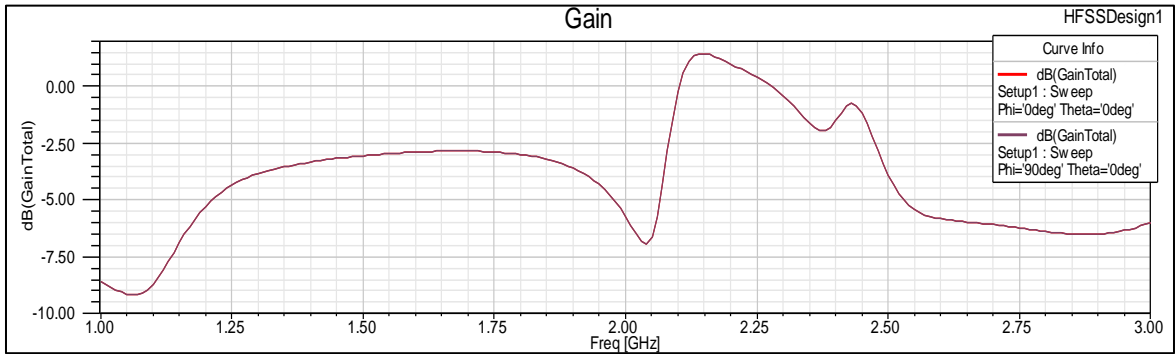


Fig 4. 8 Gain of Antenna on RT Duroid and without slot

The gain is plotted, and is presented in Fig 4.8. The plot shows high gain value of 3dB at 2.15 GHz in the resonating frequency range of 1.9 GHz to 2.3 GHz. The exact gain calculations are demonstrated in section 4.5 separately.

4.2.4 VSWR

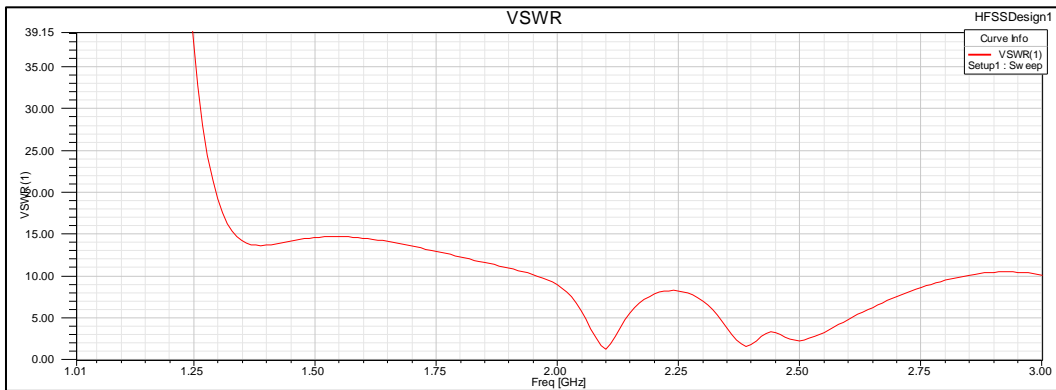


Fig 4. 9 VSWR of Antenna on RT Duroid and without slot

The VSWR plot is shown in Fig4.9. It shows that, between 1.9 GHz to 2.3GHz VSWR is less than 2 and equal to 0.18 at 2.15 GHz , proving the resonating frequency range of the antenna as discussed in Section 3.2.2

4.2.5 Axial Ratio

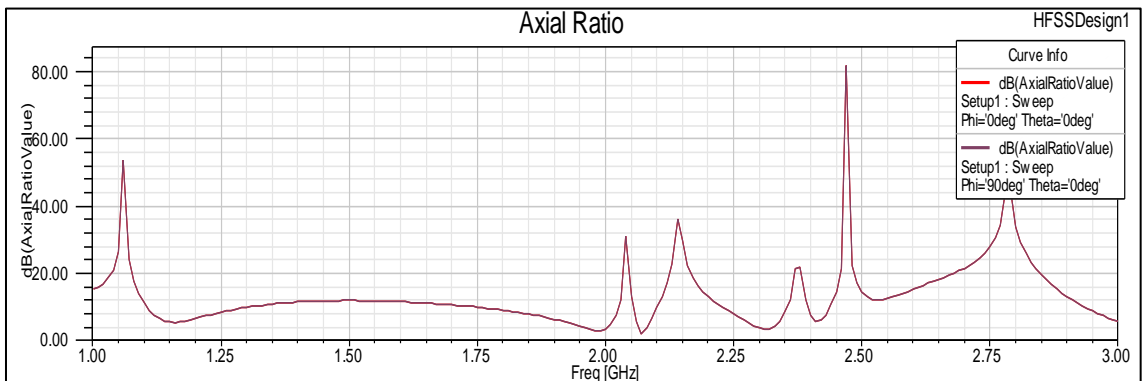


Fig 4. 10 Axial Ratio of Antenna on RT Duroid and without slot

The plot of axial ratio of antenna on RT Duroid and without slot is presented in Fig 4.10 and it depicts that, the axial ratio has varying values from 10dB to 6dB in the resonating frequency range of 1.9 GHz to 2.3 GHz.

4.3 Antenna on RT Duroid and with slot

Miniature antennas with multi-frequency are desirable in mobile applications, especially those which cover commercial bands. As discussed in Chapter 3, introducing slots in the patches on the front side of a double sided prototype resulted in the wideband antenna. The simulated and measured results of prototype antenna on RT Duroid and with Slot are discussed in following sections.

4.3.1 Return loss

The measured and simulated values of return loss are plotted in Fig.4.11. This figure clearly depicts the four resonating bands in the entire frequency range

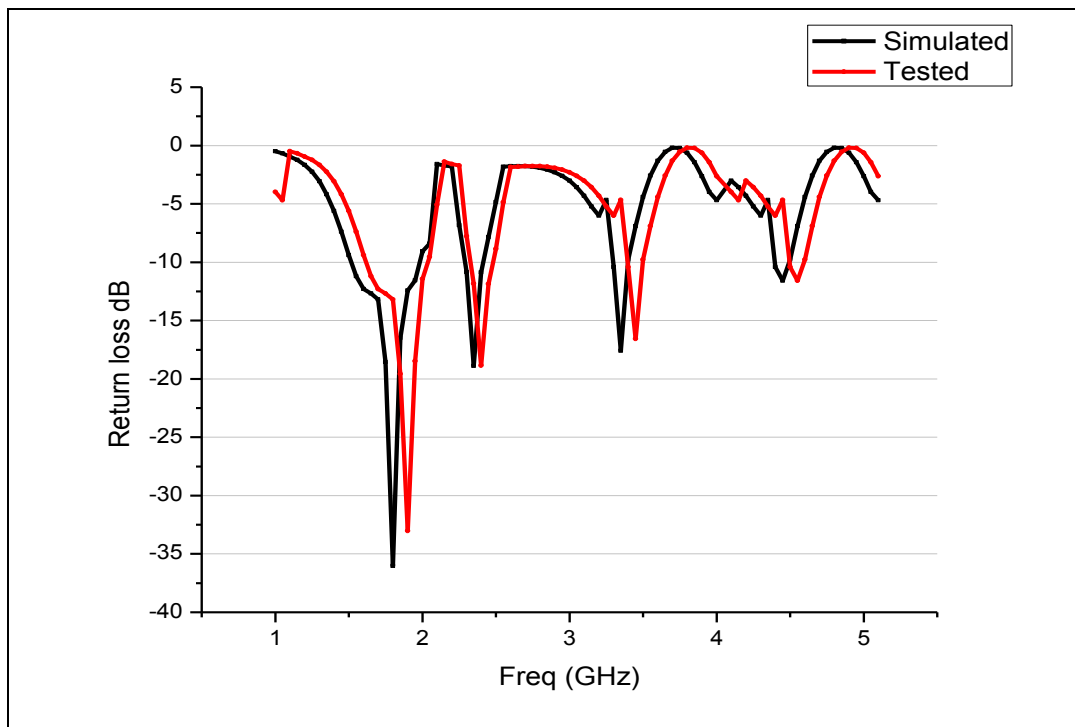


Fig 4. 11 Return loss of Antenna on RT Duroid and with slot

of interest. The bandwidth and the center frequency of each resonating band for this antenna is observed from the Fig 4.11 and tabulated in Table 4.3.

Table 4. 3 BW of Antenna on RT Duroid and with slot

S_{11}	BW1(GHz)	BW2(GHz)	BW3(GHz)	BW4(GHz)
simulated	1.6-2.05	2.3-2.45	3.3-3.4	4.4-4.5
Tested	1.6-2.05	2.35-2.5	3.4-3.5	4.45-4.6
Center frequency	1.9	2.4	3.35	4.462

As discussed in chapter 3, inclusion of slots in the patches resulted in the multi-band version of the antenna. The slot loaded metamaterial antenna exhibits distinct resonances at 1.91 GHz, 2.4GHz 3.35 GHz and 4.62 GHz. It is noted that this antenna is exhibiting better performance at lower frequency band. The two upper resonances have poor return loss. The possible reason for the weak response is poor current distributions in the structure. Further, it is observed that the central frequency for each band is shifted towards higher frequency values in case of measurement results. This shift is attributed due to losses of connector, and the fabrication anomalies. The magnitude of deviation between the simulated and tested results may define the refinement of fabrication. The ‘response’ of the prototype with slot antenna covers the commercial bands like PCS, DCS, WIBRO, BLUETOOTH, and slices of some other bands. So the antenna may fit well for different types of applications and in the different wireless sets which work in these mentioned bands [89]. The Fig.4.11 clearly demonstrates the multi frequency response due to the inclusion of slot in the patch

of antenna. The inclusion of slots probably serves as a defective ground surface (DGS) [85].

4.3.2 Radiation Pattern

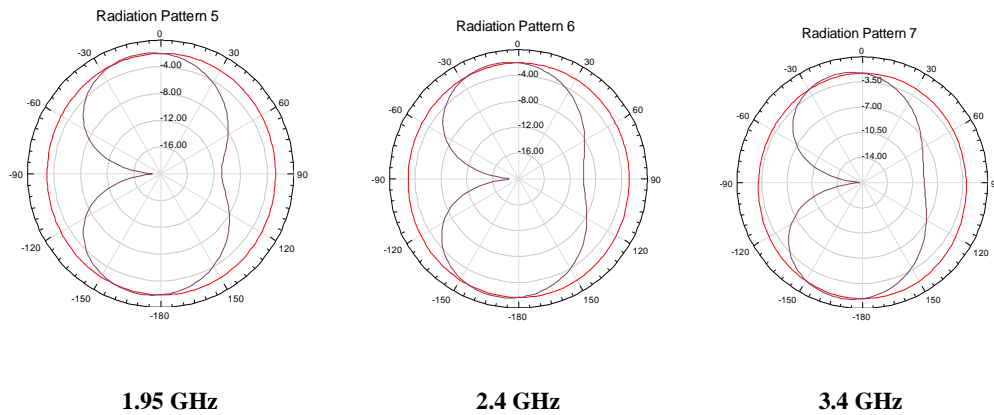


Fig 4. 12 Radiation Pattern of Antenna on RT Duroid and with slot

Fig 4.12 shows the radiation patterns at 1.9 GHz, 2.4 GHz and 3.44GHz for the antenna with slot. The magnitude of the azimuth component, red circle in the patterns of the antenna based on RT Duroid without slot, is seen to be improved. The radiation patterns of the antenna, which has slot in the patches, at different frequencies, are taken into consideration for the plotting of E and H fields. The radiation patterns don't have much variation for the two prototypes based on RT Duroid, i.e., with and without slot. As the frequency of the sample moves away from the resonant frequency the shape of the radiation pattern deteriorates towards the right side along with a minute decrease in gain.

4.3.3 Gain

Gain of the antenna in the frequency range of 1 GHz to 5 GHz with slot is shown

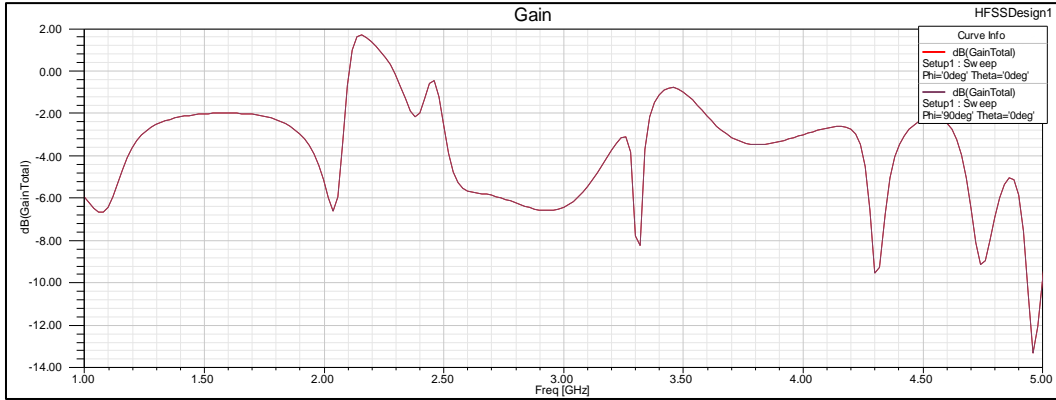


Fig 4. 13 Gain of Antenna on RT Duroid and with slot

in Fig 4.13. Gain magnitudes of the antenna for vertical and azimuth components are equal at 1.9 GHz and 2.4 GHz with -2dB and 3.44GHz with -3dB. The gain calculations through anechoic chamber, are considered in section 4.5.

4.3.4 VSWR

The plot of VSWR versus frequency for this antenna is shown in Fig 4.14.

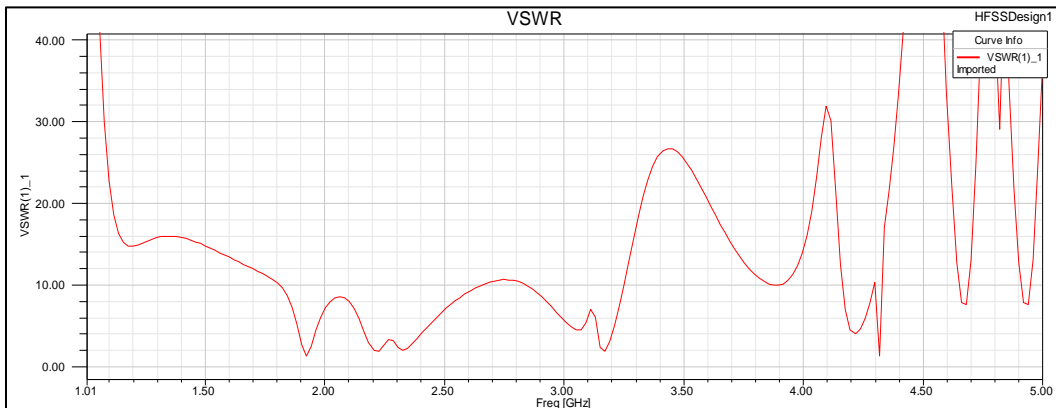


Fig 4. 14 VSWR of Antenna on RT Duroid and with slot

It shows minima at 1.9 GHz, 2.4 GHz and 4.5 GHz, respectively. These are the central resonant frequencies of the antenna based on RT Duroid with slot, discussed in detail in Section 3.2.3[90] [92].

4.3.5 Axial Ratio

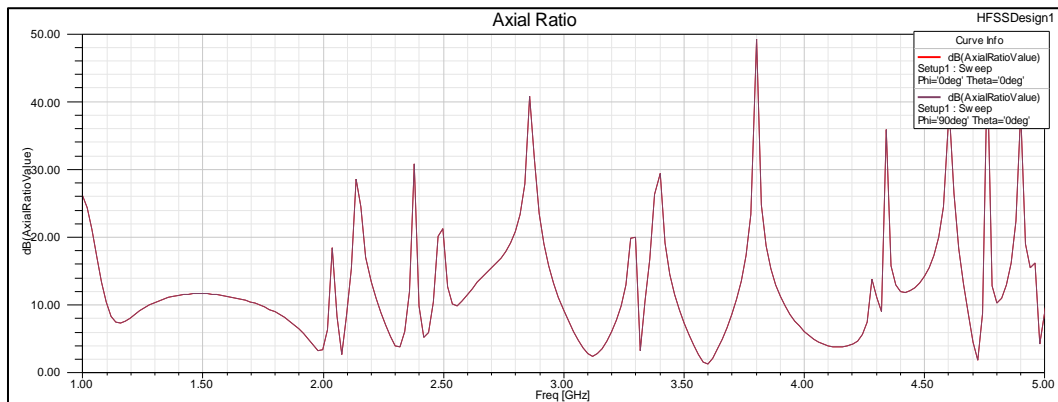


Fig 4. 15 Axial Ratio of Antenna on RT Duroid and with slot

The axial ratio of the antenna is shown in Fig 4.15 from which it is clear that the axial ratio is less than 6 dB at 1.9 GHz, 2.4 GHz, 3.44 GHz and 4.5 GHz.

4.4 Comparison of Tested Return loss of three Antennas

The Comparison of tested results of return loss of three prototypes is reported in Fig 4.16. Improvement in resonances, progressively appearing right from the first antenna prototype to the second and then to the third, is clearly observed in this figure. Gain increment is also evident from the comparison of

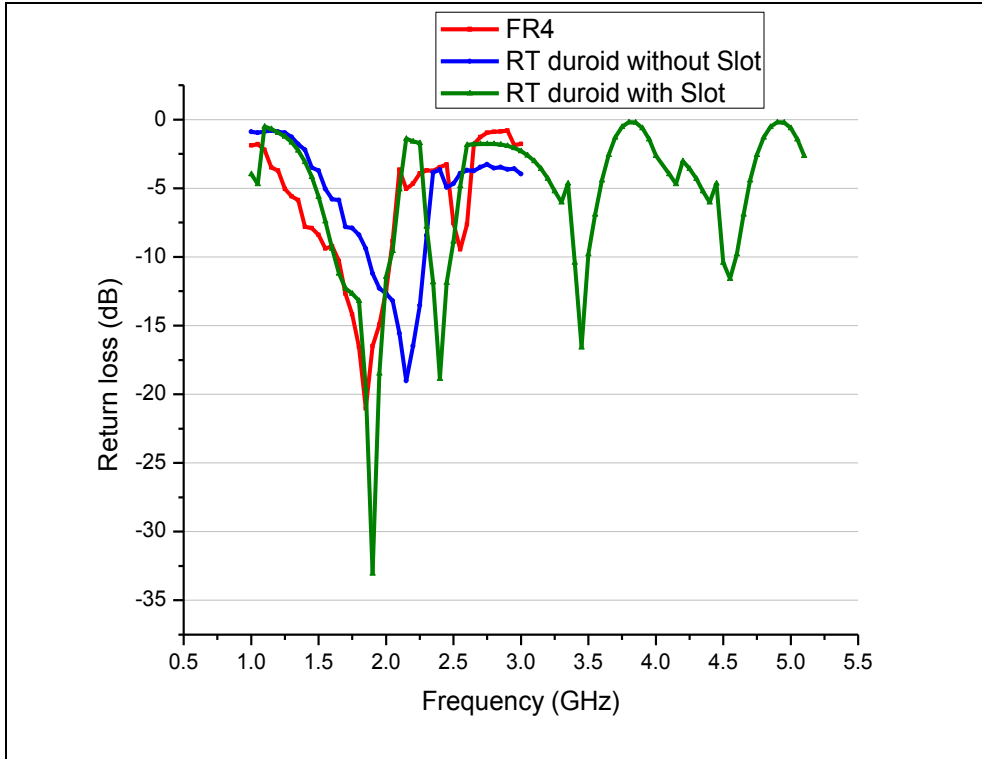


Fig 4. 16 Tested Return loss for three Prototypes

the three prototypes. The comparative values of return loss, which cross -10dB line are tabulated in the Table 4.4.

Table 4. 4 Comparison of Return loss of Three Prototypes

S. No	Antenna type	BW1(GHz)	BW2(GHz)	BW3(GHz)	BW4(GHz)
1	FR4	1.65-1.99			
2	RT Duroid WITHOUT SLOT	1.9-2.3			
3	RT Duroid WITH SLOT	1.6-2.05	2.35-2.5	3.4-3.5	4.45-4.6

From the Table 4.4, it is clearly demonstrated that the third antenna prototype not only offering the high gain at 1.9 GHz but also offering the gain for the most of mobile applications like GSM, PCS DCS, BLUETOOTH, partial WIFI and a part of WIBRO (Wireless Broadband) [86].

4.5 Gain measurement

Gain of an antenna is measured through the pattern by obtaining half power beam widths (HPBW) of mutually perpendicular Electric and Magnetic fields from the rectangular radiation pattern [5]. The gain and directivity are further obtained as discussed in section 1.4 of Chapter 1. The rectangular radiation pattern is measured with the arrangement mentioned below using a anechoic Chamber [80]. Further the antenna is then rotated from -180° to $+180^{\circ}$ for measuring power of E and H fields. This arrangement is adopted to measure the radiation pattern in the anechoic chamber for the test antenna prototypes. For the Horn feed and microstrip antennas, they are rotated by 90-deg to match the E-field at 0-deg position, for the measurement of E plane. Antenna is bent with feed and antenna's relative facing is same in H-plane measurement [93].

4.5.1 Antenna on FR4

The two dimensional plots measured for E field and H field are presented here for the antenna on FR4 Substrate.

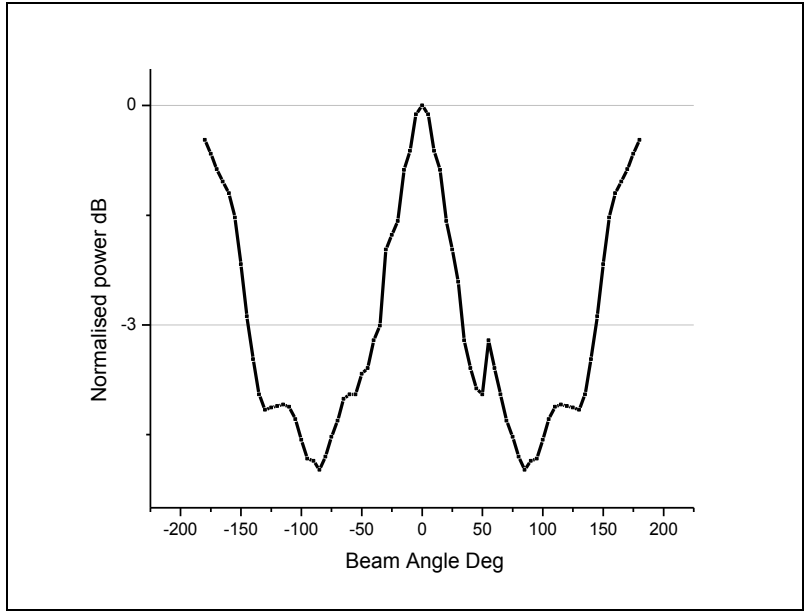


Fig 4. 17 E Plane of Antenna on FR4

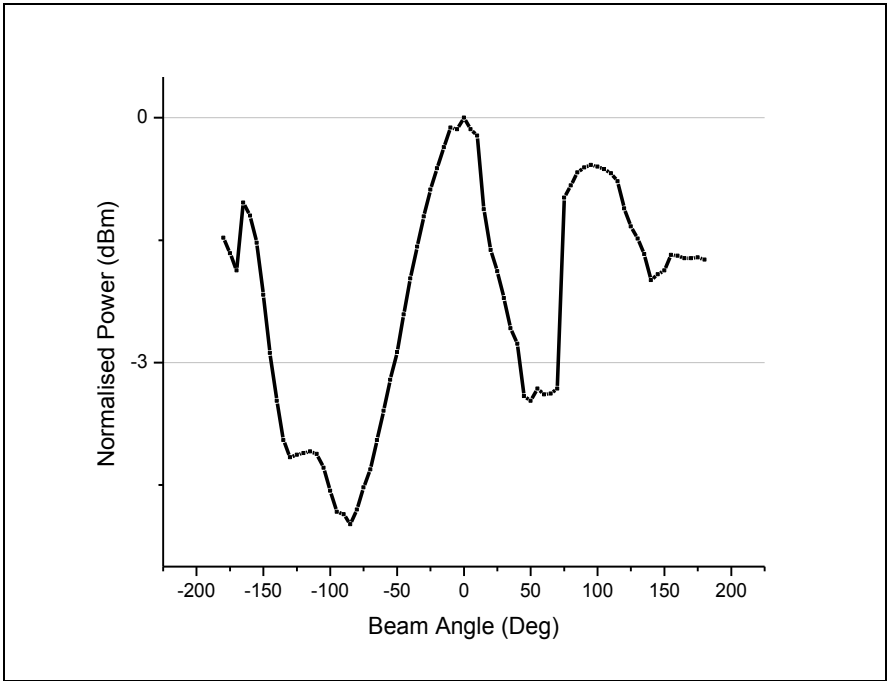


Fig 4. 18 H Plane of Antenna on FR4

From the equation 1.8, chapter 1, the two angles of half power beam widths corresponding to θ and ϕ are as shown in Fig 1.3. These can be measured in degrees in the above two figures of Fig 4.17 and Fig 4.18 as,

$$\text{HPBW E Plane- } \theta_1=54^\circ$$

$$\text{HPBW H Plane- } \theta_2= 56^\circ$$

$$D_o= [4\pi(180/ \pi)^2]/ \theta_1\theta_2 \approx 41,253/54^\circ \times 56^\circ =13.6$$

4.5.2 Antenna on RT Duroid and without slot

The rectangular plots measured for E field and H field are now presented for the antenna on RT Duroid and without slot.

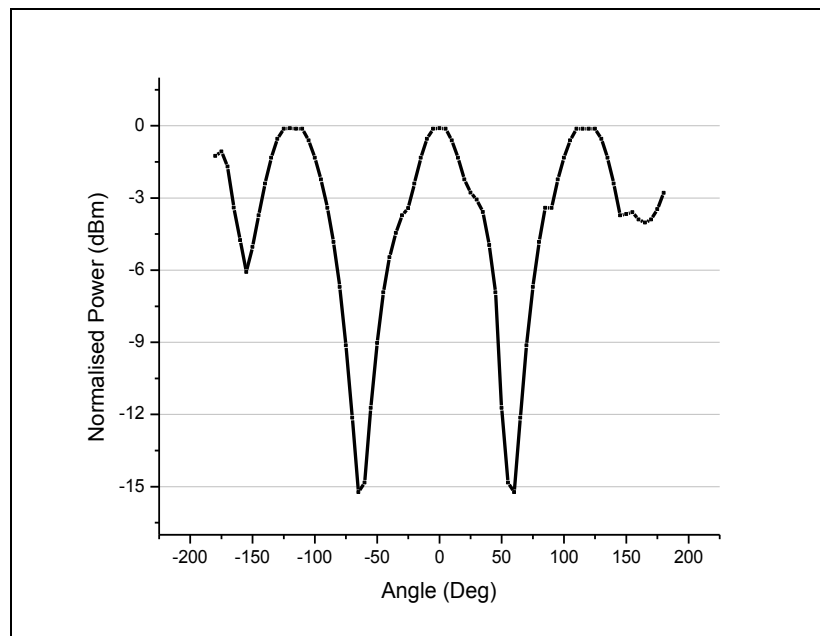


Fig 4. 19 E Plane of Antenna on RT Duroid and without slot

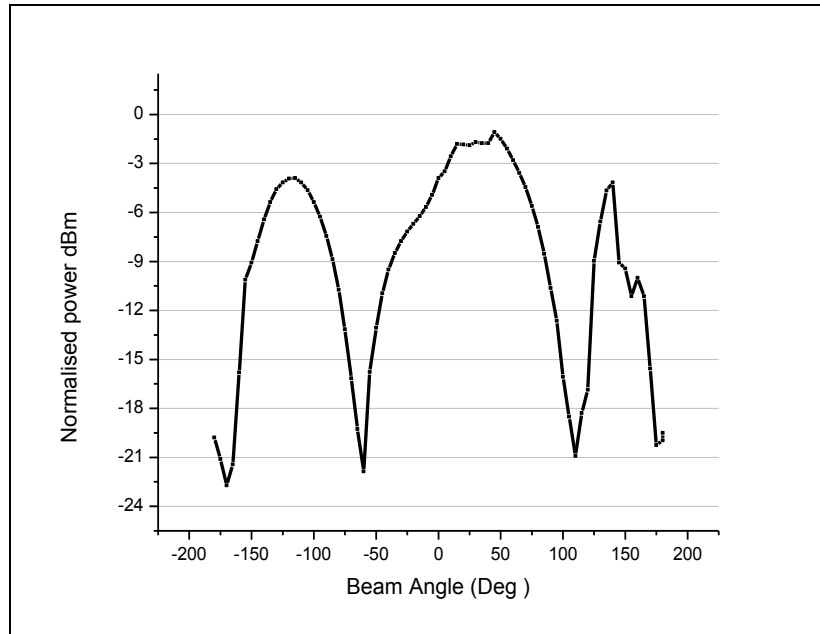


Fig 4. 20 H Plane of Antenna on RT Duroid and without slot

From the equation 1.6, chapter 1, the two angles of half power beam widths corresponding to θ and ϕ are as shown in Fig 1.3. These can be measured in degrees in the above two figures, Fig 4.19 and Fig 4.20, as

$$\text{HPBW E Plane- } \theta_1=45^0$$

$$\text{HPBW H Plane- } \theta_2= 56^0$$

$$D_0= [4\pi(180/ \pi)^2]/ \theta_1\theta_2 \approx 41,253/45^0 \times 56^0 =16.4$$

The antenna prototype with slot is also arranged as Horn feed and microstrip antennas rotated by 90-deg to maintain matching of E-field at 0-deg position for the measurement of E plane[83].

4.5.3 Antenna with slot

The radiation plots measured for E field and H field for the antenna on RT Duroid and with slot are presented in figures 4.21 and 4.22.

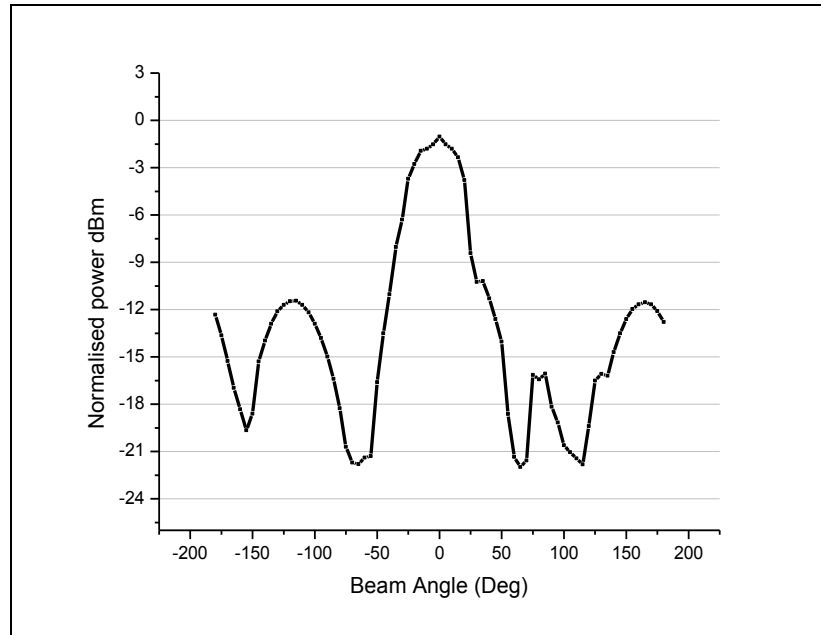


Fig 4. 21 E Plane of Antenna on RT Duroid and with slot

Antenna was bent Sideways with respect to feed and antenna's relative facing same, as in H-plane measurements as mentioned earlier.

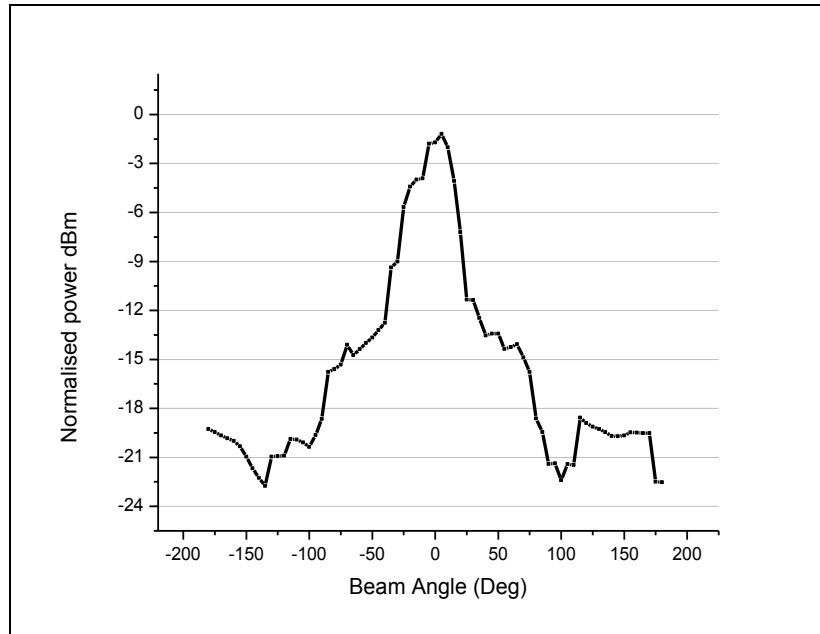


Fig 4. 22 H Plane of Antenna on RT Duroid and with slot

The HPBW angle in θ plane, corresponding to the E-field is measured from Fig 4.21. The HPBW angle in ϕ plane, corresponding to H-field is noted from Fig 4.22.

HPBW E Plane- $\theta_1=25^\circ$

HPBW H Plane- $\theta_2= 50^\circ$

$$D_o = [4\pi(180/\pi)^2] / \theta_1\theta_2 \approx 41,253/(25^\circ \times 50^\circ) = 33.1$$

Table 4. 5 Directivity

S. No	Antenna case	Directivity
1	FR4	13.6
2	Without slot	16.4
3	With slot	33.1

The directivity obtained for the three antenna samples are listed in table 4.5. A progressive improvement of gain is observed, beginning with the first antenna prototype to the third. It is clear that the inclusion of slots in the third antenna has aided sharpening of the beam.

4.6 Input Impedance of Antenna on RT Duroid and with slot

The graph for input impedance for the antenna prototype, shown in Fig 4.23, is obtained from the MATLAB code after considering the individual values of components of the antenna prototype. This graph shows the reactive term of the input impedance [82].

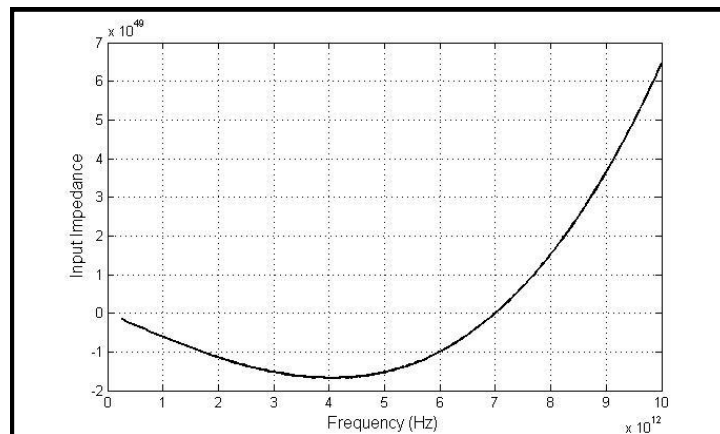


Fig 4. 23 Input Impedance of the Antenna on RT Duroid with slot

The input impedance value is derived from equation 3.7, considering the individual ‘nutshells’ of the antenna equivalent considering CRLH, SRR and Patch, with the slot on the either side of the two sided prototype antenna. The order of the nutshells of antenna indicates the current flow from source to sink.

From this graph, it is seen that the reactance is negative in entire range of frequency of interest. The result is also similar to the result reported in the paper [94], [95].

4.7 Summary of the Chapter

An extensive list of output parameters is discussed in this chapter, for the antennas fabricated according to the ideas reported in literature. Parameters like return loss, radiation pattern, gain measurement and input impedance plot are discussed in detail.

The resonant frequency of the antenna on FR4, from the simulation results, it resonates from 1.58 GHz to 1.95 GHz. The measured values for the same are in the range of 1.65 GHz to 1.99 GHz. This antenna covers the PCS and DCS bands. Limitation of this antenna is that for optimum power, its feeding increases the thickness of the mobile or wireless sets. The second prototype, antenna on RT Duroid and without slot, has size reduction in two aspects. Antenna size is reduced by 1 mm and also the overall PCB size is reduced by 20 mm. A wider band version of the antenna, with improved gain is achieved with a larger frequency bandwidth. The simulation results show that the antenna resonates from 1.95 GHz to 2.45 GHz. The measured values for the same were shifted towards left on the plot, i.e., towards lower frequencies, within 1.9 GHz to 2.3 GHz. This antenna covers the PCS, DCS and BLUETOOTH bands. The third prototype, the slot loaded metamaterial antenna exhibits resonances at 1.91 GHz, 2.4GHz 3.35GHz and 4.62 GHz. The prototype which has slots on the radiating

patches is proved to be resonating more number of bands compared to the prototype which doesn't have slots on the front side. It is seen that considering even these small deviations, there is a very good agreement between the design and experimental results of the work. Latter part of the chapter discusses the rectangular radiation patterns measured through an anechoic chamber. The half power beam widths (HPBW) for Electric and Magnetic fields are obtained by it. The gain and directivity were further measured, and discussed here. Amongst the gain obtained for the three prototypes, antenna based on RT Duroid and with slot has highest gain at resonant frequency.

Lastly, this chapter deals with the response of reactance of input impedance. It also supports that the resonating frequency of the third antenna, matches with the return loss response at 1.9 GHz.

Summary of the results is tabulated in Appendix 1. The frequency calculations of the structure are given in Appendix 3.

CHAPTER 5

CONCLUSIONS

Three prototype antennas were designed in the present work with the intention of using the concept of metamaterial structure, and thus, develop a revolutionary miniaturization method for RF devices. These antennas are of meander structure and printed on both sides of PCB. Improvements in antenna performance, as those regarding bandwidth and efficiency are achieved in this work by using CRLH, two unsymmetrical different sized SRRs and patches. The first prototype, fabricated on FR4, is suitable for PCS and DCS communications. The test results for the second prototype clearly demonstrate the antenna miniaturization achieved by the collective effect of using edge feeding, patch and the substrate RT Duroid. This prototype also exhibits wider bandwidth with slightly improved gain, and works in the PCS, DCS and partial BLUETOOTH bands. Whereas, slots were introduced in the radiating patches for the third prototype, and this has led to increased power of radiation in the overall structure. This third prototype has broad bandwidth and high gain and covers PCS, DCS, WIBRO, BLUETOOTH and slices of the other bands. Hence, it is also very useful in RF devices like, wireless sets which are lightweight and compact. These antennas can also fit in slim mobile handset working in different commercial bands since the proposed antenna is implemented on PCB.

Parameters like return loss, radiation pattern, gain measurement and input impedance show that the third antenna is very efficient for mobile applications. The mechanical etching method used for in its fabrication has also proved to be better than the chemical method.

The resonating bands of the three antennas are discussed in this work considering the -10dB power of return loss response of individual antennas. The resonating frequencies, according to response of reactance component of input impedance, and that according to the return loss response of the antenna, both, show that their values match very well at 1.9GHz.

CHAPTER 6

FUTURE SCOPE

The final prototype antenna (3rd in sequence) designed and fabricated in the present work is lightweight, slim, low cost and can be employed for batch process. Also, this prototype is integrable in RF systems. Though, this work has led to development of antenna with such qualities in RF range, it can further be extended to be used for other frequency ranges corresponding to wireless systems. The developed prototype can operate at different frequency bands for various applications, if it is setup in working communication range. The presented antenna can also be fabricated with-in the chip of SOC (System on Chip). Furthermore, the estimation of Specific Absorption Rate (SAR) levels of the presented antenna may also be done while it is used for mobile handsets. Also, this antenna can be used very effectively in small wireless sets for near distance communications. Besides the above, some of the following may also be taken up for future work:

- Dimensions of individual cells of an antenna can be varied, for antenna to resonate in the desirable frequency bands.
- Array of SRRs with meander structure can also be used for conformal antennas with flexible substrate.
- Estimate the field strength at different nodes.

- Determination of negative values of epsilon and mu in resonant frequency range through Mathematical Analysis.
- Correction/reduction of Axial ratio anomalies.
- Correction/reduction of irregularity in H-plane pattern.

REFERENCES

- [1] “White paper on Spectrum”. Technical white paper, Huawei. February 3, 2013.
- [2] Howell, J. Q., “Microstrip Antennas,” IEEE Trans. Antennas Propagation, Vol. AP-23, January 1975, pp. 90–93.
- [3] H. T. Chattha, Y. Huang, and Y. Lu, “A Further Study of Planar Inverted-F Antenna” IEEE Antennas and Propagation Magazine; pp: 4244-4396 March 2009.
- [4] P.S. Hall, C. T. P. Song, H.H. Lin, H.M. Chen, Y.F. Lin, P.S. Cheng, “Parametric study on the characteristics of planar inverted-F antenna” IEEE Proceedings; Microwaves. Antennas and Propagation., Vol.152, No.6, December 2005.
- [5] John Kraus, Antennas, 2nd edition, McGraw-Hill, Inc.
- [6] C. A. Balanis; ANTENNA THEORY: ANALYSIS AND DESIGN, 2nd ED John Wiley & Sons, 01-Sep-2007.
- [7] Trevor S. Bird “Definition and Misuse of Return Loss” IEEE Antennas & Propagation Magazine, April 2009.
- [8] D. Slater, Near-Field Antenna Measurements, Artech House, Boston, 1991.

- [9] DAVID M. POZAR Microstrip Antennas PROCEEDINGS OF THE IEEE, VOL. 80, NO. 1, JANUARY 1992.
- [10] Marek Bugaj, Rafal Przesmycki, Leszek Nowosielski, and Kazimierz Piwowarczyk "Analysis Different Methods of Microstrip Antennas Feeding for Their Electrical Parameters" PIERS Proceedings, Kuala Lumpur, MALAYSIA, March 27-30, 2012.
- [11] K. Tilley, D Wu and K Chang , "Coplanar waveguide fed coplanar strip dipole antenna", *Electronic Letters*, Vol 30 no30 pp 176,177, 1994.
- [12] Lin, Y.-F.; Liao, P.-C.; Cheng, P.-S.; Chen, H.-M.; Song, C.T.P.; Hall, P.S.; , "CPW-fed capacitive H-shaped narrow slot antenna," *Electronics Letters* , vol.41, no.17,pp. 940- 942, 18 Aug. 2005.
- [13] Garg, Ramesh; Reddy, V.S., "Edge feeding of microstrip ring antennas," *IEEE Transactions on Antennas and Propagation*, vol.51, no.8, pp.1941, 1946, Aug. 2003.
- [14] D .T. Emerson, "The work of Jagadish Chandra Bose: 100 years of millimeter-wave research" *Microwave Theory and Techniques*, *IEEE Transactions* 45 (12), pp 2267 1997-12.
- [15] Engheta, Nader; Richard W. Ziolkowski. "Metamaterials: physics and engineering explorations", Wiley & Sons. pp. 5, Chap 1. 2006.
- [16] Lindell, Ismo V.; Sihvola, Ari H., and Kurkijarvi, Juhani, "Karl F. Lindman: The last Hertzian, and a harbinger of electromagnetic chirality" , *IEEE Antennas and Propagation Magazine* 34 (3): 24–30, June 1992.

- [17] Re H. S. Chen, L. X. Ran, T. Jiang, F. Huang, X. M. Zhang, and K. S. Chen, "Magnetic properties of S-shaped split-ring resonators," *Progress Electromagnetics Research.*, vol. 51, pp. 231–247, 2005 retrieved 2010.
- [18] Eleftheriades, George V.; Balmain, Keith G. *Negative-refraction metamaterials: fundamental principles and applications.* Wiley-IEEE Press. pp. v, xiii, xiv, 4–7, 12, 46–48, 53, July 2005.
- [19] V. G. Veselago, "The electrodynamics of substances with simultaneously negative values of ϵ and μ ," *Sov. Phys. Uspekhi*, vol. 10, no. 4, pp. 509-514, Jan-Feb. 1968.
- [20] Pendry, J.; Holden, A.; Stewart, W.; Youngs i, I. "Extremely Low Frequency Plasmons in Metallic Mesostructures". *Phys. Rev. Lett.* 76 (25): 4773–4776, 1996.
- [21] El Mrabet, O.; Aznabet, M.; Falcone, F.; Essaaidi, M.; Sorolla, M., "A compact antenna based on Split Ring Resonator," *Antennas and Propagation (EuCAP), 2010 Proceedings of the Fourth European Conference on* , vol., no., pp.1,3, 12-16 April 2010.
- [22] A. Gummalla, M. Achour, G. Poilasne, and V. Pathak, "Compact Dual-Band Planar Metamaterial Antenna Arrays For Wireless LAN", *Antennas and Propagation Society International Symposium 2008,IEEE*, 7-11 July 2008.
- [23] G.V. Eleftheriades, M.A. Antoniadis and F. QureshiSome , "Antenna Applications of Negative-Refractive-Index Transmission-Line (NRI-TL)

Metamaterials” On page(s): 402 - 405 Antennas and Propagation Society International Symposium 2006, IEEE .

- [24] Mittra, R.; “Performance enhancement of small antennas using metamaterials”., 19th International Conference challenges and future directions Applied Electromagnetics and Communications, 2007. page(s)1 – 4.
- [25] Shah Nawaz Burokur, Mohamed Latrach and Sergre Toutain, “Theoretical Investigation of a Circular Patch Antenna in the Presence of a Left-Handed Mematerial, IEEE Antennas and Wireless Propagation Letters, Vol. 4, 2005.
- [26] A. Yu, F. Yang, and A. Elsherbeni “ A Dual Band Circularly Polarized Ring Antenna Based on Composite Right and Left Handed Metamaterials” Progress In Electromagnetics Research, PIER 78, 73–81, 2008.
- [27] Ning Zhu, Peng Jin, Richard W. Ziolkowski and Hao Xin “Design of a GPS L1 Rectenna by Using a Metamaterial-inspired Electrically Small Antenna” AP-S/URSI 2011. 889-892.
- [28] Qingshan Yang, Xiangkun Zhang, and Yunhua Zhang, “A Improved Structure for Substrate Integrated Waveguide Composite Right/Left-handed Cell” Progress In Electromagnetics Research Symposium Proceedings, Moscow, Russia, August 19-23, 2012. 645-647.
- [29] Dalin Jin; Bing Li; Jingsong Hong, "Gain improvement of a microstrip patch antenna using metamaterial superstrate with the zero refractive

- index," Microwave and Millimeter Wave Technology (ICMMT), 2012 International Conference on , vol.3, no., pp.1,3, 5-8 May 2012.
- [30] Andryieuski, A.; Malureanu, Radu; Alabastri, A.; Lavrinenko, A.V., "Bulk metamaterials: Design, fabrication and characterization," ICTON Mediterranean Winter Conference,2009. ICTON-MW 2009. 3rd , vol., no., pp.1,5, 10-12 Dec. 2009.
- [31] Ghanshyam Singh, "Double Negative Left-Handed Metamaterials for Miniaturization of Rectangular Microstrip Antenna", J. Electromagnetic Analysis & Applications, pp. 347-351, Feb 2010.
- [32] "Electronic Design Software, HFSS User's Guide" Ansoft Corporation 2003.
- [33] Chunchen Lin, Iftekhar O. Mirza, Shouyuan Shi, and Dennis W. Prather Tuneable Meta-Material Split-Ring Resonators For Impedance Matching Antennas for Broadband Applications.
- [34] Juan Domingo Baena, Jordi Bonache, Ferran Martín, Ricardo Marqués Sillero, Francisco Falcone, Txema Lopetegui, Miguel A. G. Laso, Joan García-García, Ignacio Gil, Maria Flores Portillo, and Mario Sorolla, "Equivalent-Circuit Models for Split-Ring Resonators and Complementary Split-Ring Resonators Coupled to Planar Transmission Lines." IEEE Transactions on Microwave Theory and Techniques, vol.53,NO.4, April2005.

- [35] Tang, T.G., Tieng, Q.M.; Gunn, M.W., "Equivalent circuit of a dipole antenna using frequency-independent lumped elements," *Antennas and Propagation, IEEE Transactions on*, vol.41, no.1, pp.100,103, Jan 1993.
- [36] D.E. Zelenchuk, V.F. Fusco "Planar High-Gain WLAN PCB Antenna";*IEEE Antennas and Wireless Propagation Letters (Impact Factor: 1.67)*. 02/2009.
- [37] Mazinghi, A.; Albani, M.; Freni, A., "Conductor losses effect on RLSA antennas," *ICECom, 2010 Conference Proceedings*, vol., no., pp.1,3, 20-23 Sept. 2010.
- [38] Y. Wang, J. Li, and L.-X. Ran, "An equivalent circuit modeling method for ultra-wideband antennas," *Progress In Electromagnetics Research*, Vol. 82, 433-445, 2008.
- [39] M. Ansarizadeh and A. Ghorbani R. A. Abd-Alhameed, "An Approach to Equivalent Circuit Modeling of Rectangular Microstrip Antennas"; *Progress In Electromagnetics Research B*, Vol. 8, 77–86, 2008.
- [40] Atsushi Sanada, Christophe Caloz, and Tatsuo Itoh, "Characteristics of the Composite Right/Left-Handed Transmission Lines" *IEEE Microwave and Wireless Components Letters*, VOL.14, NO.2, February 2004.
- [41] Qingshan Yang, Xiang kun Zhang and Yunhua Zhang ; "A Improved Structure for Substrate Integrated Waveguide Composite Right/Left-handed Cell" *Progress In Electromagnetics Research Symposium Proceedings, Moscow, Russia, August19{23,2012*

- [42] J. J. Sanchez-Martinez, E. Marquez-Segura, P. Otero and C. Camacho-Penalosa “Artificial Transmission Line with Left/Right-Handed Behavior Based on Wire Bonded Interdigital Capacitors” Progress In Electromagnetics Research B, Vol.11,245–264,2009.
- [43] Andrea Alù, Filiberto Bilotti, Nader Engheta, and Lucio Vegni, “Subwavelength, Compact, Resonant Patch Antennas Loaded With Metamaterials” ;IEEE Transactions on Antennas and Propagation, vol.55, NO.1, January 2007.
- [44] Koray., Aydinand., Ekmel., Ozbay., “Negative refraction through an impedance-matched left-handed metamaterial slab”,Vol.23,No.3/March2006/Journal of Optics Society. America. B.
- [45] B.Chen ,Y.-C.Jiao, F.-C.Ren, L.Zhang, and F.-S. Zhang “Design of Open Slot Antenna for Bandwidth Enhancement with a Rectangular Stub” Progress In Electromagnetics Research Letters, Vol. 25,109-115,2011.
- [46] Hamid, M.; Hamid, R., "Equivalent circuit of dipole antenna of arbitrary length," Antennas and Propagation, IEEE Transactions on , vol.45, no.11, pp.1695,1696, Nov 1997.
- [47] Yuandan Dong and Tatsuo Itoh, “Miniaturized Patch Antennas loaded with plementary Split-Ring Resonators and Reactive Impedance Surface” EuCAP 2011 - Convened Papers.
- [48] S. S. Karthikeyan and R. S. Kshetrimayum “Compact Wideband Bandpass Filter using Open Slot Split Ring Resonator and CMRC ;Progress In Electromagnetics Research Letters,Vol.10,39-48,2009.

- [49] A.B. Mutiara, R.Refianti, Rachmansyah "Design of Microstrip Antenna for Wireless Communication at 2.4 GHZ Journal of Theoretical and Applied Information Technology 30th November 2011. Vol. 33 No.2.
- [50] J. Montero-de-Paz, E. Ugarte-Munoz and F. J. Herraiz-Martinez "Multifrequency Self-diplexed Single Patch Antennas Loaded with Split Ring Resonators" Progress In Electromagnetics Research, Vol. 113, 47-66, 2011.
- [51] Kai-Cheng Chil, Shih-Yuan Chen, and Powen Hsu "Miniaturization of Slot Loop Antenna Using Split-Ring Resonators" Antennas and Propagation, IEEE Transactions on , vol.56, no.7, pp.3513,3516, July 2009.
- [52] Han, T. C.; Rahim, M. K A; Masri, T.; Karim, M. N A, "Left Handed Metamaterial Design for Microstrip Antenna Application," Microwave Conference, 2007. APMC 2007. Asia-Pacific , vol., no., pp.1,4, 11-14 Dec. 2007.
- [53] D. Laila, R. Sujith, S. M. Nair, C. K. Aanandan, K. Vasudevan, and P. Mohanan, "Mobile antenna with reduced radiation hazards towards human head," Progress In Electromagnetics Research Letters, Vol. 17, 39-46, 2010.
- [54] X. Sun, G. Zeng, H.-C. Yang, Y. Li, X.-J. Liao, and L. Wang, "Design of an edge-fed quad-band slot antenna for GPS/wimax/WLAN applications," Progress In Electromagnetics Research Letters, Vol. 28, 111-120, 2012.

- [55] John Coonrod, "High frequency PCBs using Hybrid and Homogenous Constructions," PCB West 2010, September 2010.
- [56] Si, L.-M. and X. Lv, "CPW-FED multiband omnidirectional planar microstrip antenna using composite metamaterial resonators for wireless communications," *Progress In Electromagnetics Research*, Vol. 83, 133-146, 2008.
- [57] H. Mirzaei and G.V. Eleftheriades, "A compact frequency-reconfigurable metamaterial-inspired antenna", *IEEE Antennas and Wireless Propagation Letters*, vol. 10, pp. 1154-1157, Oct, 2011.
- [58] Wenquan Cao; Bangning Zhang; Aijun Liu; Tongbin Yu; Daosheng Guo; Yi Wei, "Gain Enhancement for Broadband Periodic Endfire Antenna by Using Split-Ring Resonator Structures," *Antennas and Propagation, IEEE Transactions on* , vol.60, no.7, pp.3513,3516, July 2012.
- [59] Ziolkowski, R.W., "Design, fabrication, and testing of double negative metamaterials," *Antennas and Propagation, IEEE Transactions on*, vol.51, no.7, pp.1516,1529, July 2003.
- [60] Rashed, J.; Chen-To Tai, "A new class of resonant antennas," *Antennas and Propagation, IEEE Transactions on* , vol.39, no.9, pp.1428,1430, Sep 1991.
- [61] Wook-Ki Park; Soon-Soo Oh; Young-Hwan Lee; Hyo-Dal Park, "Frequency-Tunable Waveguide Antenna With Miniaturized Aperture Using a Varactor-Loaded Split-Ring Resonator," *Antennas and Wireless Propagation Letters, IEEE* , vol.9, no., pp.1233,1236, 2010.

- [62] Alici, Kamil Boratay; Ozbay, E., "Electrically small split ring resonator antennas," *Journal of Applied Physics* , vol.101, no.8, pp.083104,083104-4, Apr 2007.
- [63] Sidana, Y.; Chaudhary, R.K.; Srivastava, K.V., "A novel dual-band hexagonal patch antenna coupled with complementary split ring resonator," *Microwave Conference Proceedings (APMC), 2012 Asia-Pacific* , vol., no., pp.1343,1345, 4-7 Dec. 2012.
- [64] Kim, O.S.; Breinbjerg, O., "Miniaturized planar split-ring resonator antenna," *Antennas and Propagation Society International Symposium, 2009. APSURSI '09. IEEE* , vol., no., pp.1,4, 1-5 June 2009.
- [65] Gupta, S.; Mumcu, G., "A small complementary split ring resonator loaded circularly polarized patch antenna," *Electromagnetic Theory (EMTS),s Proceedings of 2013 URSI International Symposium on* , vol., no., pp.94,96, 20-24 May 2013.
- [66] Mirza, I.O.; Shouyuan Shi; Fazi, C.; Mait, J.N.; Prather, D.W., "A study of loop antenna miniaturization using split ring resonators," *Antennas and Propagation Society International Symposium, 2007 IEEE* , vol., no., pp.1865,1868, 9-15 June 2007.
- [67] A. Yu, F. Yang, and A. Elsherbeni, A Dual Band Circularly Polarized Ring Antenna based on Composite Right and Left handed Metamaterials. *Progress In Electromagnetics Research, PIER78,73–81,2008.*
- [68] Data sheet,"RT/duroid 5880LZ High Frequency Laminates" Rogers corporation.

- [69] C. Deng and Y. J. Xie y J. F. “Yuan Dual Band-Notched Design of Rectangular Monopole Antenna for UWB Applications” Progress In Electromagnetics Research C, Vol. 14, 213-225, 2010.
- [70] Jia Chen, Enrang Zheng, and Wanzhao Cui “Symmetric Unit Cell Models for Composite Right/Left-handed Transmission Lines (CRLH-TL)” Metamaterials Progress In Electromagnetics Research Symposium, Beijing, China, pp: 619-624, March 23-27, 2009.
- [71] Vit Sipal, Alireza Ajami, and Dirk Heberling “Effect of Substrate Dimensions on Zeroth-Order Resonator Antennas”; IEEE Antennas and Wireless Propagation Letters, vol.9,2010.
- [72] Y. Liu and X. Chen “A Novel Microstrip-fed Dielectric ROD Antenna Array with High Gain” Progress In Electromagnetics Research Symposium Proceedings, Moscow, Russia, August 19–23, 2012. 1187.
- [73] Dau-Chyrh Chang, Bing-Hao Zeng and Ji-Chyun Liu “High Performance Antenna Array with Patch Antenna Elements PIERS Proceedings, Xi’an, China, March 22–26, 2010.
- [74] Hyung Kuk Yoon, Jin A. Park, Yohan Lim, Young Joong Yoon, and Cheon-Hee Lee “Miniaturization of a Ultra Wide Band Antenna” PIERS Proceedings, Cambridge, USA, July 5–8, 2010.
- [75] L.J. Rogla, J. Carbonell and V.E. Boria “Study of equivalent circuits for open-ring and split-ring resonators in coplanar waveguide technology “IET Microwaves, Antennas Propagation., Vol. 1, No. 1, February 2007.

- [76] M. Ansarizadeh, A. Ghorbani and R. A. Abd-Alhameed, "AN APPROACH TO EQUIVALENT CIRCUIT MODELING OF RECTANGULAR MICROSTRIP ANTENNAS", Progress In Electromagnetics Research B, Vol. 8, 77–86, 2008.
- [77] Herraiz-Martinez, F.J.; Gonzalez-Posadas, V.; Segovia-Vargas, D., "Multi-frequency microstrip patch antennas based on metamaterial structures," Antennas and Propagation Society International Symposium, 2007 IEEE , vol., no., pp.3484,3487, 9-15 June 2007.
- [78] C. J. Lee, K. M. K. H. Leong, and T. Itoh, "Composite right/left-handed transmission line based compact resonant antennas for RF module integration," IEEE Transaction on Antennas and Propagation, col. 54, issue 8, pp. 2283-2291, Aug. 2006.
- [79] Yamaguchi, R.; Komiya, K., "Gain measurement of base station antenna using short reference antenna," Antennas and Propagation (EUCAP), 2012 6th European Conference on Antennas and Propagation, vol., no., pp.1581,1584, 26-30 March 2012.
- [80] M Ramanujam, P.; Lopez, L. F.; Fermella, L.R.; Reynolds, R. L., "Phase-center effects on wide-band horn pattern measurements in small anechoic chambers," Antennas and Propagation Society International Symposium, 1995. AP-S. Digest , vol.4, no., pp.1742,1745 vol.4, 18-23 June 1995.
- [81] Hamid Torpi and Yasin Damgac "Design of Dual-band Reconfigurable Smart Antenna" Progress In Electromagnetics Research Symposium , Prague, Czech Republic, pp 425-30, August 27-30, 2007.

- [82] Geyi, W., P. Jarmuszewski, and Y. Qi, "The Foster reactance theorem for antennas and radiation Q," IEEE Trans. Antenna Propagation., Vol. AP-48, No. 3, 401–407, 2000.
- [83] Rodriguez, V., "A cone shaped taper anechoic chamber for antenna measurements in the 200 MHz to 18GHz frequency range," Antennas and Propagation Society International Symposium (APSURSI), 2012 IEEE , vol., no., pp.1,2, 8-14 July 2012.
- [84] YU-Ming Lee, Shuming T. Wang, Hsien Chiao Teng and Shen Cherng, "A Functional Microstrip Circuit Module for Annular Slot Antenna" Progress in Electromagnetics Research., Vol 136, pp.255-267, 2013.
- [85] Liu, J., , W.Y. Yin, and S. He, , "A new defected ground structure and its application for miniaturized switchable antenna," Progress In Electromagnetics Research, Vol. 107, 115-128, 2010.
- [86] Ao Tang; Ji Xian Sun; Ke Gong, "Mobile propagation loss with a low base station antenna for NLOS street microcells in urban area," Vehicular Technology Conference, 2001. VTC 2001 Spring. IEEE VTS 53rd , vol.1, no., pp.333,336 vol.1, 2001.
- [87] Phillip H. Smith, "Transmission Line Calculator," Electronics, Vol. 12, No. 1, pp 29-31, January 1939.
- [88] Tanabe, M.; Masuda, Y., "Axial ratio characteristics of an Archimedean spiral antenna on a thin magnetic material," Electromagnetics in Advanced Applications (ICEAA), 2010 International Conference on , vol., no., pp.414,417, 20-24 Sept. 2010.

- [89] Y.-Q. Zhang, X. Li, L. Yang, and S.-X. Gong, "Dual-band Circularly Polarized Antenna with Low Wide-Angle Axial-Ratio for Tri-Band GPS Applications", *Progress In Electromagnetics Research C*, Vol. 32, 167-179, 2012.
- [90] M. Dogan, G. K. Sendur, and F. Ustuner, " Optimization of Aperture Coupled Microstrip Patch Antennas", *Progress In Electromagnetics Research Symposium Proceedings*, Cambridge, USA, pp:657-660, July 5-8, 2010.
- [91] C. D. Nikolopoulos, K. D. Stravoskoufis, and C. N. Capsalis, "A New Small and Low-cost Wideband PIFA with Corrugations Based on Digital Dividend", *PIERS Proceedings*, Moscow, Russia, 1566-69, August 19-23, 2012.
- [92] S. N. Khan, J. Hu, J. Xiong, and S. He, "Circular fractal monopole antenna for low VSWR UWB applications," *Progress In Electromagnetics Research Letters*, Vol. 1, 19-25, 2008.
- [93] Rodriguez, V., "An open-boundary quad-ridged guide horn antenna for use as a source in antenna pattern measurement anechoic chambers," *Antennas and Propagation Magazine, IEEE* , vol.48, no.2, pp.157,160, April 2006.
- [94] Ayca Erentok, Richard W. Ziolkowski, "Metamaterial-Inspired Efficient Electrically Small Antennas" *IEEE Transactions on Antennas and Propagation*, Vol. 56, NO. 3, pp:691-701. MARCH 2008.

- [95] James T. Aberle, “Non-Foster Reactances for Electrically-Small Antennas, High-Impedance Surfaces, and Engineered Materials”, IEEE Waves and Devices., 19 Feb 2010.

APPENDIX 1

S. No	Antenna Type	Center Frequency	Parameter		
			Gain dB	VSWR	Axial Ratio dB
1	FR4	1.8 GHz	-0.1	0.01	8
2	WITHOUT SLOT	2.15GHz	3	0.18	6
3	WITH SLOT	1.9 GHz	-2	1.2	2
		2.4 GHz	-2	2	5
		3.44GHz	-3	>2	5
		4.5GHz	-2	3	12

APPENDIX 2

MATLAB CODE FILE FOR COMPUTATION OF INPUT IMPEDANCE EQUATION

```
f = 1*10^12:0.1*10^12:12*10^12;
[w] =2*pi*f;
freq=f;
[A]=(12.5*w.^8)*10.^(-8))-5.23*10.^-54*w.^6+2.4*10.^-24*w.^4-2.16*10.^-
21*w.^2+1;
[B]=50*10.^-94*w.^9-99.5*10.^-75*w.^7+17.4*10.^-54*w.^5-2.4*10.^-
33*w.^3+13.2*10.^-12*w;
[C]=49.8*10.^-85*w.^8-17.4*10.^-45*w.^6+17.4*10.^-45*w.^4-14.3*10.^-
24*w.^2;
[D]=(-12.4*10.^-73*w.^7)+2.4*10.^-45*w.^5-6.42*10.^-32*w.^3+1.08*10.^-
12*w;
A=A';
B=B';
C=C';
D=D';
f=f';
Z= (A+iB)/(C+iD);
plot(f, Z);
```

APPENDIX 3

FREQUENCY CALCULATIONS

$$\delta_L = 1.9 \text{ GHz}$$

$$\delta_R = 4.6 \text{ GHz}$$

$$\delta_L = \frac{1}{2\pi\sqrt{1.0 \times 10^{-9} \times (x) \times 10^{-12}}}$$

$$\Rightarrow 1.9 \times 10^{12} = \frac{1}{2\pi\sqrt{x \times \sqrt{10 \times 10^{-10}}}}$$

$$\Rightarrow \sqrt{x} = \frac{0.026}{10^2}$$

$$\Rightarrow x = \frac{6.8 \times 10^{-4}}{10^4}$$

$$\Rightarrow x = 0.68 \times 10^{-9}$$

$$f_h = \frac{1}{2\pi\sqrt{(1 \times 10^{-9} \times 1 \times 10^{-12})}}$$

$$= \frac{1}{2\pi\sqrt{(1 \times 10^{-21})}}$$

$$\therefore \omega = \frac{1}{\sqrt{(1 \times 10^{-9} \times 1 \times 10^{-12})}}$$

$$= \frac{1}{\sqrt{(10^{-21})}}$$

$$f_h = \frac{1}{2\pi\sqrt{10 \times 10^{-10}}}$$

$$\begin{aligned}
&= \frac{10^{10}}{2\pi\sqrt{10}} \\
&= 0.05 \times 10^{10} \\
&= 5 \times 10^{12}
\end{aligned}$$

$$f_c = 1.9 \times 10^{12} \text{ Hz}$$

$$\omega = \sqrt{LC}$$

$$\omega = \frac{1}{\sqrt{Lr \times Cc}}$$

$$\Rightarrow 2\pi F = \frac{1}{\sqrt{Lc \times Cr}}$$

$$\Rightarrow 2\pi \times 1.9 \text{ GHz} = \frac{1}{\sqrt{1 \times 10^{-9} \times c}}$$

$$\Rightarrow \sqrt{c} = \frac{1}{\sqrt{10 \times 2\pi \times 10^{-4} \times 1.9 \times 10^{12}}}$$

$$\Rightarrow \sqrt{c} = \frac{10^{-8}}{\sqrt{10 \times 3.8\pi}}$$

$$\Rightarrow \sqrt{c} = 0.026 \times 10^{-8}$$

$$\therefore c = 6.7 \times 10^{-4} \times 10^{-16}$$

$$= 6.7 \times 10^{-20}$$

$$f_h = 4.62 \text{ GHz}$$

$$4.62 \times 10^{12} = \frac{1}{2\pi \sqrt{\frac{1 \times 10^{-9}}{L} \times \frac{x \times 10^{-12}}{C}}}$$

$$\Rightarrow 4.62 \times 10^{12} = \frac{1}{2\pi \times \sqrt{x} \times \sqrt{10 \times 10^{-10}}}$$

$$\Rightarrow \sqrt{x} = \frac{1}{\sqrt{10} \times 2\pi \times 4.62 \times 10^{12} \times 10^{-10}}$$

$$\Rightarrow \sqrt{x} = 0.011 \times 10^{-2}$$

$$\therefore x = 1.21 \times 10^{-6}$$

$$= 1\mu F$$

$$f_h = 4.62 \text{ GHz}$$

$$4.62 \times 10^{12} = \frac{1}{2\pi \times \sqrt{\frac{1 \times 10^{-9}}{L} \times \frac{x \times 10^{-12}}{C}}}$$

$$\sqrt{x} = \frac{1}{\sqrt{10} \times 4.62 \times 10^{12} \times 10^{-10}}$$

$$= 0.068 \times 10^{-2}$$

$$\therefore x = 0.47 \times 10^{-6}$$

CURRICULAM VITAE



Email: prasanti@ddn.upes.ac.in

Working as Assistant Professor in the College of Engineering, University of Petroleum and Energy Studies, Dehradun, Uttarakhand. She has 13 years of Experience in Teaching. Her research interests are

- Antenna Design
- RF Networks
- FPGA Synthesis
- VLSI & Embedded System
 - Ph.D (Pursuing) from University of Petroleum and Energy Studies, Dehradun, India since June 2010.\
 - B. Tech. ECE from Jawahar Lal Nehru Technological University, Kakinada, Andhra Pradesh.
 - M. Tech. DSCE from Jawahar Lal Nehru Technological University Ananthapur, Andhra Pradesh

RESEARCH PUBLICATIONS

1. N. Prasanthi Kumari, Praful Ranjan, Piyush Kuchhal “DESIGN AND FABRICATION OF MINIATURIZED METAMATERIAL ANTENNA FOR MOBILE AND WIRELESS APPLICATIONS” International Journal of Advances in Engineering & Technology, Sept. 2013. ©IJAET ISSN: 22311963 1687 Vol. 6, Issue 4, pp. 1687-1692.
2. N. Prasanthi Kumari, Dr. Ravi Gowri, Praful Ranjan, Dr. Piyush Kuchhal, “Design of Double sided Metamaterial Antenna for Mobile Handset Applications IEEE International Conference SPIN-2014, Delhi, India.
3. N. Prasanthi Kumari, Dr. Piyush Kuchhal, Dr. Ravi Gowri, Mukul K. Gupta Miniaturization of sub-wavelength Antennas for mobile applications using SRRs with DNG Metamaterials; International Conference on Advances in Electrical & Electronics Engineering (ICAEET-2011) February 25-26, 2011, at Moradabad Institute of Technology, Moradabad (U.P.), India;
4. N. Prasanthi Kumari, Dr. Piyush Kuchhal, Dr. Ravi Gowri "Design of Miniaturized Dual Band Metamaterial Antenna for Mobile Handset Applications," IEEE International Conference on Wireless Information Technology and Systems, Maui, Hawaii, USA on November 11-16, 2012.
5. N. Prasanthi kumari, Dr. Vijay Kumar. K “Design of sub-wavelength Antennas for mobile applications using SRRs with DNG Metamaterials;

(RACE-2011) NATIONAL CONFERENCE ON Recent Advancements in Communications & Electronics conducted by IETE.

6. N. Prasanthi Kumari, Dr. Ravi Gowri, Dr. Prashant Raawat, Dr. Piyush Kuchhal, “Bandwidth enhancement of Metamaterial Antenna for Mobile and wireless Applications using slots” Communicated.
7. N. Prasanthi Kumari, Dr. Ravi Gowri, Dr. Prashant Raawat, Dr. Piyush Kuchhal, “Reactance response of metamaterial antenna for mobile handsets” Communicated.